

**AQUIFER PARAMETER INVESTIGATIONS OF THE WASATCH AND FORT
UNION FORMATIONS IN THE POWDER RIVER BASIN, WYOMING, UTILIZING
MODFLOWP**

by
Michael P. Brenneis

A thesis submitted to the Department of Geology and Geophysics
and The Graduate School of The University of Wyoming
in partial fulfillment of the requirements
for the degree of

**MASTER OF SCIENCE
in
GEOLOGY**

**Laramie, Wyoming
December, 1997**

Brenneis, Michael P., Aquifer Parameter Investigations of the Wasatch and Fort Union Formations in the Powder River Basin, Wyoming, Utilizing Modflowp, M.S., Department of Geology and Geophysics, December, 1997.

A geostatistical model of the Wyodak coal seam of the Tongue River Member of the Paleocene Fort Union Formation and the sand lens aquifer of the Eocene Wasatch Formation was constructed from 1766 driller's logs. The resulting model was then discretized and formatted for use in the finite-difference groundwater flow models Modflow and Modflowp. The conceptual model of the aquifer system and the aquifer parameters of the coal were modified to improve calibration. The vertical hydraulic conductivity of the confining layer separating the Wyodak coal from the Wasatch sand lens was estimated at 4.5E-06 feet/day.

Heterogeneity was introduced into the coal and was found to further improve calibration. The vertical hydraulic conductivity of the confining layer separating the Wyodak coal from the Wasatch sand lens was estimated again, with heterogeneous coal, at 9.0E-06 feet/day.

TABLE OF CONTENTS

CHAPTER 1.	INTRODUCTION	PAGE
	Introduction	1
	Objectives	1
	The inverse problem and data adequacy	1
	Modflow and Modflowp	6
	Geographic setting	6
	Geologic setting	6
	Stratigraphy	9
	Hydrogeologic setting	11
CHAPTER 2.	MODEL PREPARATION	
	Method	13
	Conceptual model	13
	Model layers	13
	Sand lens layer	13
	Implicit confining layer	13
	Coal layer	14
	Starting head gradients	14
	Boundaries	14
	Anisotropy	17
	Stratigraphic model	17
	Compilation and correlation of stratigraphic data	17
	Construction of the geologic model	18
	Discretization	19
	Model domain - grid	19
	Model layers	32
	Model modifications	32
	Setup of specific model inputs	34
	Top and bottom of coal layer	34
	Top and bottom of the sand lens layer	34
	IBOUND arrays	39
	Hydraulic conductivity arrays	39
	VCONT	45
	Coal layer starting head	45
	Sand lens layer starting head	46
	Recharge	46
	Calibration points	46
CHAPTER 3.	CALIBRATION OF THE CONCEPTUAL MODEL	
	Introduction	47
	Method	48

	Results	52
	Conclusions	61
CHAPTER 4.	INVESTIGATION OF VERTICAL HYDRAULIC CONDUCTIVITY IN THE CONFINING BED SEPARATING THE WYODAK COAL FROM THE OVERLYING WASATCH SAND LENS AQUIFER	
	Introduction	68
	Method	68
	Results	71
	Conclusions	71
CHAPTER 5.	INVESTIGATION OF HETEROGENEITY IN THE COAL	
	Introduction	86
	Method	86
	Results	91
	Conclusions	97
CHAPTER 6.	ESTIMATION OF VERTICAL HYDRAULIC CONDUCTIVITY GIVEN BEST ESTIMATE HETEROGENEOUS COAL	
	Introduction	98
	Method	98
	Results	98
	Conclusions	112
CHAPTER 7.	CONCLUSIONS	
	Aquifer parameters	113
	Boundaries	113
	Coal heterogeneity	113
	Vertical hydraulic conductivity of the confining layer	113
	Recommendations for future study	114
	Boundary conditions	114
	Hydrogeologic properties of the Wasatch	114
	Leaky aquifer test	114
	Modeling	115
REFERENCES		116

LIST OF FIGURES

Chapter	Figure	Description	Page
1.	1-1	Study area, including coal and coal bed methane permits.	2
	1-2	Drawdowns at BLM monitoring wells	3
	1-3	Drawdowns at BLM monitoring wells	4
	1-4	Study area, including sand lens	5
	1-5	Data locations	7
	1-6	Regional location map	8
	1-7	Stratigraphic column, with hydrostratigraphic units	10
2.	2-1	Coal geometry interpretations	15
	2-2	Results of Theis solution	16
	2-3	Map of coal structure data	20
	2-4	Example of a fitted covariance function	22
	2-5	Structural contour, top of coal, kriged	24
	2-6	A seam isopach	25
	2-7	B seam isopach	26
	2-8	B2 seam isopach	27
	2-9	B1 seam isopach	28
	2-10	Parting isopach	29
	2-11	Structural contour, bottom of sand lens	30
	2-12	Sand lens isopach	31
	2-13	Modflow grid	33
	2-14	Structural contour, top of coal layer	35
	2-15	Isopach map of coal layer	36
	2-16	Structural contour, top of sand lens layer, detailing construction	37
2-17	Confining layer isopach	38	
2-18	Sand lens layer isopach	40	
2-19	IBOUND array, layer 2	41	
2-20	IBOUND array, layer 1	42	
2-21	Starting K, layer 2	43	
2-22	Starting K, layer 1	44	
3.	3-1	Zone array for case 1	49
	3-2	Results from case 1	50
	3-3	Zone array for case 2	51
	3-4	Zone array for case 3a and 3b	53
	3-5, 3-6	Results from case 2	55, 56
	3-7, 3-8	Results from case 3a	58, 59
	3-9, 3-10	Results from case 3b	62, 63
	3-11	Head calculated in case 3b, layer 2	65

LIST OF FIGURES (continued)

Chapter	Figure	Description	Page
3.	3-12	CH vs. mean residual and budget discrepancy	66
4.	4-1	Zone array for case KV2	69
	4-2	Zone array for case KV3	70
	4-3, 4-4	Results from case KV1	72, 73
	4-5	Head calculated in case KV1, layer 1	75
	4-6	Head calculated in case KV2, layer 2	76
	4-7 to 4-9	Results from case KV2	77-79
	4-10 to 4-12	Results from case KV3	81-83
5.	5-1	Fitted correlation function for K	87
	5-2	K array kriged from 38 data points	88
	5-3	K array conditionally simulated from 6 conditioning points	89
	5-4	Residuals from Modflowp run with 6 point conditionally simulated K array	90
	5-5	K array conditionally simulated from 16 conditioning points	92
	5-6	Residuals from Modflowp run with 16 point conditionally simulated K array	93
	5-7	Head calculated with 16 point conditionally simulated K array, layer 1	95
	5-8	Head calculated with 16 point conditionally simulated K array, layer 2	96
6.	6-1, 6-2	Results of Modflowp KV runs with heterogeneous coal, one zone kv	99, 100
	6-3	Head calculated with 16 point conditionally simulated K array and KV=9E-6, layer 1	102
	6-4	Head calculated with 16 point conditionally simulated K array and KV=9E-6, layer 2	103
	6-5 to 6-7	Results of Modflowp KV runs with heterogeneous coal, two zone KV	104-106
	6-8 to 6-10	Results of Modflowp KV runs with heterogeneous coal, three zone KV	108-110

LIST OF TABLES

Chapter	Table	Description	Page
2	2-1	Descriptive Statistics of Geologic Model Input Files.	21
2	2-2	Results of Covariance Modeling and Kriging Parameters	23
3	3-1	Results from case 1	54
3	3-2	Results from case 2	57
3	3-3	Results from case 3a	60
3	3-4	Results from case 3b	64
4	4-1	Results from case KV1	74
4	4-2	Results from case KV2	80
4	4-3	Results from case KV3	84
5	5-1	Results from investigations of heterogeneous coal	94
6	6-1	Results from KV estimation, one zone	101
6	6-2	Results from KV estimation, two zones	107
6	6-3	Results from KV estimation, three zones	111

This page intentionally left blank.

Chapter 1. Introduction

I. Introduction

Coal mining in the Powder River Basin of northeastern Wyoming began in earnest in the middle 1970s, with an increase in production during the 1980s. The 1990s saw the beginning of coal-bed methane production to the west of the coal mines (Figure 1-1). Of interest to many parties has been the determination of the effects of drawdowns in the coal aquifer, due both to strip-mining and coal-bed methane production, on the water supply of the Powder River Basin.

The Bureau of Land Management has been recording water levels in a pair of wells, which monitor both the coal and the sand lens aquifers, since 1993 (Brogan and Meyer, 1996)(Figure 1-2 and 1-3). A steady drawdown in the coal has been observed over this period. A drawdown in the sand lens aquifer is evident as well. What is unknown is whether the drawdowns observed in the sand lens aquifer are caused by drawdowns in the coal aquifer.

II. Objectives

This study examines the confining layer separating the Eocene Wasatch Formation from the underlying Wyodak coal seam of the Paleocene Fort Union Formation from a modeling perspective. Specifically, this study attempts to estimate the vertical hydraulic conductivity of the material separating a particular sand lens (Figure 1-4) in the Wasatch Formation from the underlying Wyodak coal bed. In addition this study details how the Wyodak coal layer should be represented in the model.

III. The inverse problem and data adequacy

Solving the groundwater flow equation for groundwater elevation using known aquifer parameters, stresses and boundary conditions is the direction in which such problems are generally solved. Solving the groundwater flow equation for aquifer parameters, stresses and boundary conditions using known ground water elevations is referred to as solving the inverse problem. The difficulty of this approach in this case is

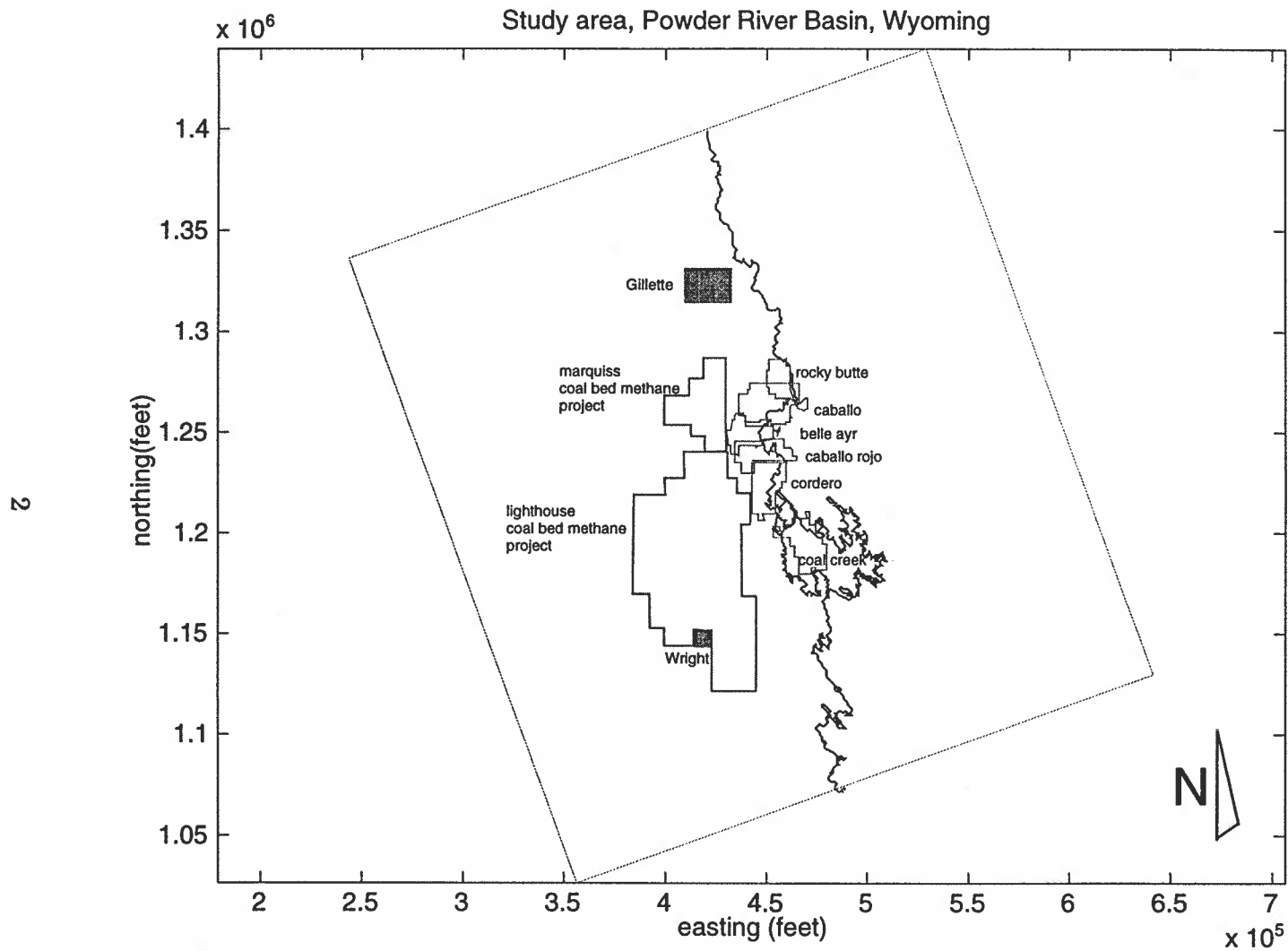


Figure 1-1. Map view of study area showing locations of mine permits, cities, and the full seam coal line also known as the cropline. In the area of Coal Creek mine the two lines shown represent the cropline of two different coal seams.

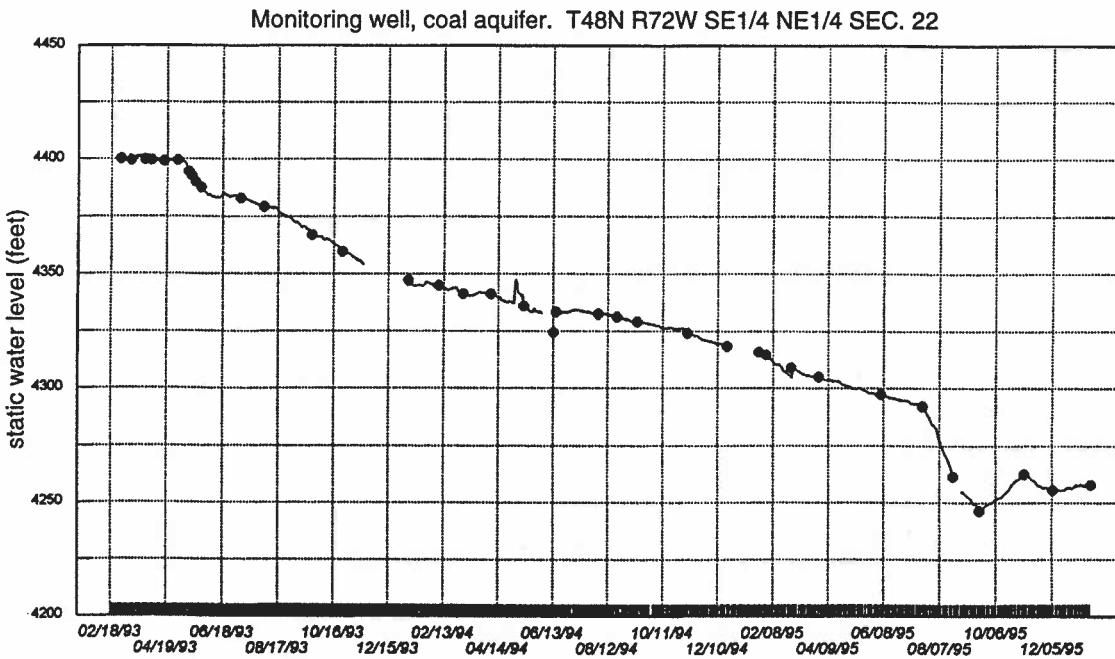
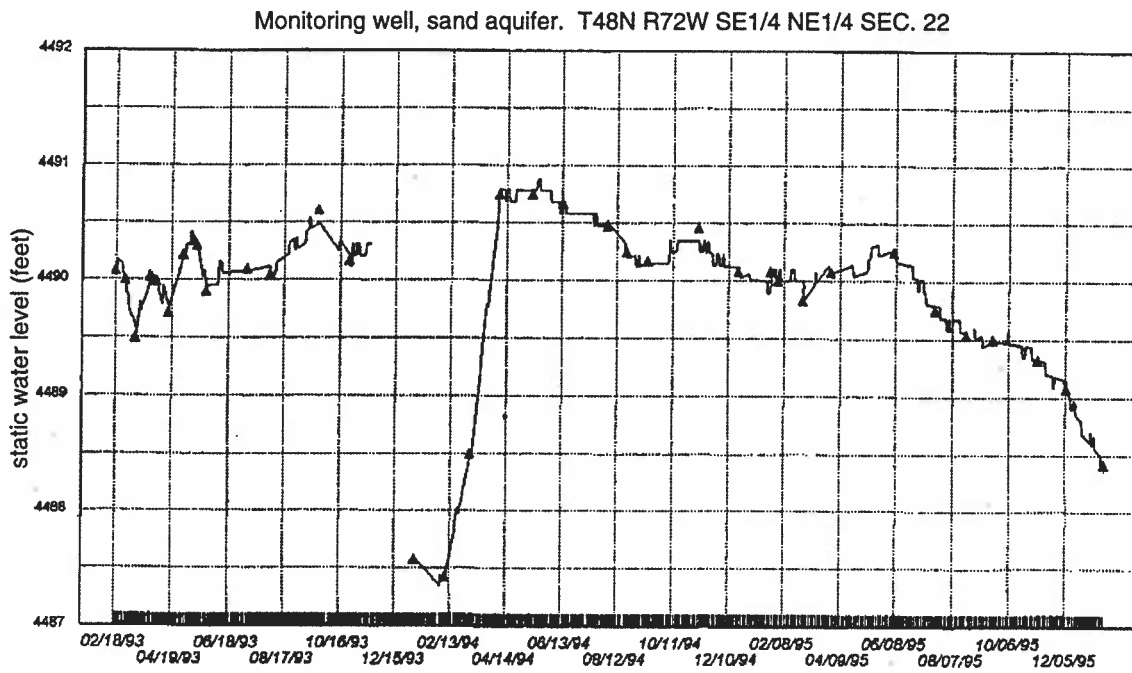


Figure 1-2. Plots of water level over time, in a well which monitors both the sand lens and coal aquifers.

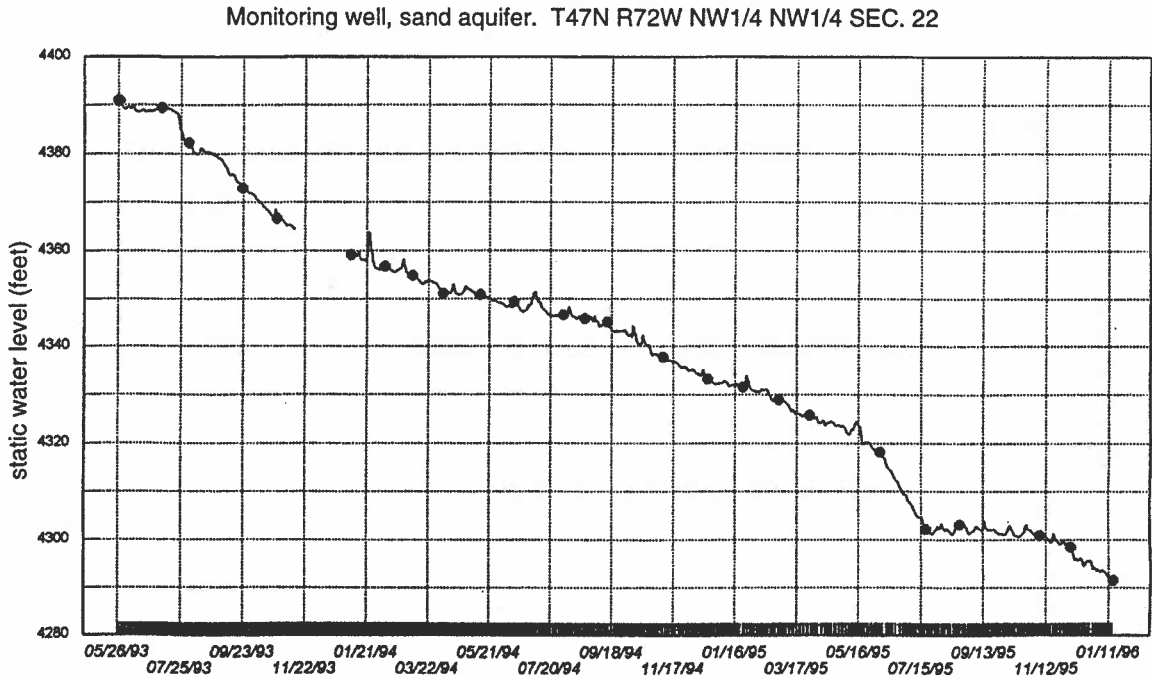
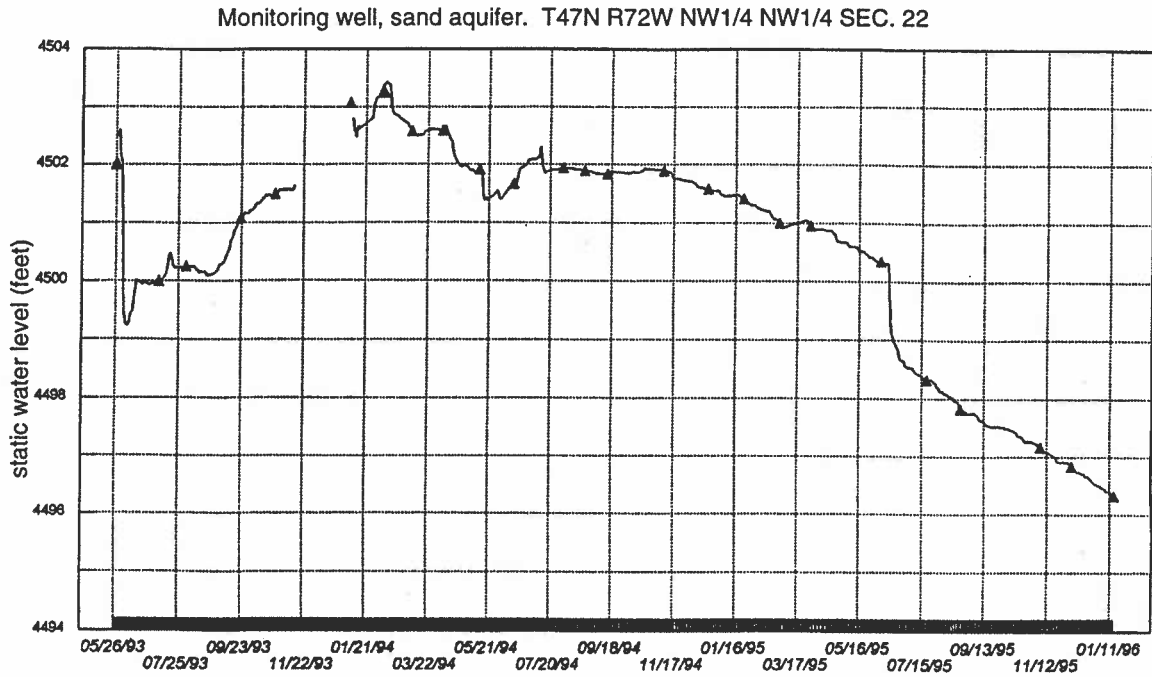


Figure 1-3. Plots of water level over time, in a well which monitors both the sand lens and coal aquifers.

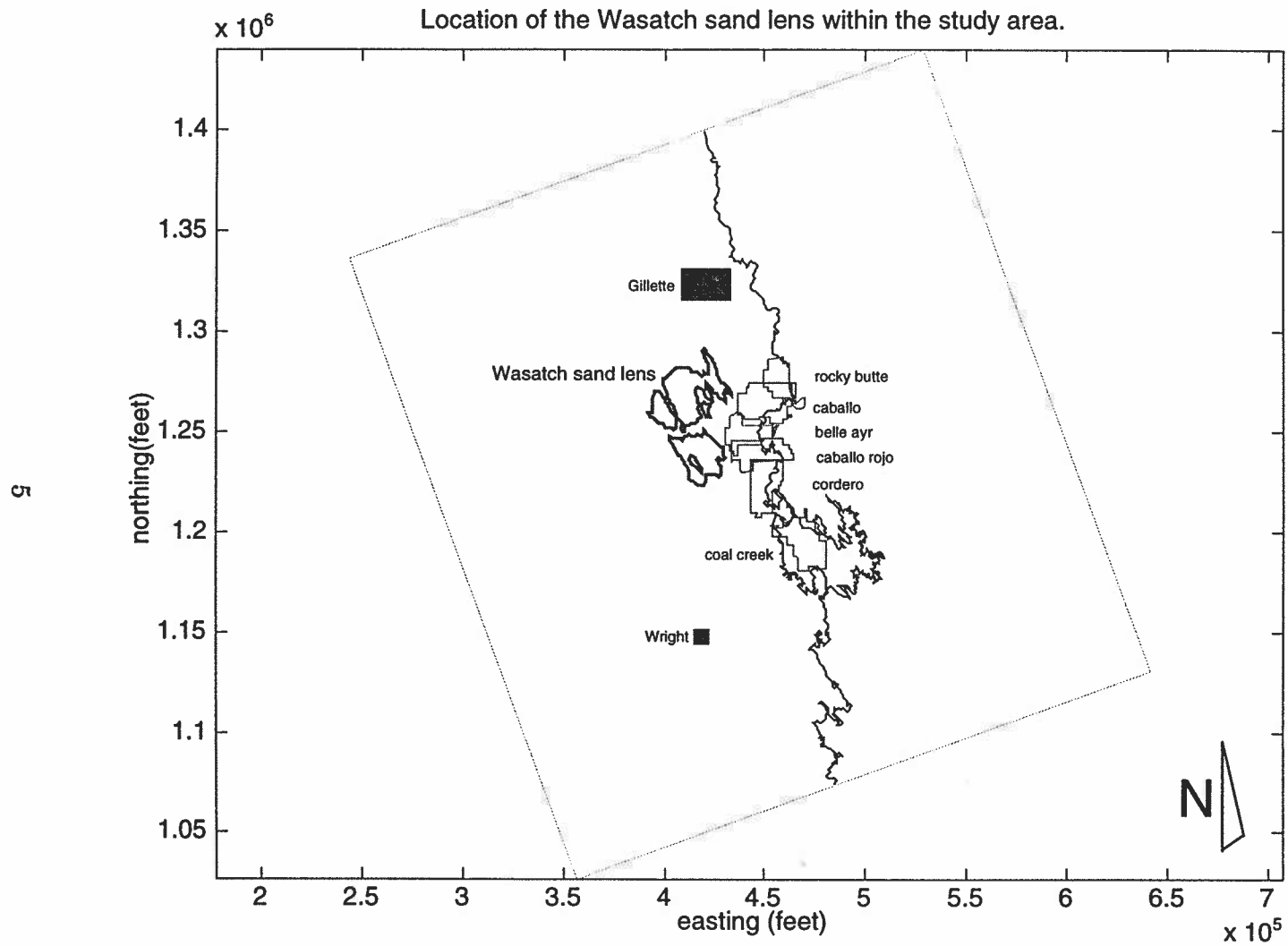


Figure 1-4 . Map of the study area including the location of the Wasatch sand lens west of the mines. The sand lens is represented by the 20 foot isopach.

compounded by a paucity of data. The majority of the data were collected by industry, in the vicinity of the mines. No systematic data collection for the domain is available. For this reason geologic data and water level data are clustered near the eastern boundary of the domain (Figure 1-5). There is a large expanse to the west which contains little or no data. As a result, conceptualization of the natural system plays an important role in the construction of the model.

IV. Modflow and Modflowp

The United States Geological Survey (USGS) computer codes Modflow (McDonald and Harbaugh, 1988) and Modflowp (Hill, 1990) were utilized to solve the ground water flow equation. Modflow utilizes a finite difference approach to solve the groundwater flow equation, and forms the core of Modflowp. Modflowp allows the modeler to estimate aquifer parameters and determine how they affect the heads and fluxes of the model. Modflowp cycles these estimates through Modflow, determines how closely the resulting head matches given calibration points and alters the estimates to improve the calibration. Modflowp is an evolving program; in fact a new version was released during the course of this investigation.

V. Geographic setting

The model domain for this study is located in the Powder River Basin of northeast Wyoming, and extends from Gillette, to the north, to south of Wright, to the south, in Campbell County, Wyoming (Figure 1-6). The study area encompasses Rocky Butte, Caballo, Belle Ayr, Caballo Rojo, Cordero, and Coal Creek coal mines, the Marquiss coal-bed methane project area, and the Lighthouse coal-bed methane project area.

VI. Geologic setting

The Powder River Basin, formed during the Laramide orogeny, is a large northwest trending asymmetric syncline, bounded to the west by the Bighorn Mountains, to the south by the Laramie Range, to the southwest by the Casper Arch, to the southeast by the Hartville Uplift, to the east by the Black Hills, and to the northeast by the Miles

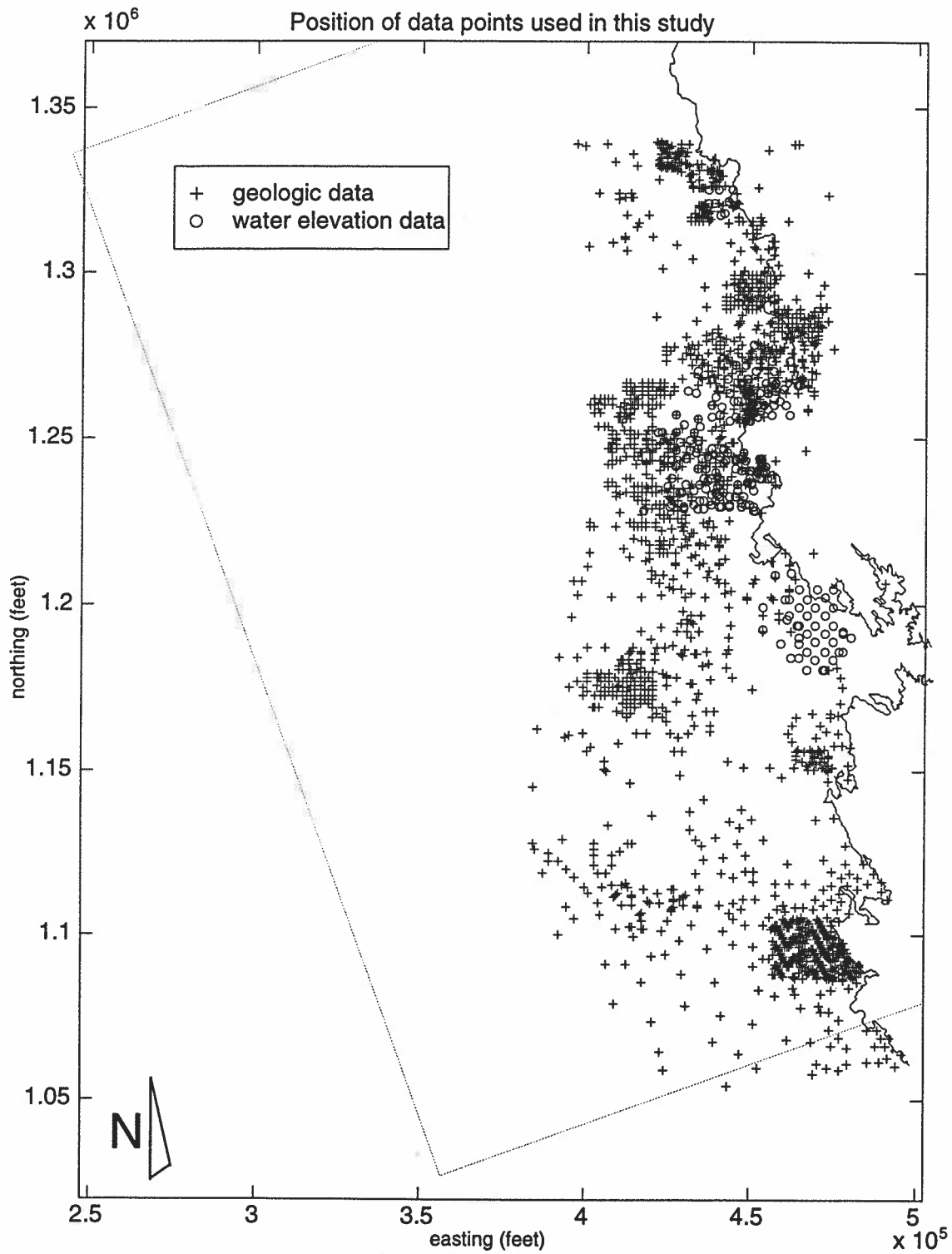


Figure 1-5. Location of data used in this study. Notice the clustering along the cropline, and the paucity of data to the west. Study domain boundary shown in gray.

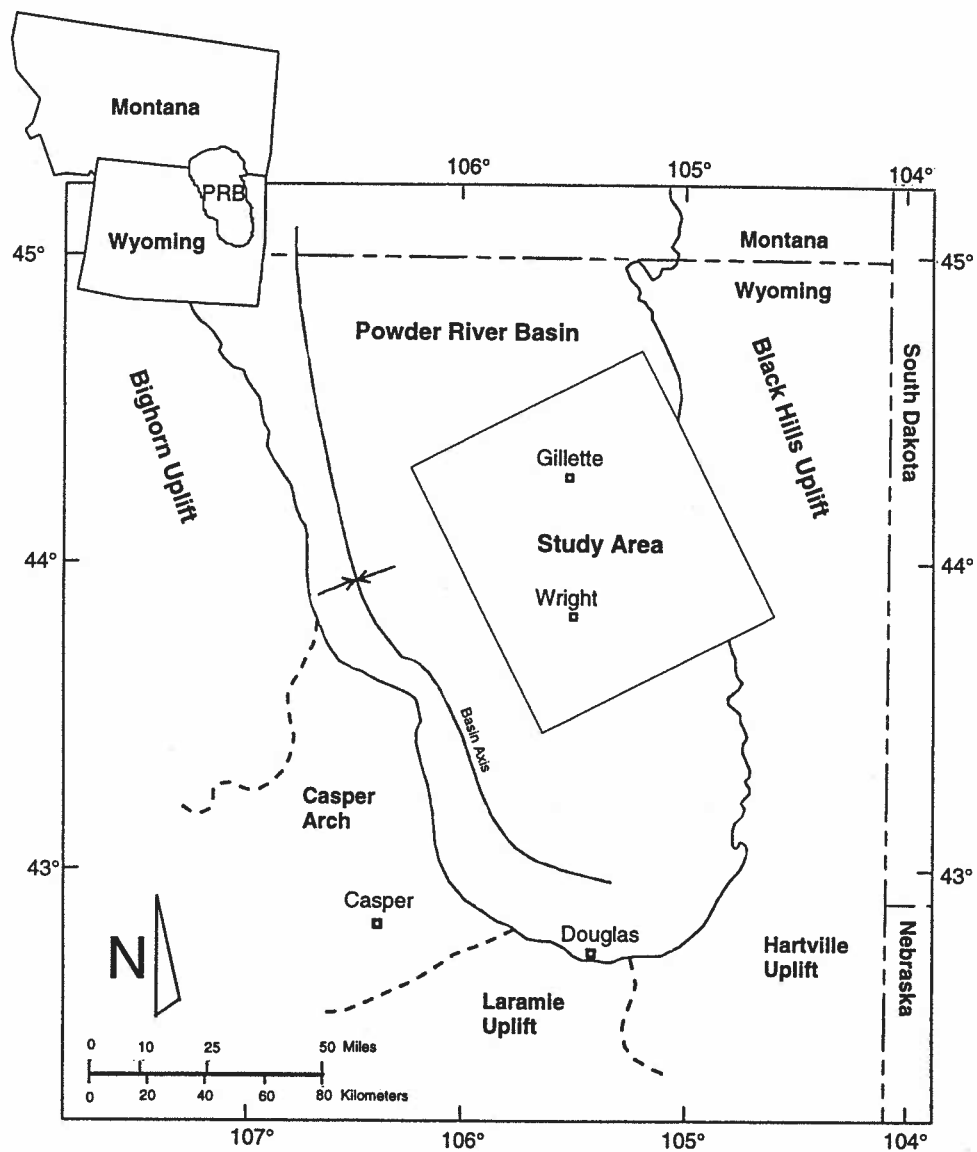


Figure 1-6. Location of study area within the Powder River Basin, Wyoming. Modified from Dobson (1996).

City Arch (Figure 1-6). The Powder River Basin contains a sedimentary package more than 13000 feet thick of Phanerozoic sediments overlying the Precambrian basement, about 6600 feet of which resulted from post deformational sediment influx and consist mainly of stream and lacustrine deposits (Lisenbee 1988).

Stratigraphy

The units of interest in the present study include those that are affected by coal and coal-bed methane production. These include the Tongue River member of the Paleocene Fort Union Formation, and the Eocene Wasatch Formation (Figure 1-7).

The Tongue River Member is the uppermost member of the Paleocene Fort Union Formation and consists of interbedded light-gray, very-fine to fine-grained, moderately-sorted, friable sandstone, gray siltstone, gray sandy shale, mudstone, and laterally continuous thick coal seams. The Tongue River member tends to be coarser and more conglomeratic on the western margin of the basin (Weaver et. al. 1987). It is typically 1200 to 1500 feet thick in the model area (Pierce et. al. 1990). Sandstone percentages in the Tongue River are highest at the basin margins with about 50% decreasing to about 30% toward the center of the basin (Curry 1971, Ayers 1986). Sand body geometry and lithofacies distribution suggest that the Tongue River Member is basin fill consisting of delta deposits prograding into ancient Lake Lebo (Ayers 1986). Primary deltaic sediment influx was from the east with minor deltas to the northwest and southwest (Ayers 1986). The Tongue River member is the most prodigious coal producing unit in the Powder River Basin (Glass 1991), and is the object of the mines in the study area.

The Eocene Wasatch Formation is lithologically similar to the Tongue River Member of the Fort Union Formation. The Wasatch Formation is second only to the Fort Union Formation in coal-bearing rocks in the basin; with as many as eight, laterally persistent, coal beds (Glass 1991). In the model area the Wasatch formation can be described from driller's logs as consisting predominantly of shale with interbedded sandstone, siltstone and coal. The shale is generally gray, sometimes sandy, silty, or carboniferous. Of particular interest in this study is a Wasatch sandstone lens which has been identified west of the coal mines (Figure 1-4). This lens consists of medium to fine-grained sandstone with pockets of coarse sand to gravel and minor pockets of

System	Series	Stratigraphic Unit		Hydrostratigraphic Unit
Tertiary	Eocene	Wasatch Formation		Wasatch Sand Lens Aquifer
				Upper Tongue River/ Lower Wasatch Confining Layer
	Paleocene	Fort Union Formation	Tongue River Member	Wyodak Coal Seam Aquifer
				Lower Tongue River Confining Layer

Figure 1-7. Stratigraphic and hydrostratigraphic units considered in this study.

argillaceous sandstone to sandy or silty shale. The Wasatch Formation is thickest in the center of the basin, about 1575 feet, and thins toward the basin flanks (Fogg et al 1991).

The Wasatch Formation and the Tongue River member of the Fort Union Formation contain clinker adjacent to coal seams. Clinker is rock that has been thermally metamorphosed by the combustion of adjacent coal, resulting in hardened, melted or sintered rock. Clinker is differentially resistant to erosion due to its increased hardness over unaltered rock and also due to its high fracture permeability, caused by heating and subsidence, which allows water to infiltrate and minimizes surface runoff, leaving clinker to cap ridges, buttes, mesas, and knobs which stand out above the eroded, unaltered and less resistant country rock (Mears et. al. 1991).

VII. Hydrogeologic setting

The study domain is divided into four hydrostratigraphic units as described from driller's logs and Martin et. al. (1988)(Figure 1-7). At the greatest depth is the Lower Tongue River confining unit. This unit consists of shale and sandy shale with minor coal, siltstone, argillaceous siltstone, and carboniferous shale.

Overlying the Lower Tongue River confining layer is the Wyodak Coal Seam aquifer. The coal aquifer is quite impermeable except in cleat and other fractures (Dobson 1996, Stone and Snoeberger, 1977). Flow through the coal is believed to be localized along fractures and may be correlated to surface lineaments (Dobson 1996).

Overlying the Wyodak Coal Seam aquifer is the Upper Tongue River / Lower Wasatch confining layer. This unit is dominated by shale. Data from paired monitoring wells in the Wyodak Coal Seam aquifer and the Wasatch Sandstone Lens aquifer indicate that this confining layer may be only semiconfining, allowing some water to pass between the two aquifers (Figures 1-2 and 1-3).

Overlying the Upper Tongue River / Lower Wasatch confining layer is the Wasatch Sandstone Lens aquifer. The Sandstone Lens aquifer is a discrete lens of Sandstone in the Wasatch Formation separated from the underlying coal by the Upper Tongue River / Lower Wasatch confining layer. The Sandstone Lens aquifer is confined from the land surface by another shale-dominated layer.

The Clinker is not a member of the aquifer / confining layer system described above, but comprises the fourth hydrostratigraphic unit. Its unique hydrologic properties affect the boundary conditions of the model.

Chapter 2. Model Preparation

I. Method

The modeling method included the formulation of a conceptual model, the approximation and discretization of the conceptual model into a mathematical model, and the solution of the mathematical model using the USGS computer programs, MODFLOW (McDonald and Harbaugh 1988) and MODFLOWP (Hill, 1990).

II. Conceptual model

The conceptual model is a simplification of an interpretation of the natural system. Such a simplification was necessary in order to construct a numerical problem solvable by MODFLOW and MODFLOWP. The conceptual model consists of three layers. Layer 1 is the Eocene Wasatch sand lens layer and was modeled explicitly. Layer 2 is the Eocene Wasatch / Upper Tongue River confining bed, which was modeled implicitly, meaning that it filled the space between the top and bottom layers, but was represented solely by a vertical hydraulic conductivity in the formulation of the model. Layer 3 is the Paleocene Wyodak coal seam of the Tongue River Member of the Fort Union Formation, which was modeled explicitly.

II.a. Model layers

II.a.1. Sand lens layer

The sand lens layer was developed about the Wasatch Sand Lens. The location of the Wasatch Sand Lens and its proportions are known to a high degree of certainty based on data, as described in section III.1. Since MODFLOW requires each layer to be continuous over the model area, layer 1 was extended arbitrarily from the sand lens to the boundaries of the model. The hydraulic conductivity of this layer was manipulated to approximate the undifferentiated Wasatch Formation material outside of the sand lens.

II.a.2. Implicit confining layer

Separating the coal, below, from the sand lens layer, above, is a confining layer. Based on the observation of driller's logs, this layer consists of undifferentiated Wasatch Formation material. As such it acts to hinder flow between the coal and sand lens layers.

II.a.3. Coal layer

Two interpretations of coal structure are supported by the data. The first is of one continuous coal seam, parted in the north and parted in the south, but unparted through the center of the study area. Alternatively, the layer of coal above the southern parting may pinch out, and not reconnect with the main body of the coal (Figure 2-1). A clear distinction can not be made between these two scenarios due to the correlation procedure, as discussed in section III.1.

II.b. Starting head gradients

A northwest gradient in the coal and sand lens layers was indicated for the study area both from raw head data and from previous studies in the area (Peacock, 1997a). The head in the sand lens layer is slightly higher than that of the coal layer.

II.c. Boundaries

The full-seam coal-line boundary, or cropline, in keeping with the conceptual model and in the interests of numerical stability, was designed as a specified head boundary. This eastern edge contains clinker, which is highly porous and permeable. Clinker in contact with the coal acts, in effect, as would a standing body of water, by flowing into the model as demanded (Peacock, 1997a).

The full-seam coal-line boundary was designed by overlaying the modflow grid and the full seam coal line, and determining on which side of the line the cells of the model fell.

The other three boundaries of the model are at a sufficient distance from the model stresses to not be reached by drawdowns in any of the layers over the time period of transient simulation. Thus they are modeled as specified head boundaries.

In order to determine the size of the model domain necessary for transient simulation, a first order approximation of the effects of the stresses on the system was made. A Theis solution was calculated with aquifer transmissivity of 840 square feet/day and a storativity of 0.00025. The coal was modeled as homogeneous and isotropic with a hydraulic conductivity (K) of 14 feet/day, which is on the order of the long axis of the K ellipse as calculated for the coal. The pumping from the Marquiss coal bed methane well field was approximated by one well pumping at a rate of 504 gallons/minute over a period of three years. The results are shown in figure 2-2. The model boundaries were constructed accordingly.

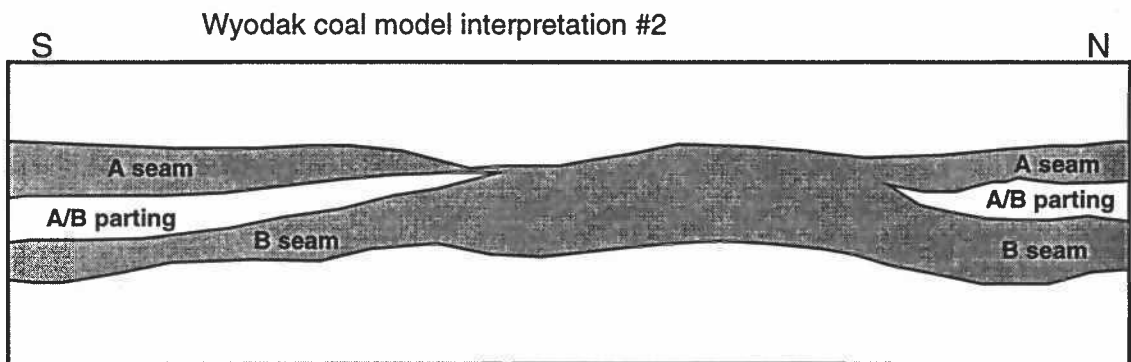
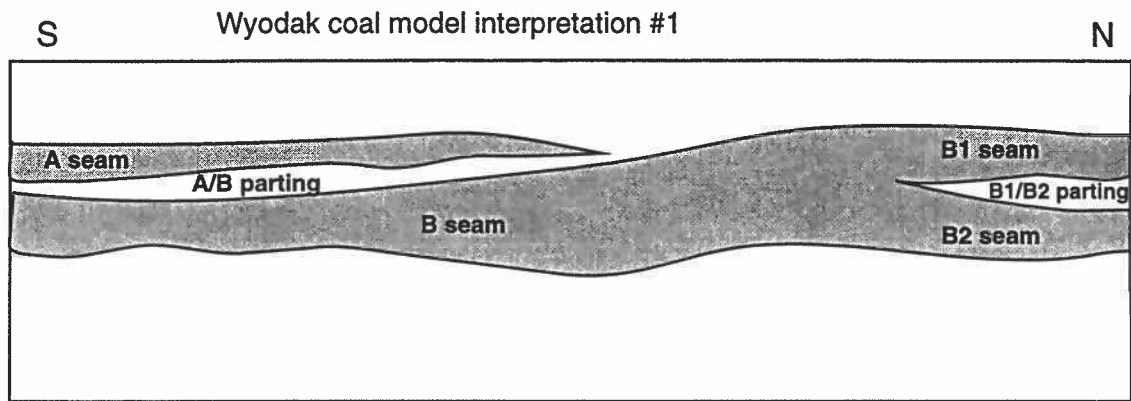


Figure 2-1. Idealized north-south cross sections through the study area of two coal structure interpretations which are indistinguishable from the data as analyzed in this study. Highly vertically exaggerated.

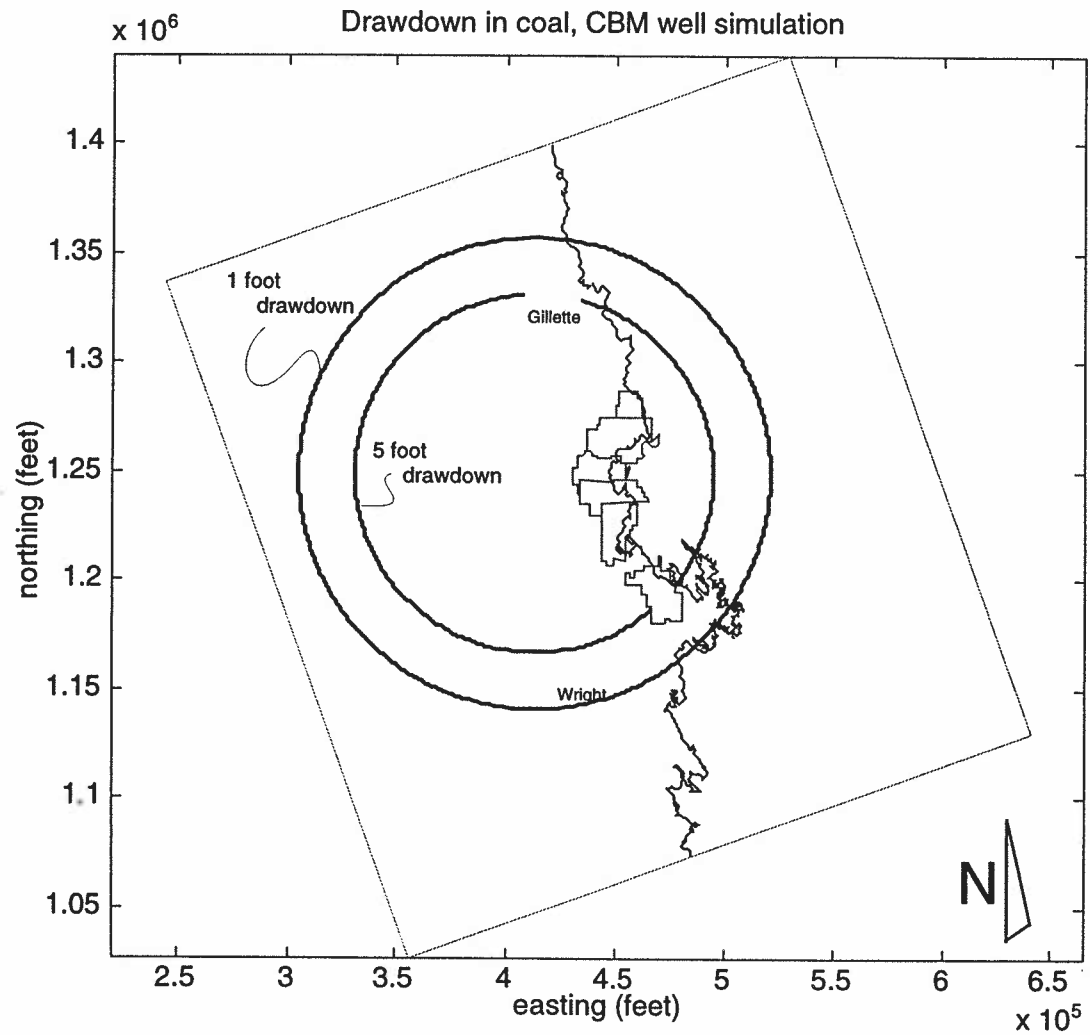


Figure 2-2 . Drawdown from aquifer stress simulation with transmissivity=840 feet²/day and a discharge of 504 gal/day over 3 years from coal bed methane wells. Mine permits and cropline shown for orientation. Modflow model boundary shown as gray rectangle.

II.d. Anisotropy

The coal was determined, by two long-range aquifer pump tests conducted by the Bureau of Land Management (BLM), to have a two to one horizontal hydraulic conductivity anisotropy in the N27W direction (Kern, 1997a).

III. Stratigraphic Model

III.1. Compilation and Correlation of Stratigraphic Data

Driller's logs were compiled from USGS Open-File Reports, the Montana Bureau of Mines and Geology, Permit to Mine Applications, Martens and Peck Stratigraphic Test Holes, a BLM database courtesy of Jim Bauer, a BLM database courtesy of Ken Peacock, and the Original BLM Public database. The accumulated logs totaled nearly 1800. The logs were entered into the relational database program STRATIFACT (StratiFact Software, 1995).

The study area was broken into manageable portions by correlating 50 cross sections, approximately half of which ran north-south and half of which ran east-west. More cross sections were constructed in areas of greater data density. Smaller cross sections were then constructed perpendicular to the 50 previously correlated, beginning and ending with points that were already correlated.

The stratigraphy was broken into six hydrostratigraphic units: the Wasatch Formation, the Fort Union Formation Wyodak A Member, the Fort Union Formation Wyodak Parting Member, the Fort Union Formation Wyodak B Member, the Fort Union Formation Wyodak Wyo Member (where no parting could be identified), and Fort Union Formation Tongue River Member. Everything above the Wyodak coal was labeled Wasatch, except for one sand lens as discussed. Everything below the Wyodak coal was labeled as Fort Union Formation Tongue River Member. In order to identify the geometry of the monitored sand lens in the Wasatch Formation, the formation was subdivided into Oversand deposits, the Wasatch Sand Lens, and Undersand deposits.

In order to minimize the number of layers to be included in the ground-water-flow model, only partings larger in vertical extent than 15 to 20 feet were correlated. Smaller partings were lumped into coal layers. In addition, only one parting per hole was correlated. In cases where there were multiple thick partings separated by thin coals, the coals were lumped in with the

partings. In cases where the interbedded coals were more substantial, all but the largest parting were lumped in with the coals. In locations with multiple substantial partings, some care was taken to maintain consistent correlation of the selected parting from one log to the next.

III.2. Construction of the Geologic Model

Data sets for the tops and bottoms of the following layers, in order of increasing depth, were generated from the correlated logs: Oversand deposits, the Wasatch Sand lens, Undersand deposits, Generic Wasatch (where no sand lens was located), Wyodak A, Generic Wyodak (where no parting was located), Parting, Wyodak B, and Fort Union Tongue River. These layers were not designed to correspond with accepted stratigraphic nomenclature. Rather, they were designed as a convention to facilitate the development of the conceptual geologic model.

As a matter of quality control the following data sets were generated: bottom of Oversand deposits, top of sand lens, bottom of sand lens, top of Undersand deposits, bottom of generic Wasatch, top of Wyodak A and top of generic Wyodak, bottom of Wyodak A, top of parting, bottom of parting, top of Wyodak B, bottom of Wyodak B and bottom of generic Wyodak, and top of the Fort Union Tongue River. The designation of Wasatch and Tongue River were conventions to describe the material above and below the coal respectively. To insure that only legitimate tops and bottoms were to be used in the geologic model, only those tops that were coincident with bottoms of overlying layers, and bottoms coincident with tops of underlying layers, were used. Logs, in which the bottom of a layer is registered without the top of the underlying layer, end in the layer being registered and do not indicate the actual bottom of the layer. Logs in which the top of a layer is registered without the bottom of the overlying layer end in the layer being registered and do not indicate the actual top of the layer. Such data points were not used in further development of the geologic model. Logs in which the top of the uppermost layer coincides with the ground surface elevation were used with ground surface elevation determining the top of the uppermost layer.

Some additional data, which was correlated by other workers, was made available and incorporated into the regional data set.

The resulting data set was manually investigated to identify errors. This resulted in the removal of two data points where the overall thickness of coal was anomalously high, 419 and 170 feet respectively, and may have been the result of correlations erroneously labeling coal

seems overlying the Wyodak seam as top of the Wyodak seam. The final data set contained 1766 logs which could be divided into four categories: Logs with two coal seams separated by a parting, logs with one coal seam and no parting, logs with a B seam only, and logs with no coal (Figure 2-3). The logs used in the development of the sand lens were a subset of these logs and are not presented on figure 2-3. Table 2-1 presents an analysis of the data sets ultimately used in the development of the geologic model.

GEOMAT (Kern, 1996), a geostatistical computer code written for MATLAB (Mathworks, 1996), was used to universally krig the individual data sets. Covariance functions were modeled for each data set (Figure 2-4) and anisotropy ellipses were determined (Table 2-2). The thickness of the parting was kriged first to determine where it dropped below 20 feet, or did not exist according to the correlation convention. The overall thickness of the coal seam, consisting of both coal and parting thickness data, where appropriate, summed, was then kriged. The top of the A seam off of which the other thickness' are to be hung was then kriged (Figure 2-5). This was followed by the A seam thickness, the B seam thickness', and the parting thickness (Figures 2-6, 2-7, 2-8, 2-9 and 2-10). The thickness' of the A seam, B seam, and parting are only defined where these layers exist. The tops of these layers were determined by arithmetic manipulation of the thickness'. In locations where the kriged parting thickness was less than 20 feet, the parting thickness was set to zero. Table 2-2 presents the results of geostatistical analyses of the data sets as well as inputs into the kriging routine.

For use in the ground water flow model, the bottom and thickness of one monitored sand lens in the Wasatch Formation was modeled using the same methods as outlined above (Figures 2-11 and 2-12).

IV. Discretization

IV.1. Model Domain - Grid

The grid consists of a rectangle with 100 cells on each side with its long axis rotated to N27W. The grid is centered on an 80 by 80 block of fully refined cells. Bordering the refined area is a layer of 10 unrefined grid cells arrived at by sequentially multiplying the refined column width by 1.34 and the row height by 1.4. The model domain is nearly square with sides of 57.4 miles in the northeast-southwest direction and 62.3 miles in the northwest-southeast direction

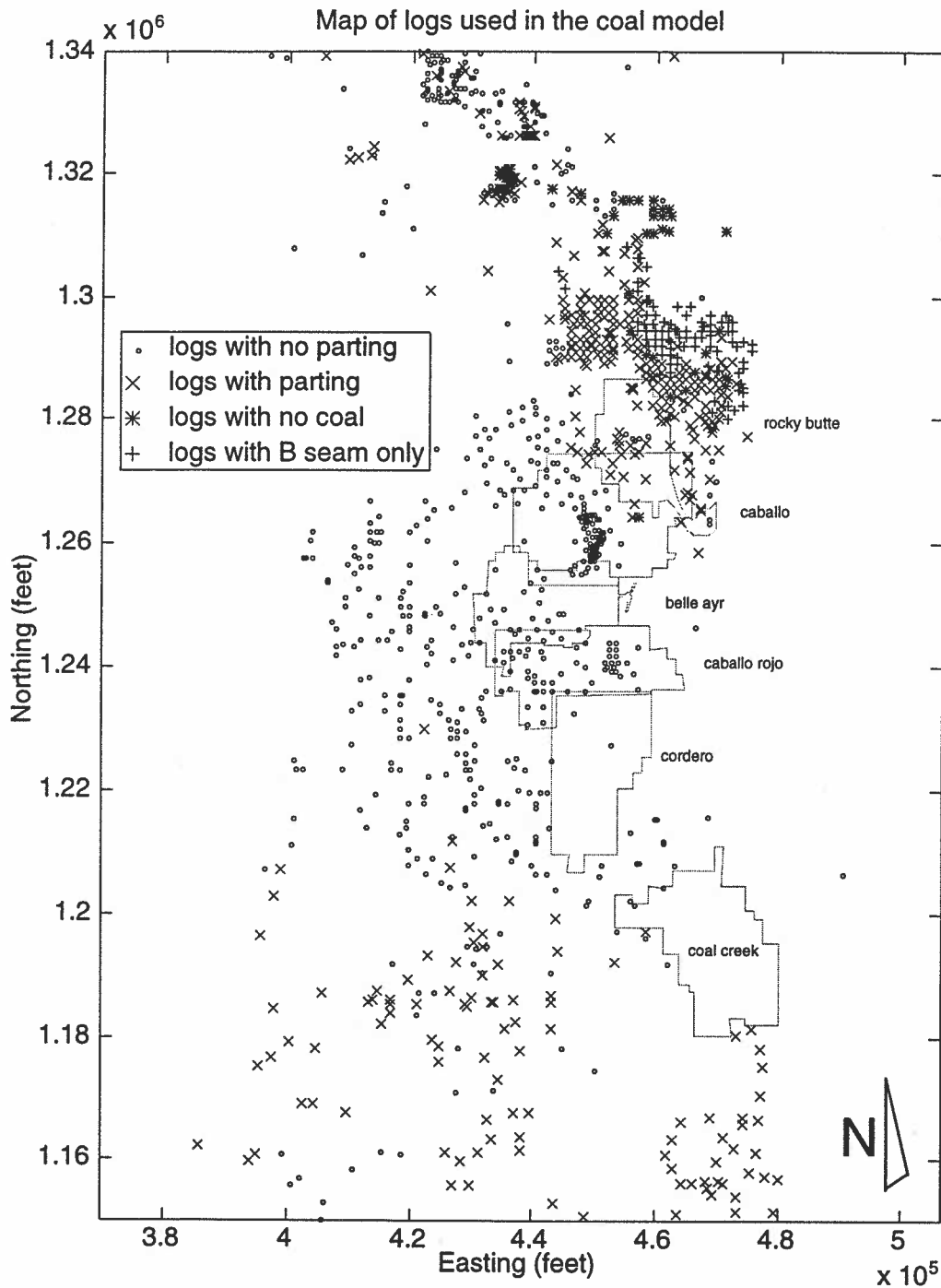


Figure 2-3. Map of the four different species of coal geometry observed in driller's logs within the study area. Mine permit boundaries shown for orientation.

Table 2-1. Descriptive Statistics of Geologic Model Input Files.

Data Set	number of points	range	mean	standard deviation
sand lens bottom	110	4292 / 4650	4494.8	52.8116
sand lens thickness	106 / 822*	2 / 264	66.88	40.8474
Wyodak A seam top	1325	3834 / 4882	4389.3	181.0438
Wyodak A seam thickness	460	0 / 170.5	43.07	27.9955
parting thickness	395 / 1766*	1 / 217	56.7	47.3667
Wyodak Bseam thickness	502	0 / 111	29.94	21.3808
overall thickness of coal	1033	0 / 293	92.96	48.7769

* indicates the number of points including points where quantity is not present. Listed statistics are for points where quantity is present.

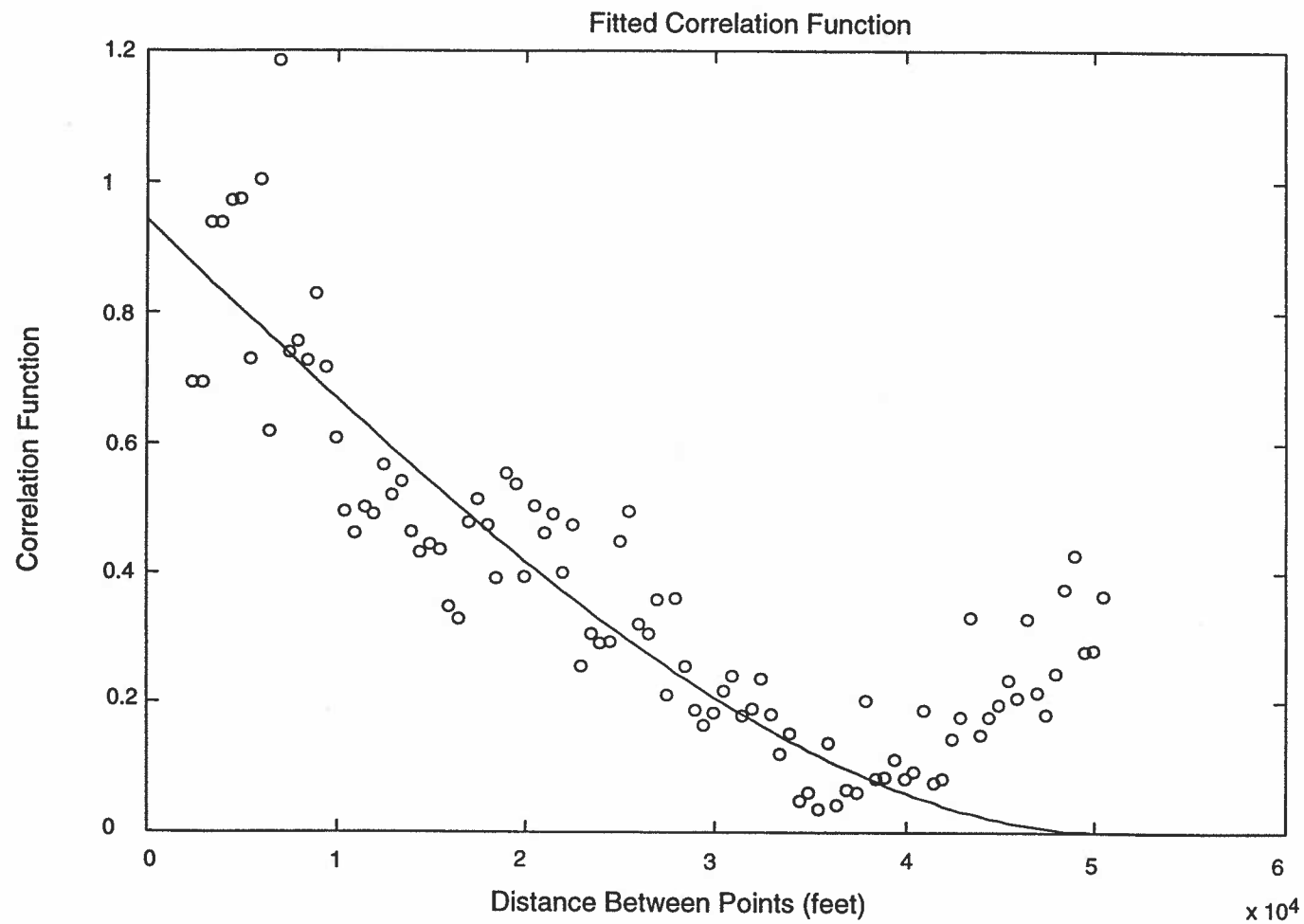


Figure 2-4. Covariance function for the overall thickness of the coal seam, oriented N60W, the direction of the major axis of anisotropy. The estimates were kernel smoothed with an effective band width of 500 feet and a maximum distance of 50000 feet. The major axis was 50773 feet in length in this case.

Table 2-2. Results of Covariance Modeling and Kriging Parameters

Data set	model	nugget	Anisotropy		Trend surface				R ²	variance	search radius for major axis (feet)	
			major axis	minor axis	equation	slope	intercept					
			angle (degrees)	length (feet)	angle	length						
overall coal thickness	spherical	0.1949	N60W	50773	N30E	17285	NA	NA	NA	NA	2380.4	60000
sand lens bottom	spherical	0.328	N50E	8152.5	N40W	2682.9	NA	NA	NA	NA	2788.6	80000
sand lens thickness	spherical	0.3774	N30W	13485	N60E	2609.9	NA	NA	NA	NA	716.5	60000
Wyodak A seam top	spherical	0.1632	N20W	90533	N70E	33003	linear in x	9.36E-03	4389.27	0.8861	32781.4	60000
Wyodak A seam thickness	spherical	0.3826	N30W	25387	N60E	10249	NA	NA	NA	NA	783.4	80000
parting thickness	spherical	0.2186	N70W	20001	N20E	7125.3	NA	NA	NA	NA	1059.3	60000
Wyodak Bseam thickness	spherical	0.2948	N70W	15180	N20E	5179.5	NA	NA	NA	NA	457.2	80000
bottom of coal	spherical	0.4235	N45W	56740	N45E	25640	linear in x	9.20E-03	4337.1	0.9506	30881.9	60000

23

Universal Kriging Parameters

1. Maximum system size = 16
2. grid of 100 x 100 cells
3. State Plane Coordinates of Grid

	min	max
x	3.50E+05	5.00E+05
y	1.15E+06	1.34E+06

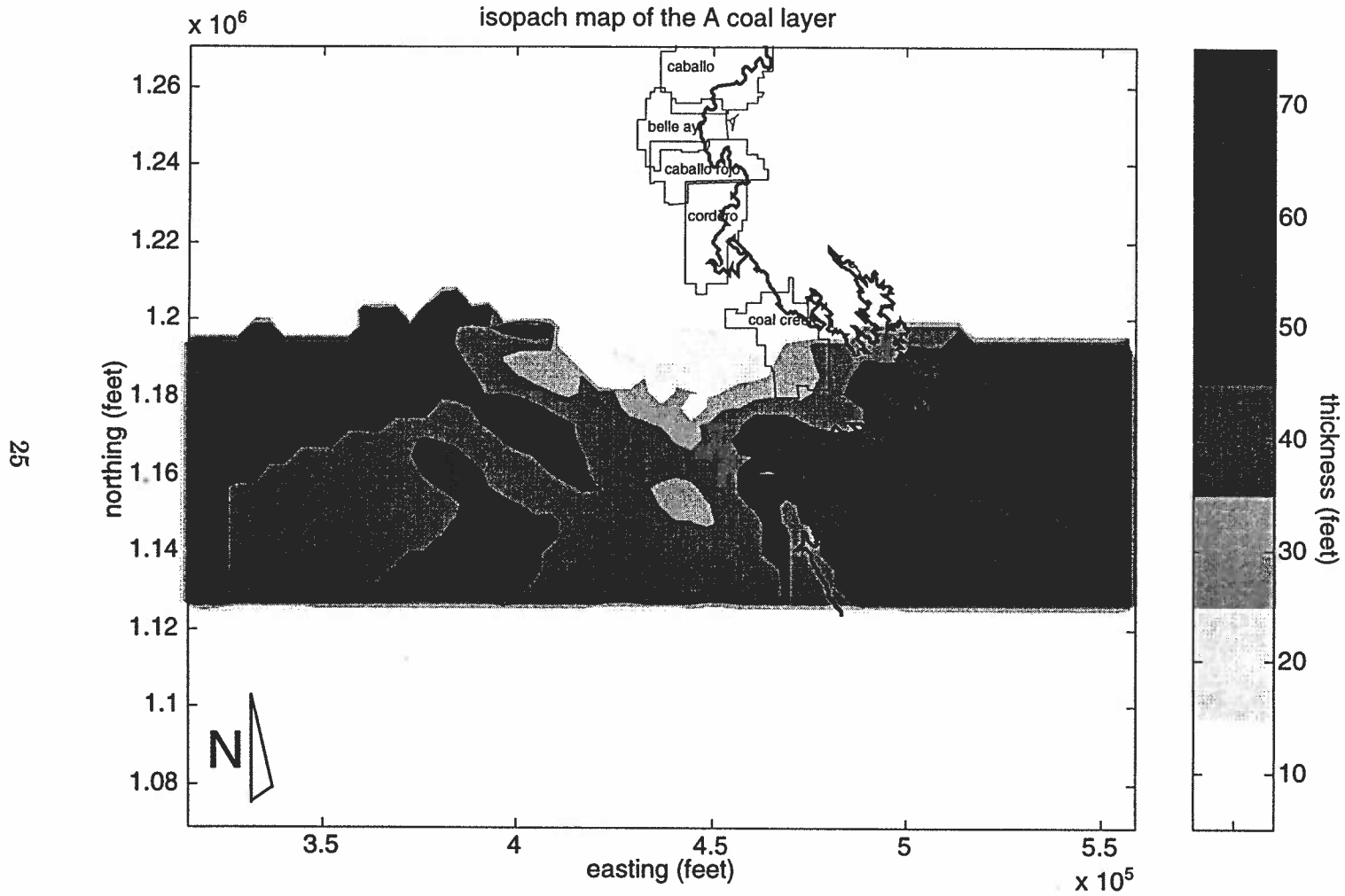
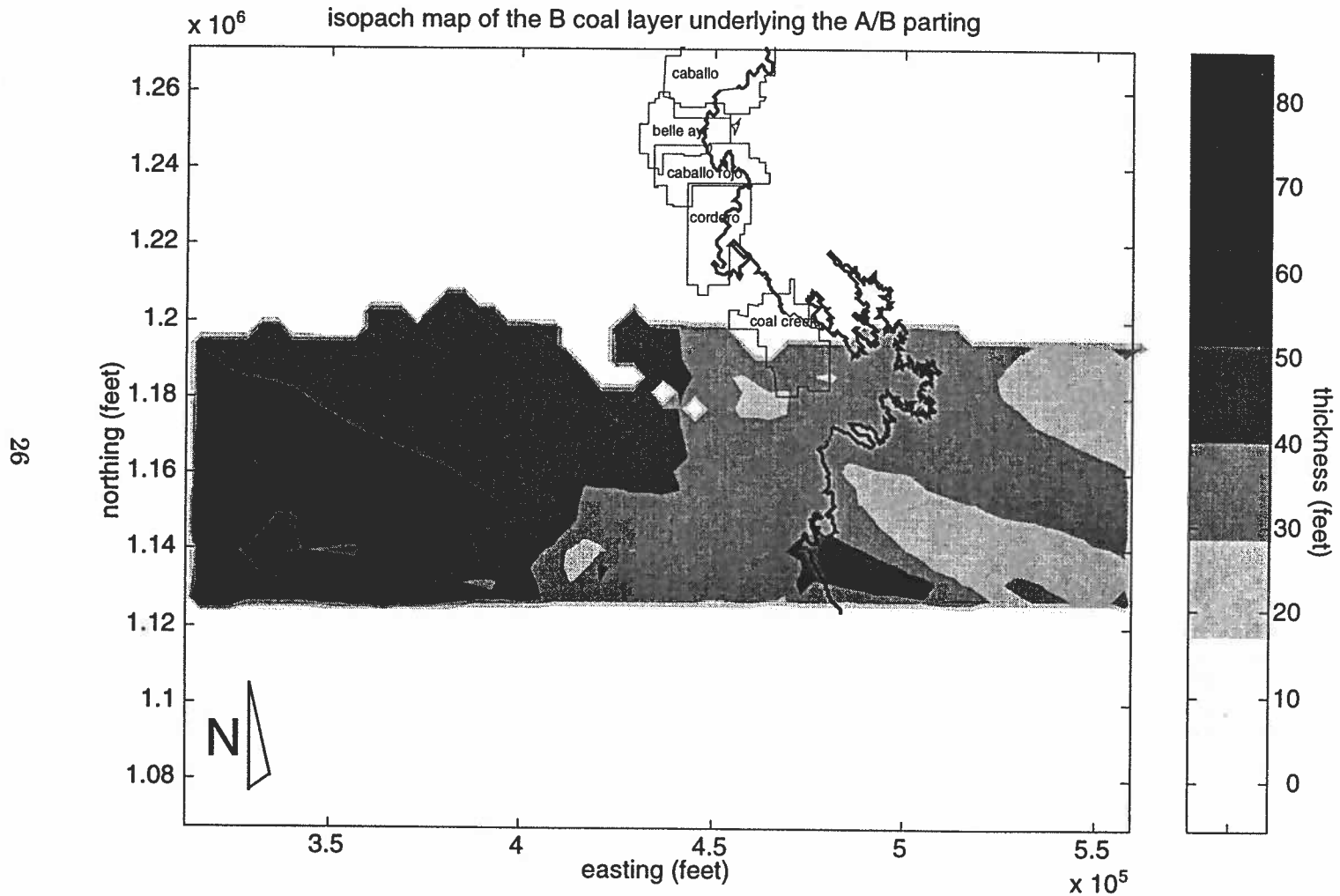


Figure 2-6. Isopach map of the A coal layer. Cropline and mine permits shown for orientation.



26

Figure 2-7. Isopach map of the B coal layer underlying the A/B parting. Cropline and mine permits shown for orientation.

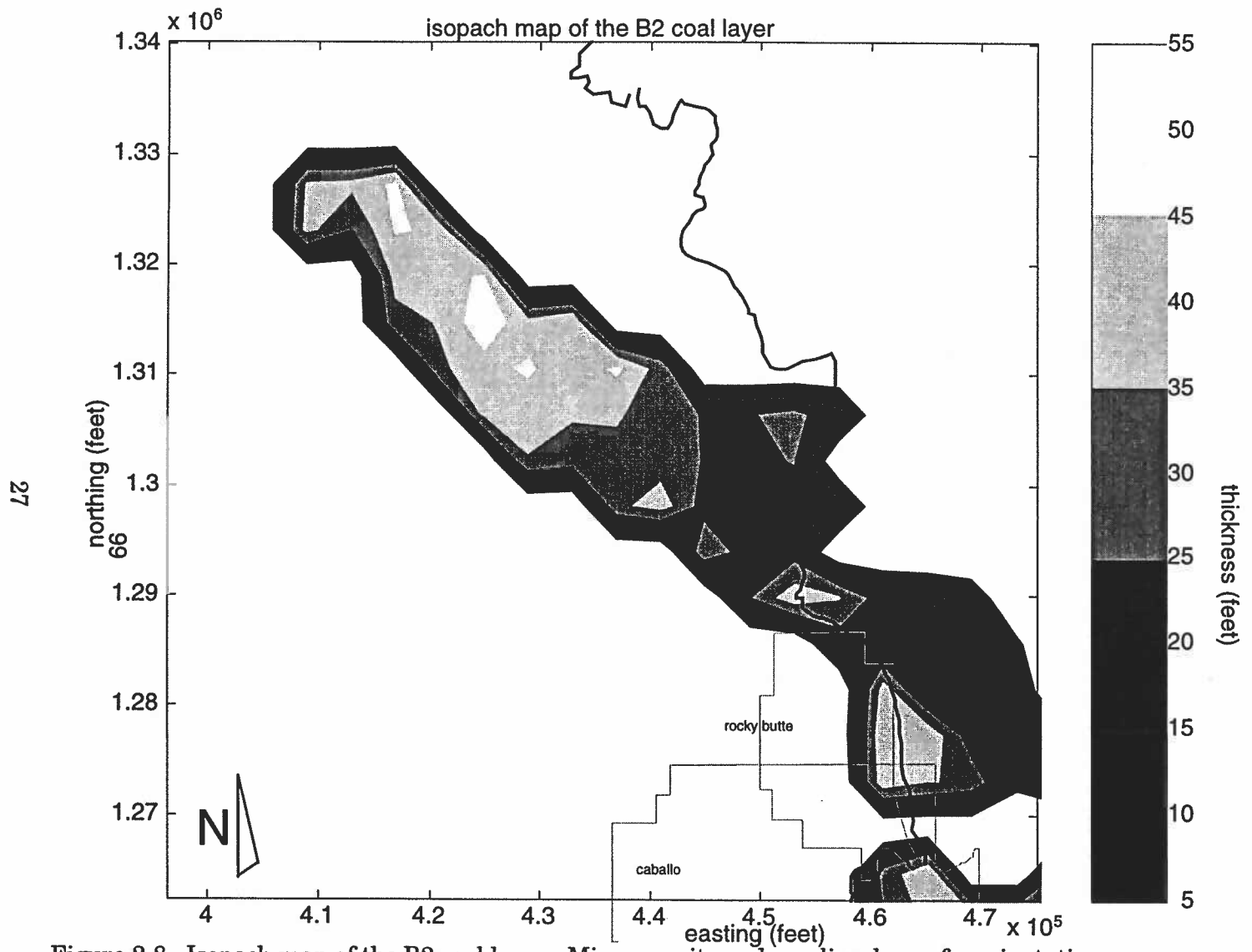


Figure 2-8. Isopach map of the B2 coal layer. Mine permits and croplines shown for orientation.

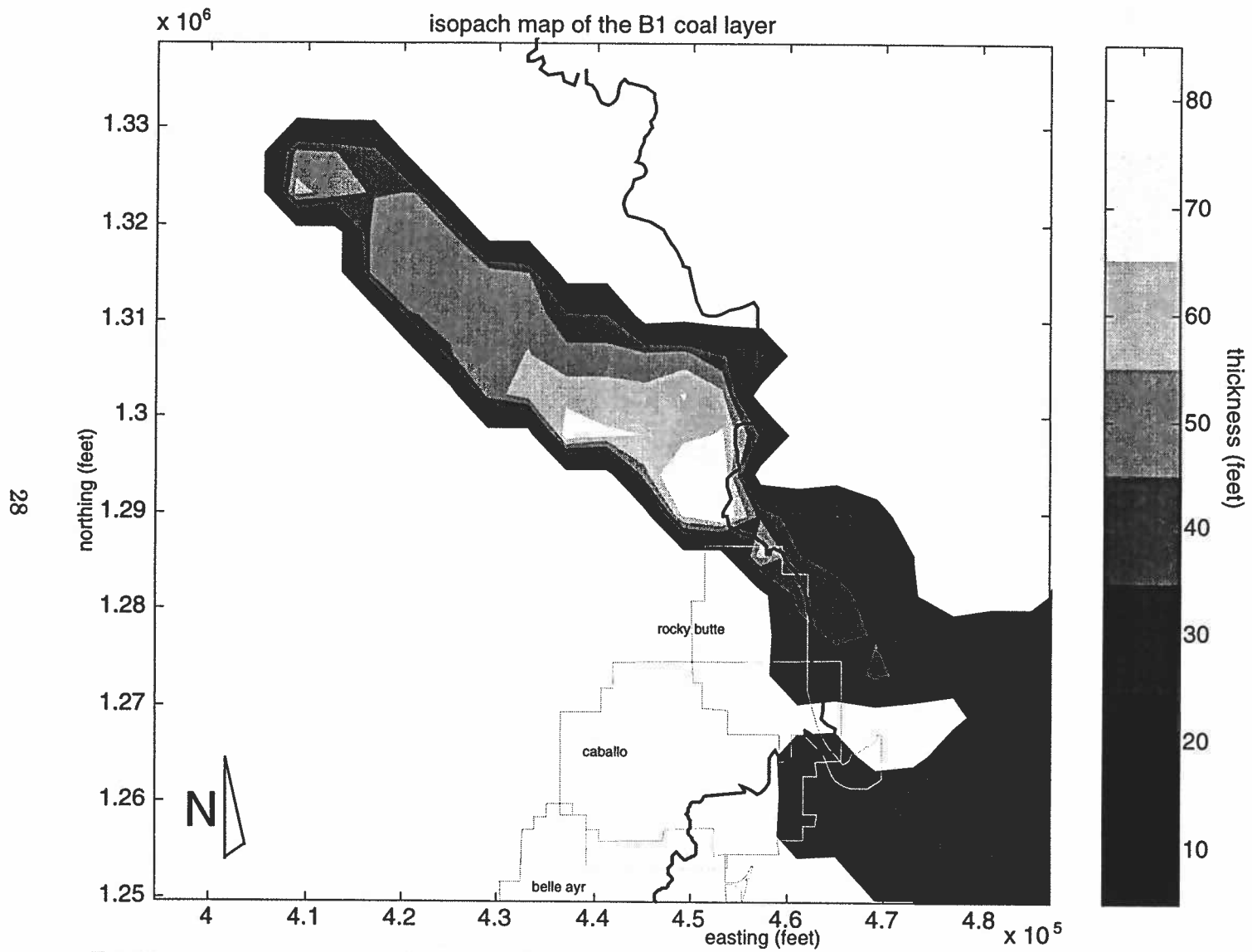


Figure 2-9. Isopach map of the B1 coal layer. Mine permits and croplines shown for orientation.

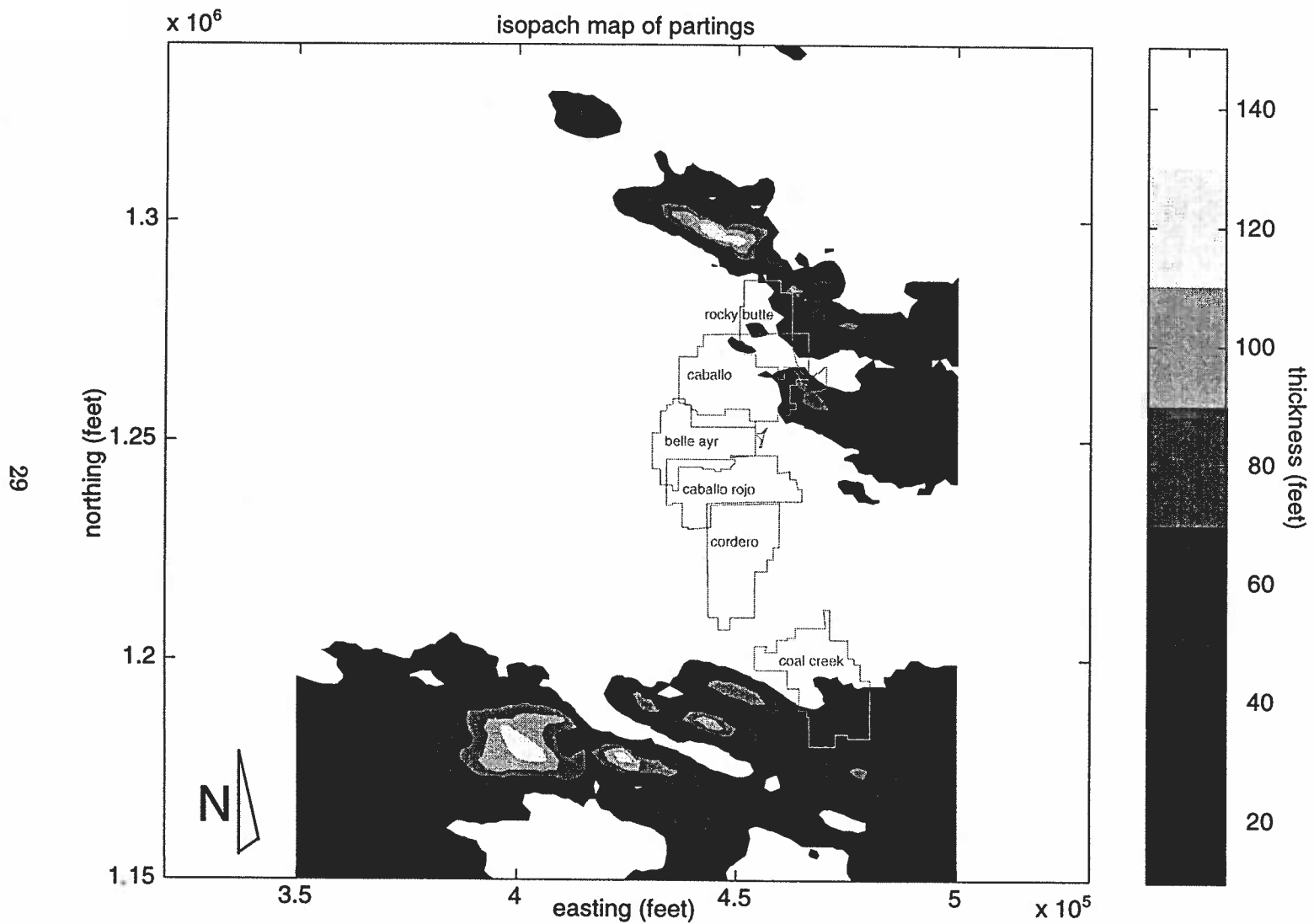


Figure 2-10. Isopach map of the partings in the coal. Mine permits shown for orientation.

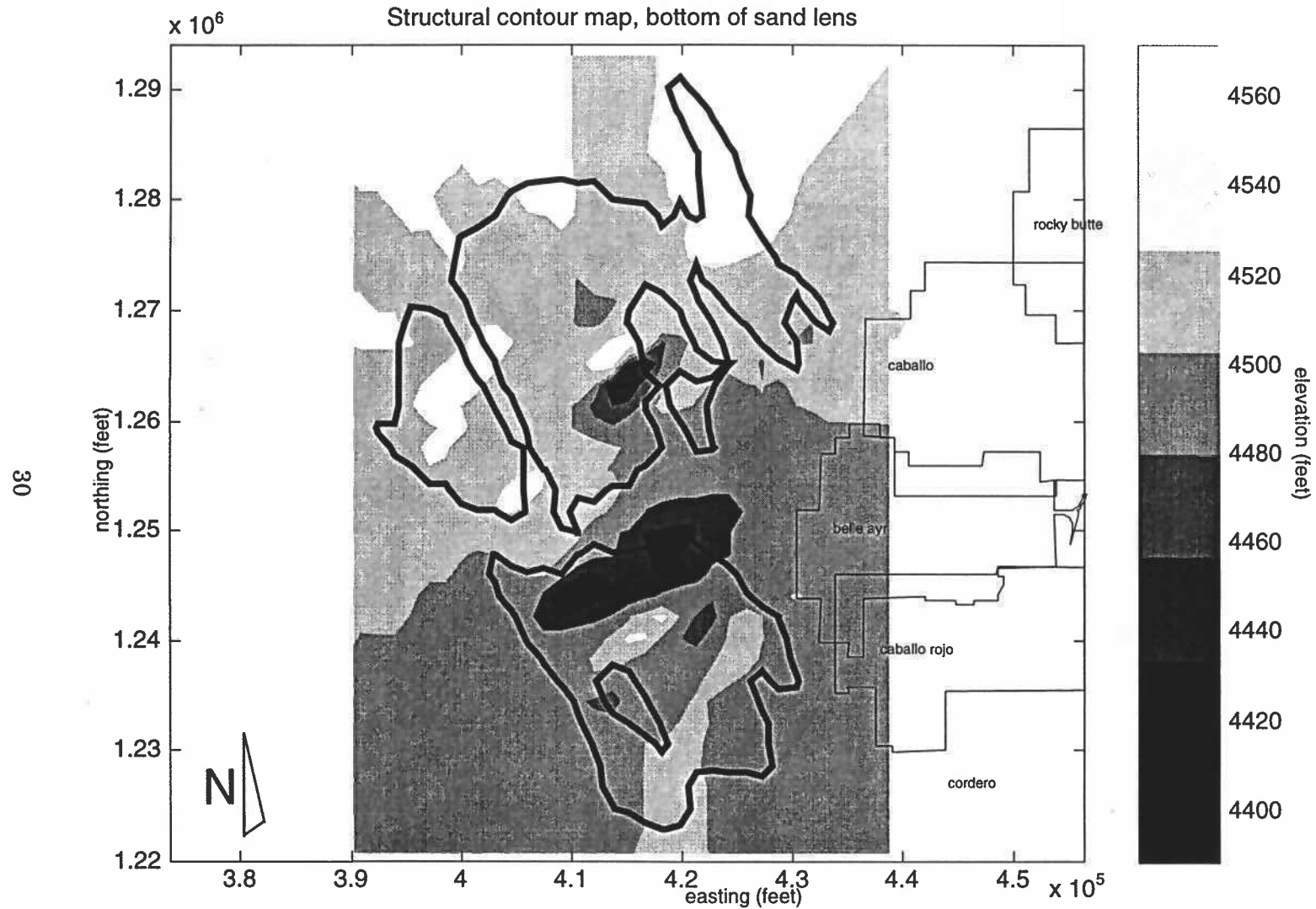


Figure 2-11. Structural contour map, bottom of the Wasatch sand lens. Mine permits shown for orientation. Surface is only defined within 20 foot isopach, shown in black.

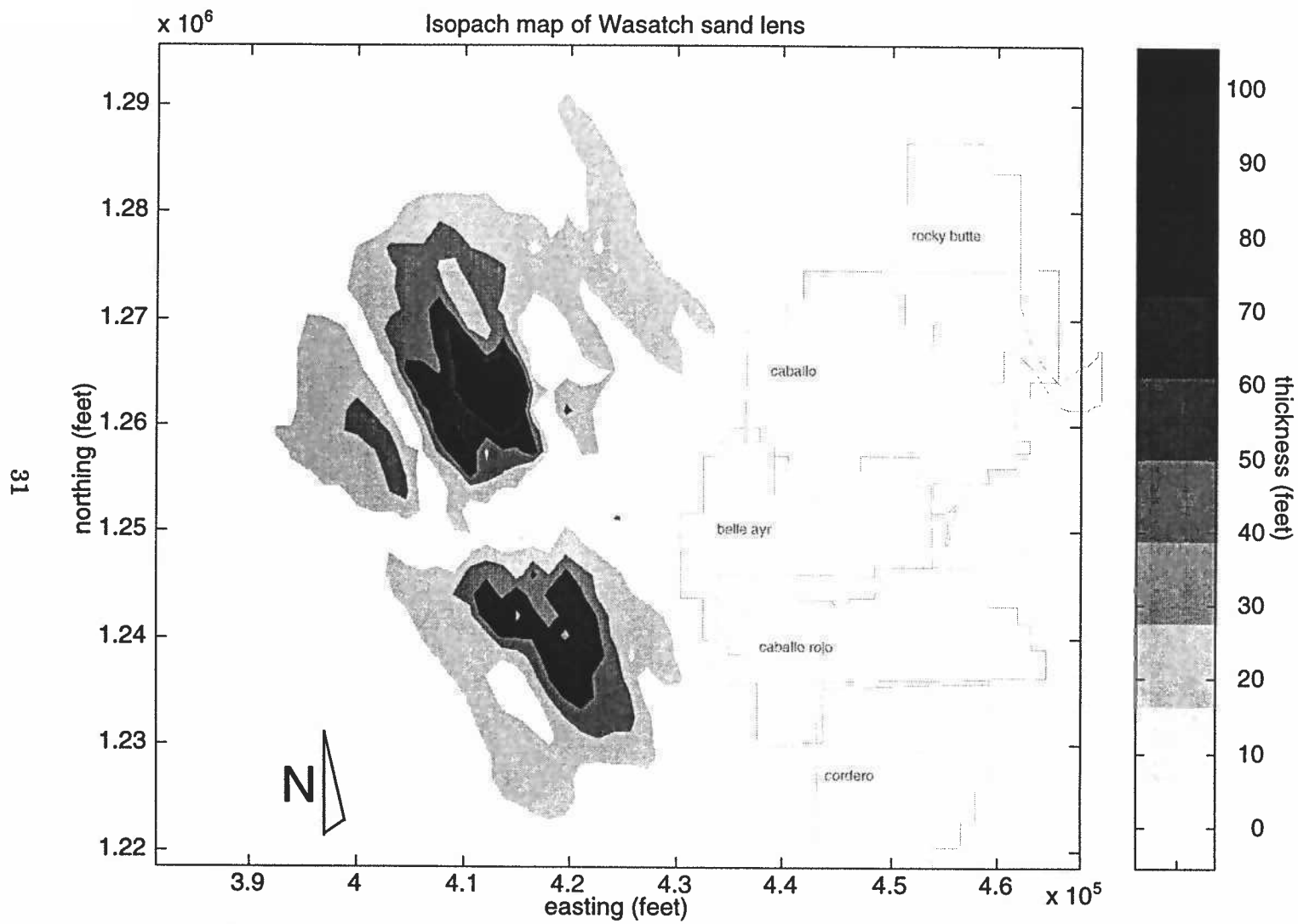


Figure 2-12. Isopach map of the Wasatch sand lens. Mine permits shown for orientation.

(Figure 2-13). The entire model grid covers an area of 3576 square miles. The row spacing varies from 1100 to 31818 feet. The column spacing varies from 1500 to 27998 feet. The most refined grid cells are 1100 feet by 1500 feet and cover an area of 1.65e6 square feet, 37.88 acres. The least refined grid cells are 31818 by 27998 feet and cover an area of 8.91e8 square feet, 20451 acres, 32 square miles. The refined area of the grid is designed to incorporate all of the stress locations and the extent of the Wasatch Sandstone Lens aquifer. The corners of the grid are, from upper right going clockwise, 528751E 1439641N, 641232E 1130602N, 356481E 1026961N, 244000E 1336000N. The grid covers T45N through T50N and R71E through R77E.

IV.2. Model Layers

The model consists of two explicit layers and one implicit layer as previously described. The thickness' of the layers were linearly interpolated from the stratigraphic model to the nodes of the modflow grid. The top of the coal layer was used as a bench-mark for the construction of the layers of the model. Thickness' were manipulated arithmetically to calculate the tops and bottoms of the model layers.

In order to minimize computer processing time and model setup time, the coal was modeled as one layer. To the south, the parting coal is located in unrefined grid cells, in an area of sparse hydraulic conductivity and starting head data. Lumping the parting and coal together was simply a matter of adjusting the hydraulic conductivity of the parting material. Since the partings consist of shale, sandy and silty shale, carboniferous shale, minor interbedded sandstone and some coal, the increase in hydraulic conductivity was less than one order of magnitude. Presently there is only indirect evidence that this adjustment is indeed incorrect. The lumping of the northern parting and coal together may be more troublesome since the parting is contained partially within fully refined cells. However, in a model of this coarseness such a simplification is necessary, and may not affect the outcome unduly.

In addition, were the coal to be modeled as two coal layers separated by parting material, starting heads would be necessary for each layer. This level of data density is simply unattainable at present.

IV.3. Model Modifications

The dip of the Wyodak coal caused some problems in reference to the discretization of the coal into the model grid. The dip of the three western-most rows had to be decreased in order

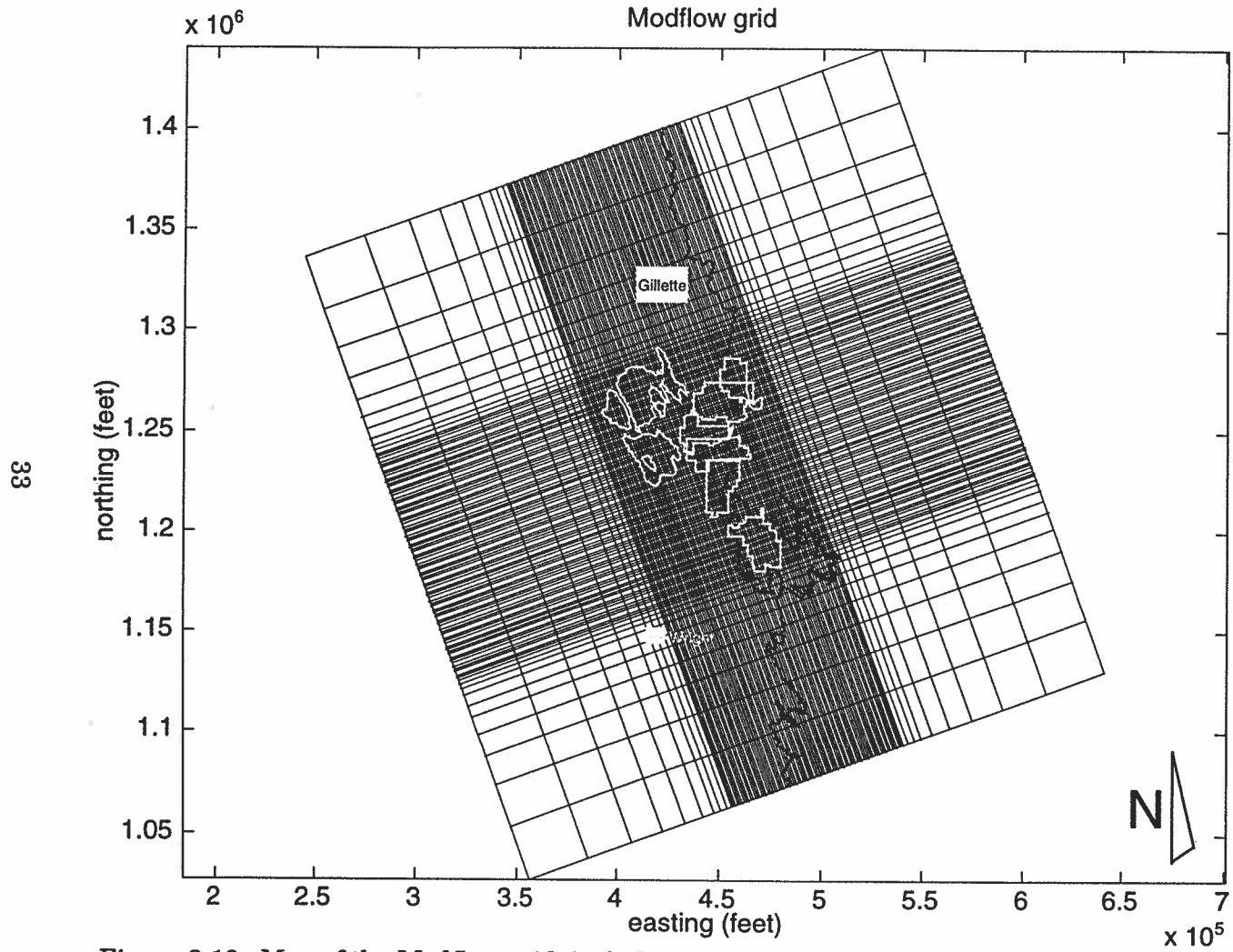


Figure 2-13. Map of the Modflow grid, including the locations of the mines, cities, Wasatch sand lens, and cropline.

to eliminate discontinuities between adjacent cells. Much more of the sand lens layer had to be modified in this fashion. However, the modification of the sand lens layer was confined to unrefined cells and did not affect the sand lens itself. Modification of the coal layer can further be justified by realizing that the axis of the Powder River Basin is in the vicinity of the western edge of the study area. Therefore, the dip of the coal must be reduced and eventually reversed in this area.

V. Setup of specific model inputs

V.1. Top and bottom of coal

The top of the coal was kriged as listed in table 2-2 (Figure 2-14). Since the coal model covered a smaller area than the modflow grid, it was necessary to expand the top of coal surface into a portion of the modflow grid with the trend surface of the top of coal. The same procedure was used to krig the bottom of the coal seam and extend it to fill the study domain (Table 2-2). The thickness of the coal was then calculated arithmetically from the top and bottom surfaces (Figure 2-15).

V.2. Top and bottom of sand lens layer

The bottom of the sand lens layer was kriged (Table 2-2) and retained within a rectangle which encompassed the sand lens 20 foot isopach. The sides of the rectangle were made up of rows 85 and 48 and columns 10 and 51 (Figure 2-16). The mean thickness of the implicit confining layer within this rectangle is 364 feet. Since the top of the coal layer was the benchmark for all other structural surfaces, the thickness of the confining layer was added to the top of the coal to generate the bottom of the sand lens layer. The thickness of the confining layer was set to the calculated values within the rectangle shown in figure 2-16. The northern boundary of the rectangle was replicated to fill the rest of the columns to the north. The same procedure was applied to the southern boundary. The thickness of the confining layer was set at 500 feet at the western edge of the model grid. A linear interpolation was made between the values in row 85 and row 100; the western edge of the model. The thickness of the confining layer was set to zero along the cropline. Thickness values between row 48 and the crop line were linearly interpolated along columns (Figure 2-17).

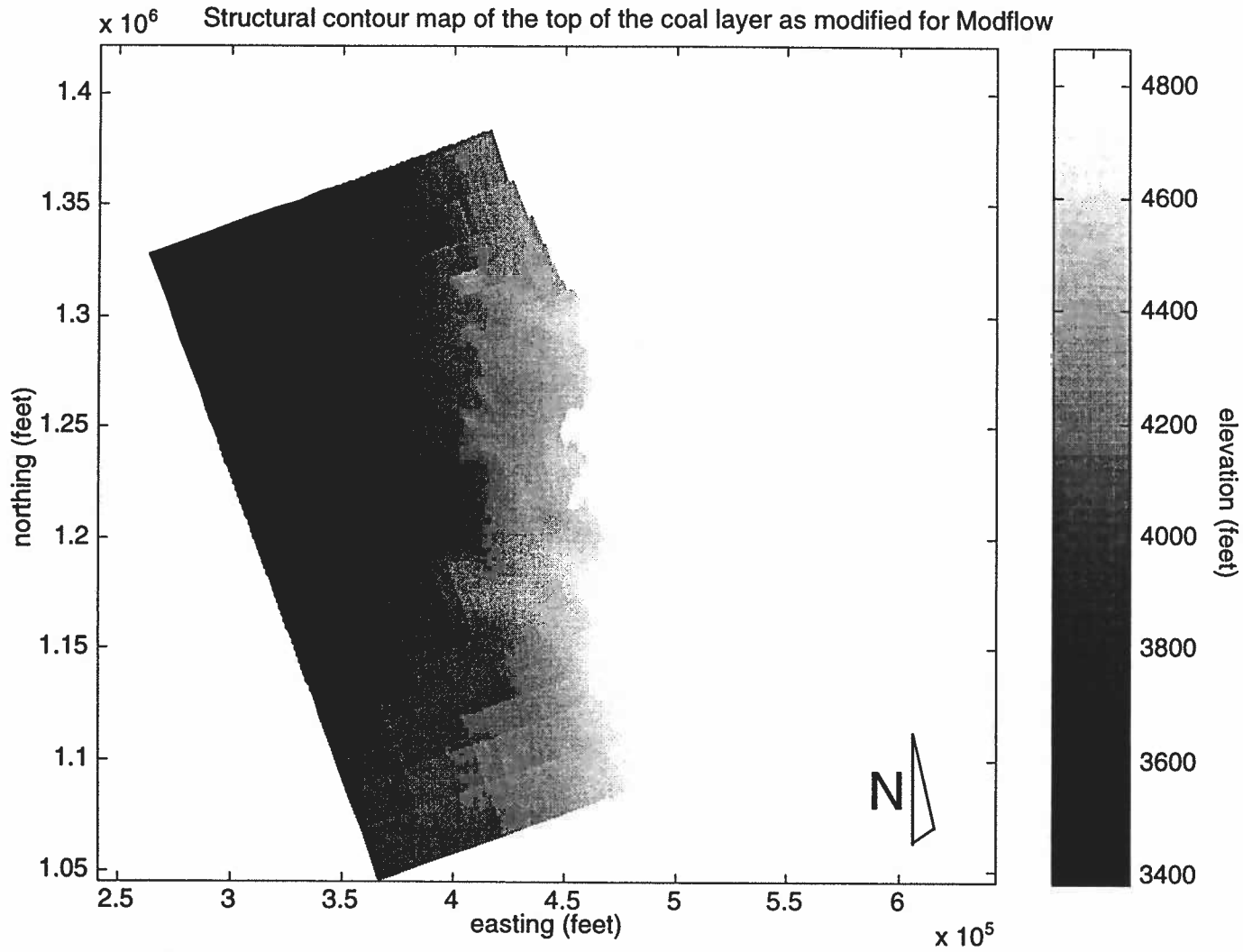


Figure 2-14 . Structural contour map of the top of the coal layer as modified for Modflow.

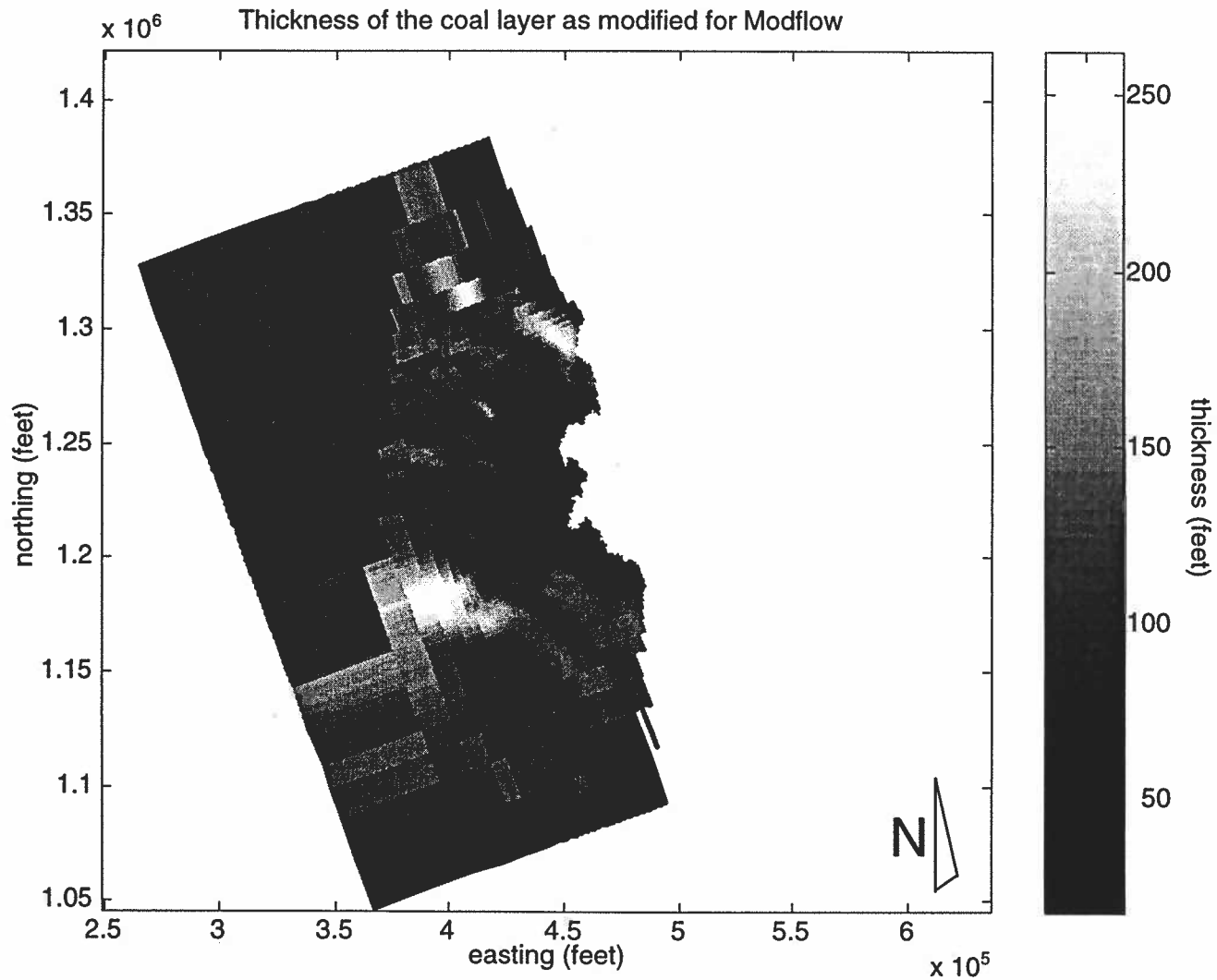


Figure 2-15 . Isopach map of the coal layer as modified for Modflow.

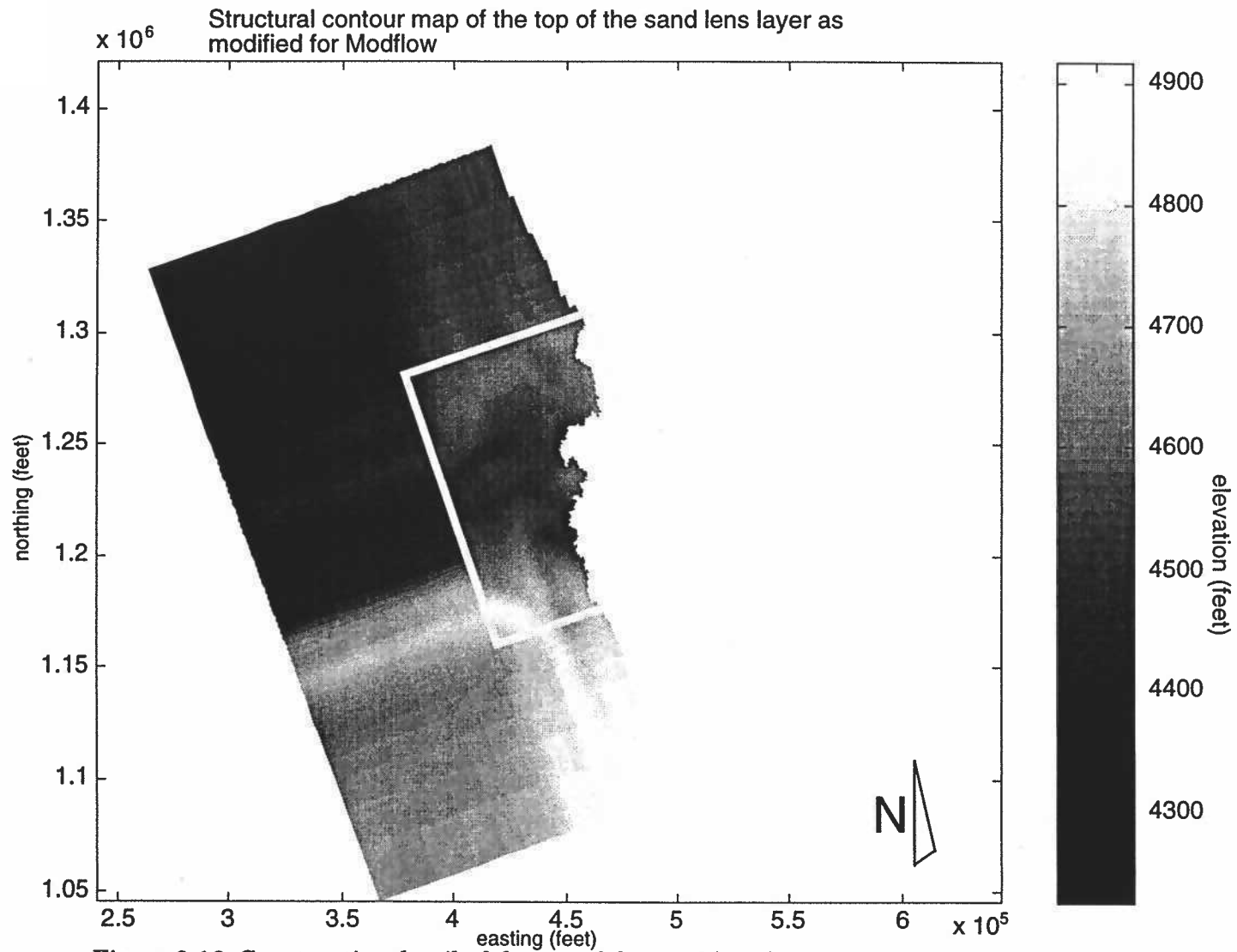


Figure 2-16. Construction detail of the top of the sand lens layer.

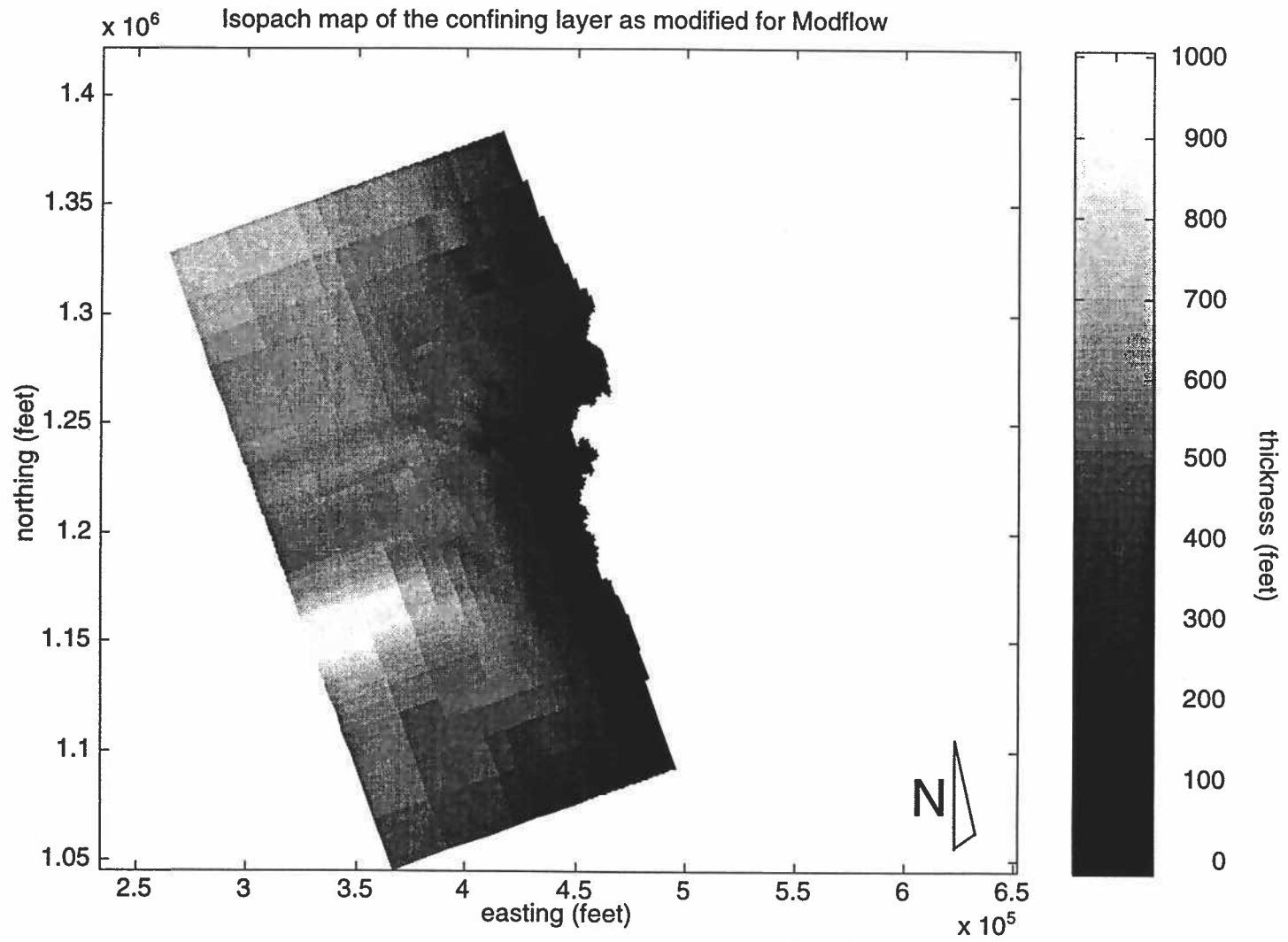


Figure 2-17. Isopach map of the confining layer as modified for Modflow.

The thickness of the sand lens layer was generated in similar fashion (Figure 2-18). The thickness of the entire layer was kriged, but only retained within the 30 foot isopach. The thirty foot isopach was used, in place of the twenty foot isopach, in order to create a thicker layer which would not be as susceptible to discontinuities due to the interaction of dip and discretization. From row 48 through 100, outside of the thirty foot isopach, the thickness of the sand lens layer was set to 30 feet. the thickness of the sand lens layer was set to zero at the crop line. Values between row 48 and the cropline were linearly interpolated.

The bottom of the sand lens layer was then determined by adding the thickness of the confining bed to the top of the coal. The top of the sand lens layer was determined by adding the thickness of the sand lens layer to the calculated bottom of the sand lens layer.

V.3. IBOUND arrays

IBOUND arrays for this model consist of 100 by 100 arrays of positive or negative numbers or zeros which indicate whether the model cells are active, specified head or inactive respectively. Specified head cells maintained the same head value throughout the simulations. An IBOUND array for the coal layer (Figure 2-19) was generated by overlaying the modflow grid onto maps of the cropline and clinker distribution (Hefferin 1997), and qualitatively determining which cells were contained within coal, clinker, or other material east of the cropline. The IBOUND array for the sand lens layer included all of the above in addition to the sand lens itself (Figure 2-20).

V.4. Hydraulic conductivity arrays

The IBOUND arrays were refined beyond what was absolutely necessary in order to be used as tools for the distribution of hydraulic conductivity (K) values in the model. East of the full seam crop line, clinker cells were distinguished from cells of other material, so that their K values could be different. The sand lens itself was distinguished from undifferentiated Wasatch in this fashion. In addition, border cells were distributed around the sand lens and between the crop line and the rest of the model in order to allow the K values to step down more gradually in the interest of numerical stability. The starting K arrays are shown in figures 2-21 and 2-22.

The values used to generate these arrays were calculated as follows. The mean of 46 coal hydraulic conductivity aquifer tests was calculated to be 3.5 feet/day. This value was accepted as the effective K for the coal. Since the anisotropy of the coal is known to be 2:1, the K value was

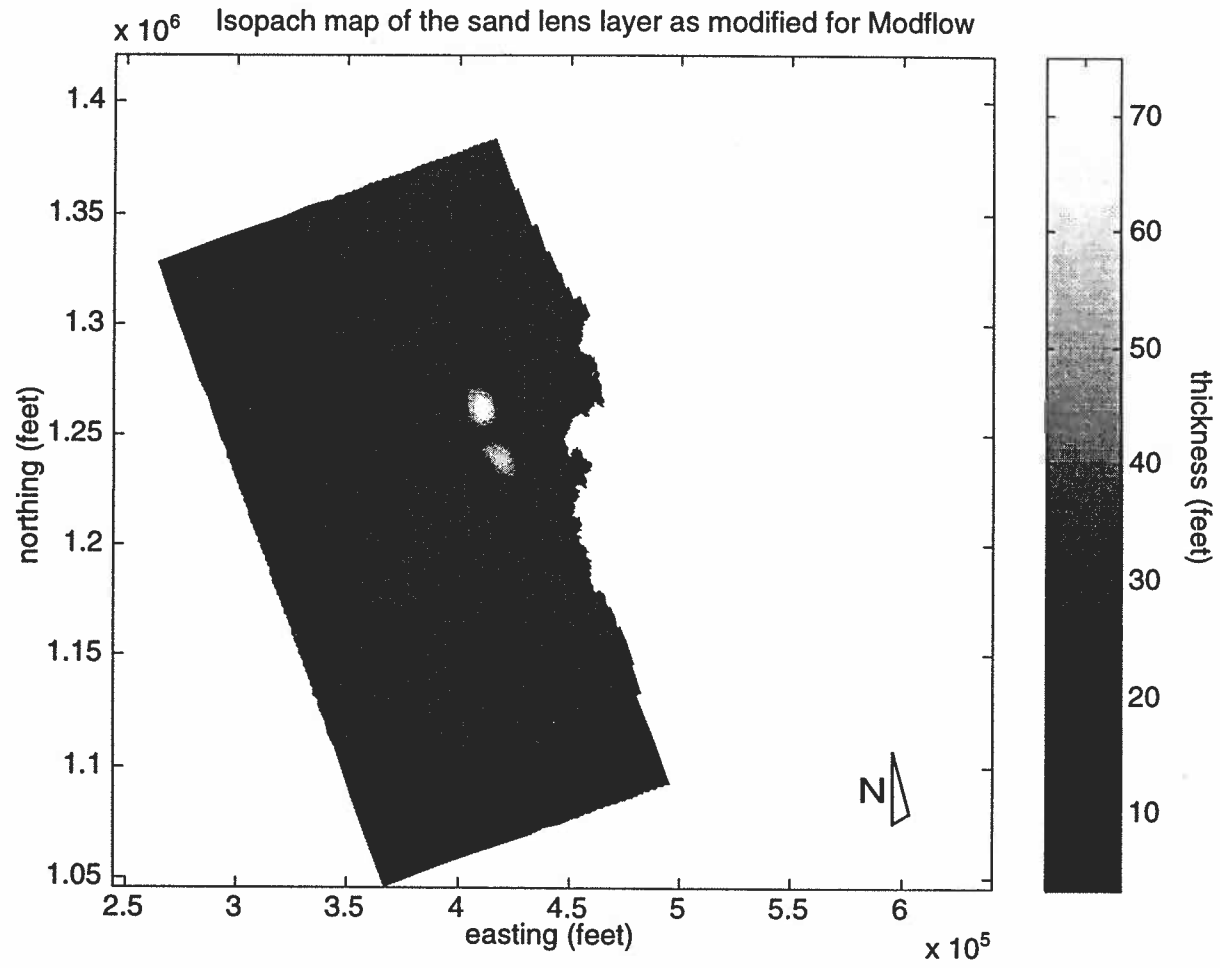


Figure 2-18. Isopach map of the sand lens layer as modified for Modflow.

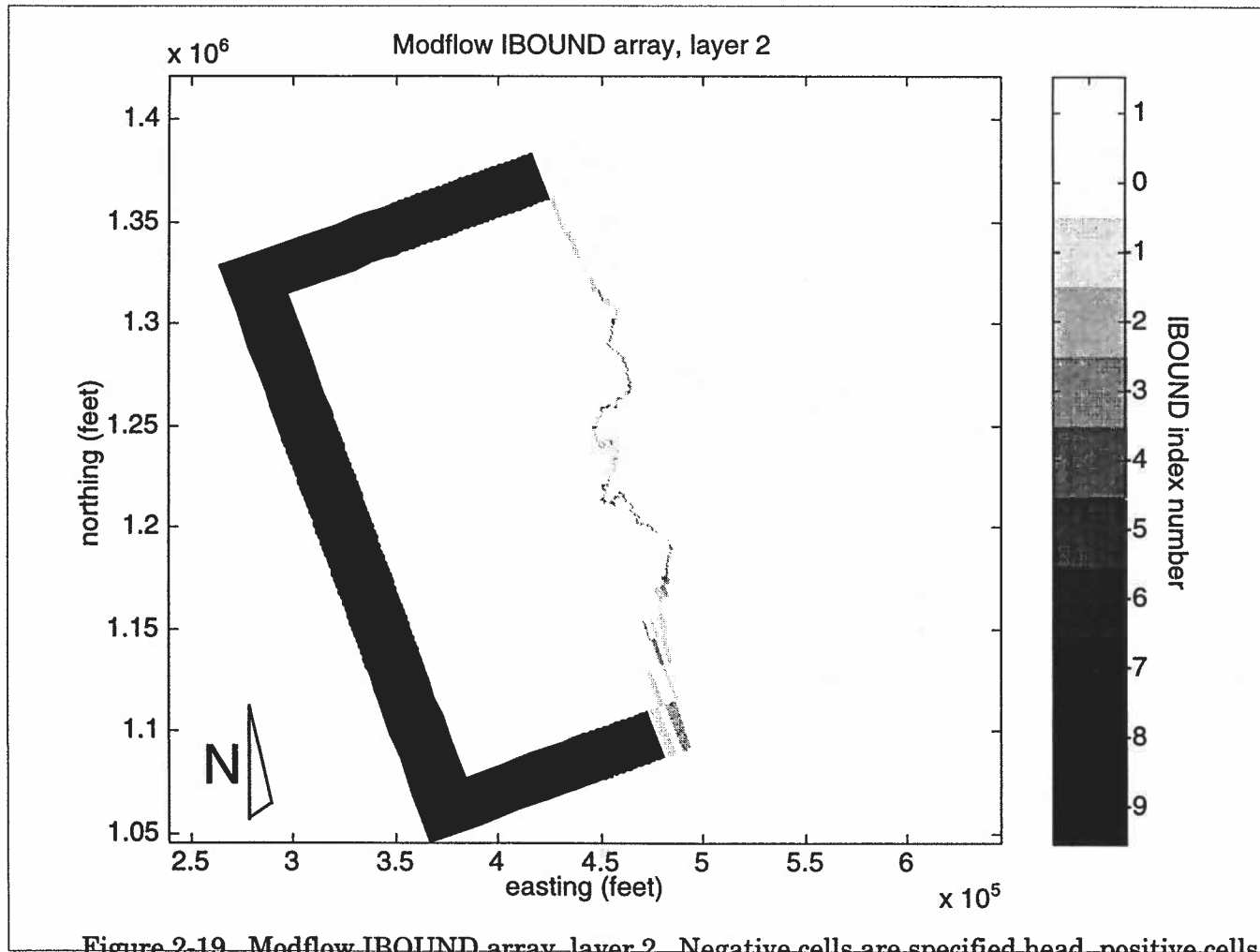


Figure 2-19. Modflow IBOUND array, layer 2. Negative cells are specified head, positive cells are active and zero indicates inactive cells.

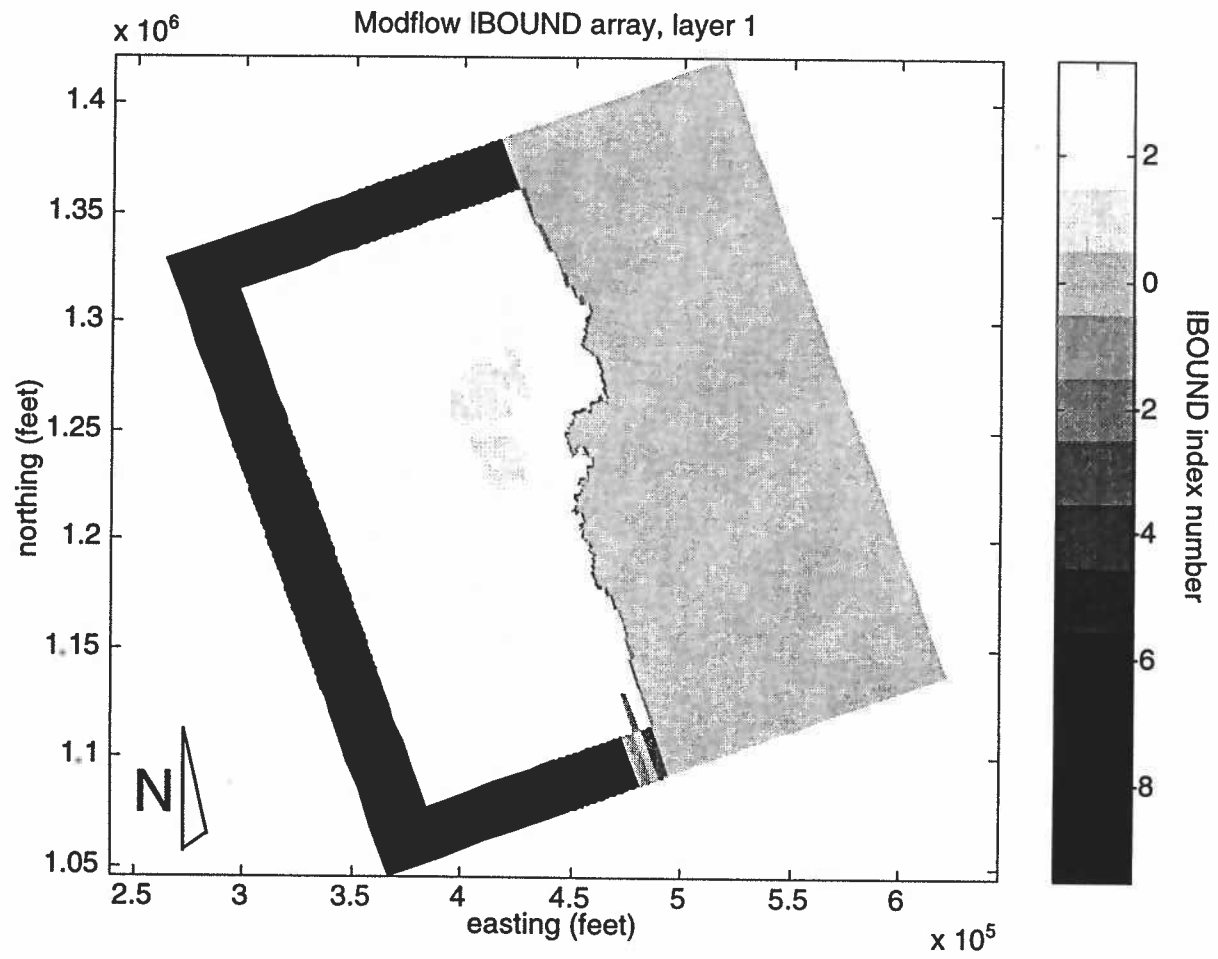


Figure 2-20. Modflow IBOUND array, layer 1. Negative cells are specified head, positive cells are active and zero indicates inactive cells.

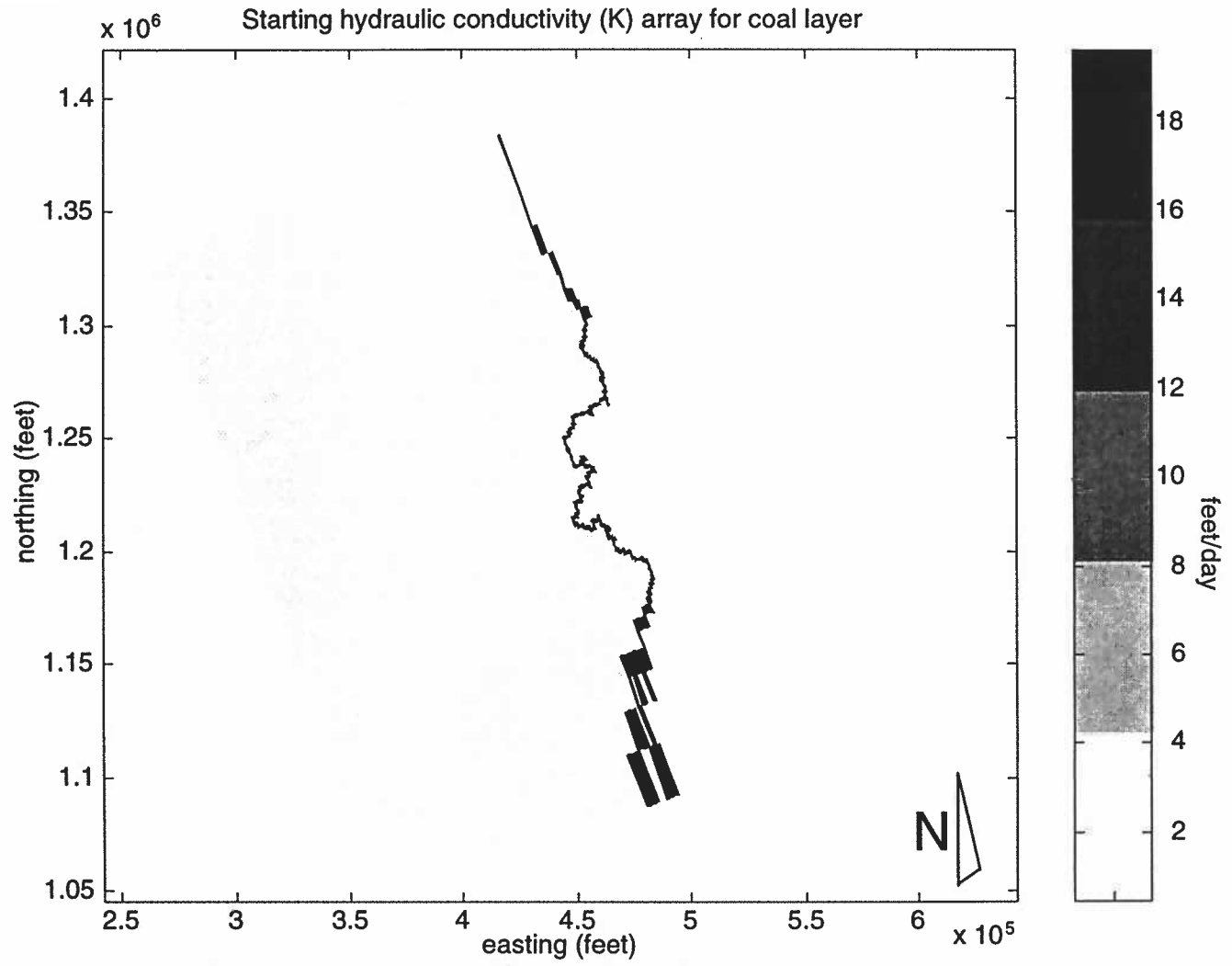


Figure 2-21. Hydraulic conductivity (K) array for coal layer as used in Modflow. Clinker cells, with a K of 12685 feet/day, are not shown on this figure, but can be seen on figure 2-19 represented by -1.

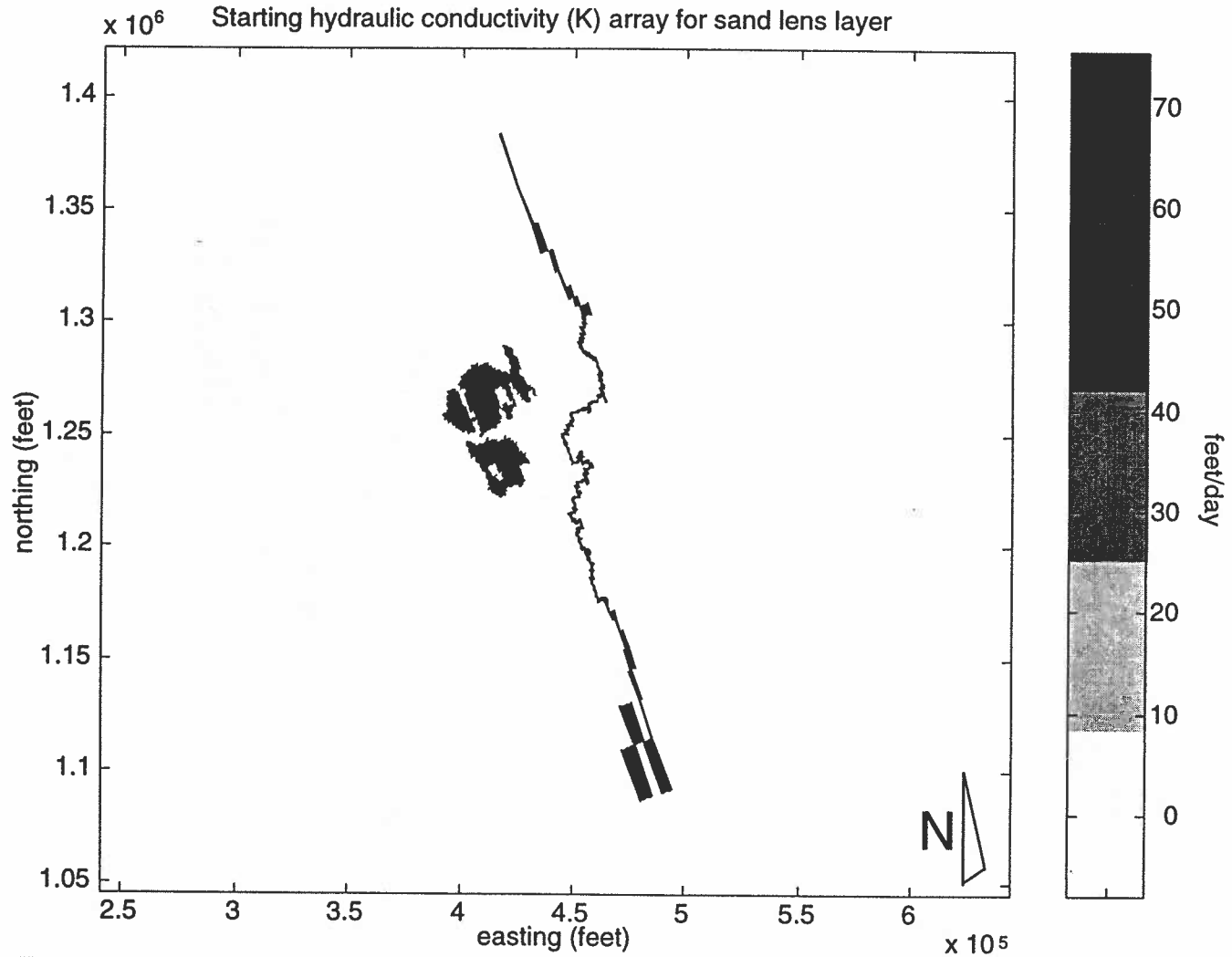


Figure 2-22. Hydraulic conductivity (K) array for sand lens layer as used in Modflow. Clinker cells, with a K of 12685 feet/day, are not shown on this figure, but can be seen on figure 2-20, represented by -1.

resolved into vectors. The resulting K along columns was 2.4 feet/day. The K value for the Wasatch Formation outside of the sand lens was calculated by taking the mean of 46 aquifer tests, resulting in a value of 0.35 feet/day. This value was also used for the confining layer in the calculation of VCONT (section V.5.). The K of the sand lens itself could only be determined qualitatively from lithology information. A value of 50 feet/day, which represents a fine-grained, moderately sorted sand was used. A value of 12685 feet/day, which is the mean of 15 aquifer tests in the clinker, was used as the K value of the clinker.

V.5. VCONT

The VCONT, or vertical hydraulic conductivity divided by thickness, array was generated using the thickness' of the sand lens layer, coal, and confining bed. In addition, vertical hydraulic conductivity was approximated as 0.1 times the horizontal hydraulic conductivity (Anderson 1993). VCONT was calculated by,

$$vcont = \frac{1}{\left(\left(\frac{dzu}{kzu} \right) + \left(\frac{dzl}{kzl} \right) + \left(\frac{dzc}{kzc} \right) \right)} \quad (\text{McDonald and Harbaugh, 1988})$$

where,

dzu=0.5*sand lens layer thickness,
 dzl=0.5*coal layer thickness,
 dzc=confining layer thickness,
 kzu=vertical hydraulic conductivity of the sand lens layer,
 kzl=vertical hydraulic conductivity of the coal layer,
 kzc=vertical hydraulic conductivity of the confining bed.

V.6. Coal starting head

The starting head in the coal layer was spline contoured through 80 data points using Earth Vision (Dynamic Graphics Inc., 1995). An effort was made to deterministically manipulate the splined coal head surface in the area of the cropline to conform with the conceptual head gradient model. The three other boundaries were modeled as specified head, with head values taken directly from the splined head surface.

V.7. Sand lens layer starting head

The starting heads for the sand lens layer began as a splined surface through 80 data points. Where the bottom of the sand lens layer was above this kriged surface the head was set to saturate the layer. Where the sand lens layer would have started out dry; where the top of the kriged head surface was below the bottom of the sand lens layer, the head was set to the top of the sand lens layer. In essence, much of the sand lens layer was constructed in the pursuit of numerical stability. This is justified given that where the sand lens itself is mapped, all data were honored, and since our interests lie only within the sand lens itself for this layer.

V.8. Recharge

According to Marston (1990), the Powder River Basin receives 0.0029 feet of precipitation per day. It is assumed that 0.02% of this precipitation infiltrates into the groundwater system (Peacock, 1997a). This calculates to $6.00E-7$ feet/day of vertical recharge, which is applied as a constant over the entire model domain.

V.9. Calibration points

In order to calibrate the early runs of the model, water level data from 55 monitoring wells was used. These wells were coal mine monitoring wells and were used to monitor drawdown over time in the vicinity of the mines. It was determined that these wells had the best observations of the premining potentiometric surface available. In addition, the two BLM monitoring wells were included to calibrate to the sand lens aquifer.

Chapter 3 Calibration of the conceptual model.

I. Introduction

In an attempt to improve the calibration of the steady-state flow model with the set of 55 coal monitoring wells, four progressively more complex scenarios or conceptual models were tested. The four scenarios were: 1) homogeneous coal with no transition zone between the coal and the crop line; 2) homogeneous coal with a homogeneous transition zone all along the cropline; 3a) homogeneous coal with a heterogeneous transition zone; 3b) homogeneous coal with a heterogeneous transition zone and only clinker cells active east of the cropline. The attempt was to alter the concept of how the parts of the natural system, about which the least is known, behave, in a logical, step-by-step manner, until the model agreed with the data that was collected.

As constructed, the partial differential equation (PDE) being solved in the steady-state flow model is the Poisson elliptical PDE with Dirichlet boundary conditions,

$$\frac{\partial^2 h}{\partial x^2} + \frac{\partial^2 h}{\partial y^2} = -\frac{R(x,y)}{T} \quad (\text{Wang and Anderson, 1982})$$

where

h = hydraulic head (feet)
T = transmissivity (square feet/day)
R = recharge (cubic feet/day).

The hydraulic head at all points on the boundary has been specified. In relation to this PDE, it can be said that the solutions of this equation can not achieve a strong relative maximum or minimum in the interior of the domain, given that vertical recharge is a constant over the entire domain (Garabedian, 1964). Hence, the maximum and minimum of the solution are dictated by the choice of heads on the boundary and occur on the boundary. This is highly significant since in many flow models of this type and size, boundary heads are one of the least known parameters. In this case the heads are fairly well established on the eastern boundary but known only poorly on the western boundary. The heads on the western boundary have been set up to

conform to the conceptual model, i.e. hydraulic heads somewhere between the top of the coal and the elevation of the land surface, with a gradient to the northwest.

II. Method

A discussion of Modflowp input is necessary at this point. Modflowp utilizes zone arrays to control the distribution of given parameters. These arrays consist of zones, each of which is made up of repetitions of a unique positive number. Each unique number is assigned a parameter value. The zone array for case one is represented graphically in figure 3-1. In addition, Modflowp allows for manipulation of the following parameters of interest in this model: 1) head on the boundary (CH); 2) hydraulic conductivity (K); and 3) vertical hydraulic conductivity of a confining bed (KV). CH consists of a single elevation value, which can be estimated, and a gradient along a row, which is fixed. At this stage CH and K will be manipulated in layer 2, the coal layer.

Case 1

Case 1 consists of homogeneous coal and no transition zone along the cropline (Figure 3-1). Models were run with coal K varying from 2 to 92 feet/day and CH varying from 4000 to 4160 feet (Figure 3-2). In measuring the quality of the fit between the predicted head and the observed head, two properties were observed: the budget discrepancy, reported in percent; and the mean residual, measured in feet. The budget discrepancy is calculated by taking water in minus water out, dividing by total quantity of water involved and multiplying by 100%. The mean residual is a measure of the bias in the model. A positive mean residual indicates that the calculated head is below the observed head. A negative mean residual indicates that the calculated head is above the observed head.

Case 2

Case 2 consists of homogeneous coal and an homogeneous transition zone (Figure 3-3). The transition zone is continuous along the entire length of the cropline and separates the coal from the clinker and non-clinker material east of the cropline. As described in chapter two, clinker has an elevated K value. Clinker formation does not cease cleanly along a line in space. There undoubtedly exists a zone between clinker, formed from fully combusted coal, and unaltered coal, in which the effects of combustion are only partial. It would be logical to assume

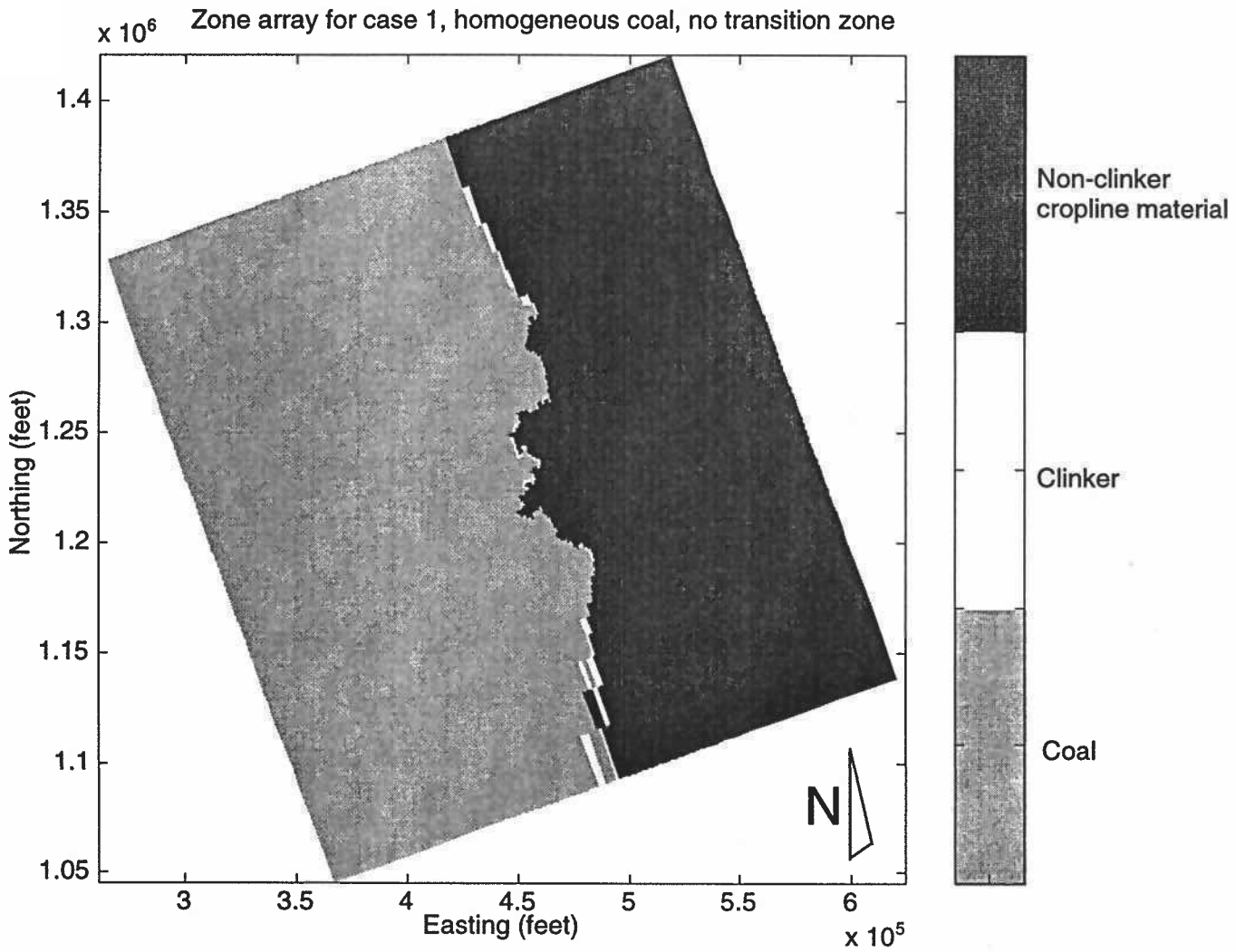
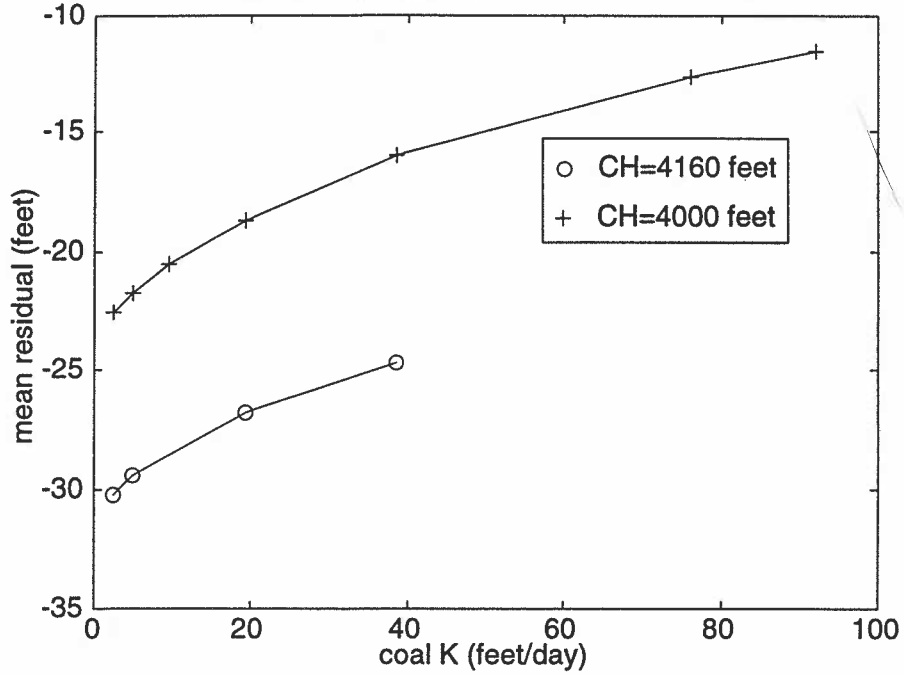


Figure 3-1. Zone array for case1, homogeneous coal, no transition zone.

coal K vs. mean residual, homogeneous coal, no transition zone, CH=4160 and 4000



coal K vs. budget discrepancy, homogeneous coal, no transition zone, CH=4160. and 4000.

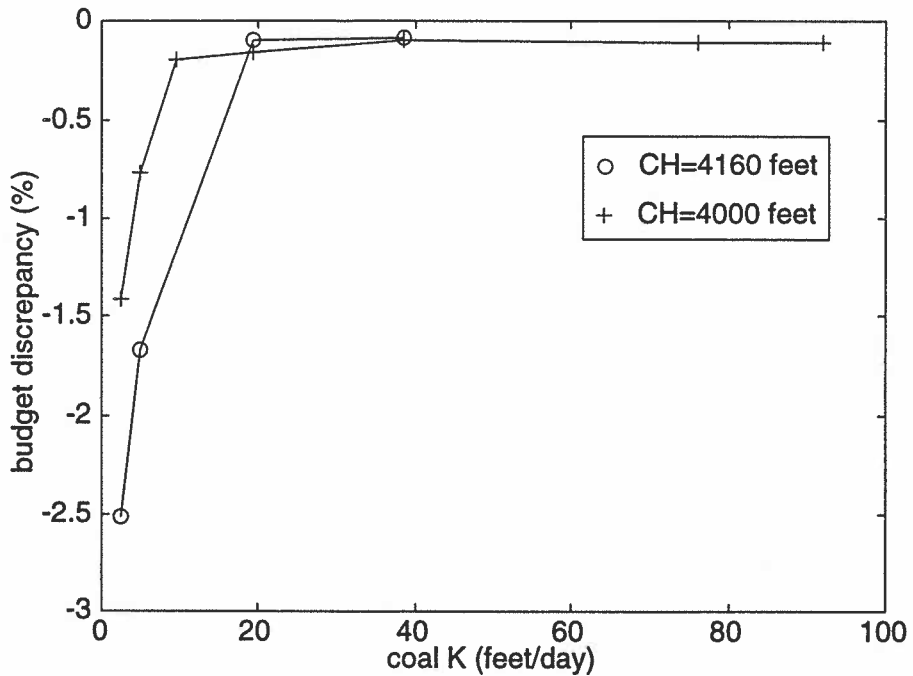


Figure 3-2. Case 1, homogeneous coal with no transition zone. Budget discrepancy and mean residual as a function of coal K. CH held constant at 4000 and 4160 feet.

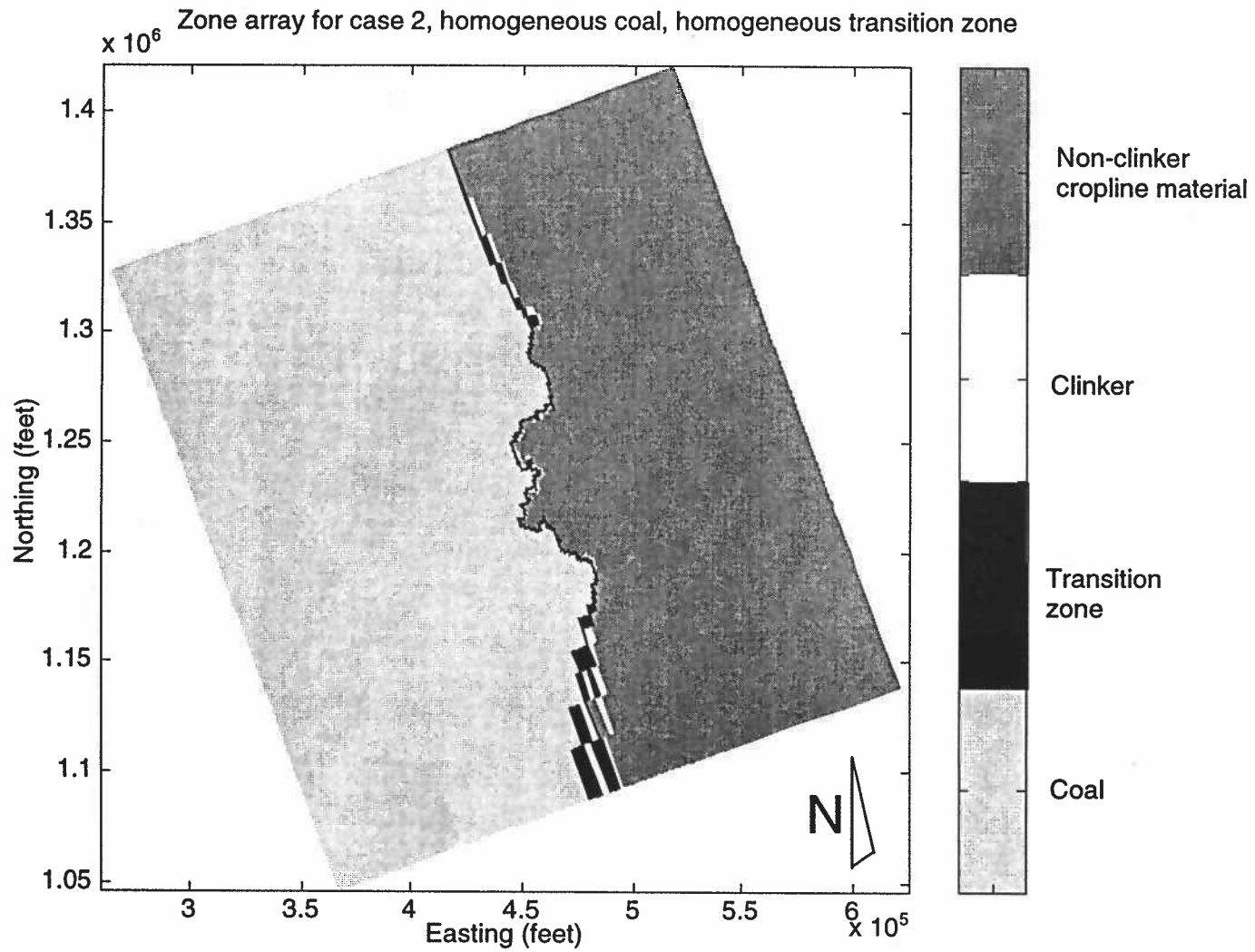


Figure 3-3. Zone array for case 2, homogeneous coal, homogeneous transition zone.

that this zone has K values between those of clinker and those of coal. Never the less, models were run with a full range of values for the transition zone, from lower than coal to somewhere between clinker and coal. CH was held fixed at 4160 feet.

Case 3a

Case 3a consists of homogeneous coal with a heterogeneous transition zone along the cropline. The transition zone was separated into five pods, each of which is adjacent to clinker cells on the cropline. All transition zone cells that were adjacent to non-clinker crop-line material were reverted to coal cells (Figure 3-4). CH was held fixed at 4160 feet.

Case3b

In an attempt to reduce the inflow of water from the east, the non-clinker cropline cells were inactivated (Figure 3-4). This model consists of homogeneous coal, heterogeneous transition zone, and inactive non-clinker cropline cells. Inactive cells are no-flow cells, and do not draw water into or out of the model. CH was held fixed at 4160 feet.

III. Results

Case 1

The results of case one are shown in figure 3-2 and table 3-1. The best fit at CH=4000 was with coal $K = 92$, resulting in budget discrepancy of -0.11% and mean residual of -11.5 feet, which indicates an overestimation of the potentiometric surface in the domain (Figure 3-2). The best fit at CH=4160 was with coal $K=38.4$, resulting in a budget discrepancy of -0.14% and a mean residual of -24.7 (Figure 3-2). This was sufficient for conclusions to be drawn; no further models were run for this case.

Case 2

The best fit scenario in case 2 occurred with coal $K=63$ feet/day and transition zone $K=16$ feet/day, resulting in a budget discrepancy of -0.10% and a mean residual of -5.39. Complete results are shown in figures 3-5 and 3-6 and table 3-2.

Case 3a

The lowest mean residual and budget discrepancy for this scenario occurred with a coal $K=63$ and a transition zone $K=2.4$, resulting in a budget discrepancy of -0.07%, and a mean residual of 0.776 feet. Complete results are shown in figures 3-7 and 3-8 and table 3-3.

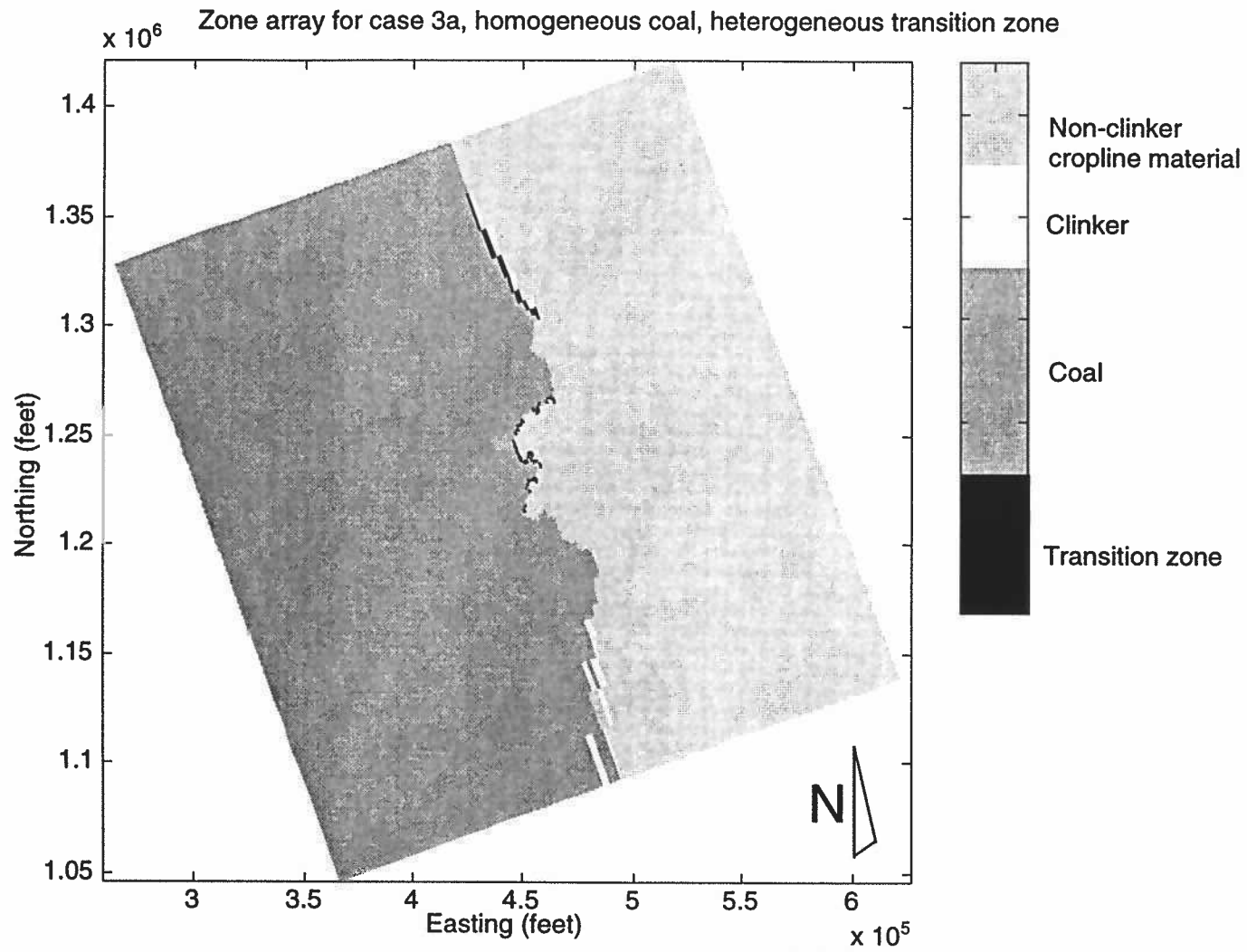


Figure 3-4. Zone array for cases 3a and 3b. In case 3b the zone labeled non-clinker cropline material is inactive.

Table 3-1. Results from chapter 3 case 1

simulation no.	coal K			sum of the squared residuals	mean residual (feet)	budget discrepancy	
	CH (feet)	(feet/day)	KV (feet/day)			%	rmse (feet)
1	4160	2.4	1.00E-11	145550	-30.2	-2.51	51.4
2	4477	2.4	1.00E-11	192330	-42.8	2.48	59.1
3	4160	4.8	1.00E-11	142210	-29.4	-1.67	50.8
4	4160	19.2	1.00E-11	132610	-26.8	-0.10	49.1
5	4160	38.4	1.00E-11	125390	-24.7	-0.09	47.7
6	4100	19.2	1.00E-11	127530	-23.8	-0.14	48.2
7	4050	19.2	1.00E-11	124210	-21.3	-0.15	47.5
8	4000	19.2	1.00E-11	121810	-18.7	-0.16	47.1
9	4000	38.4	1.00E-11	116000	-16.0	-0.10	45.9
10	4000	76.2	1.00E-11	111150	-12.6	-0.11	45.0
11	4000	92	1.00E-11	110270	-11.5	-0.11	44.8
12	3950	100	1.00E-11	110840	-8.0	-0.04	44.9
13	3950	150	1.00E-11	110930	-5.7	-0.01	44.9
14	4000	2.4	1.00E-11	131410	-22.6	-1.42	48.9
15	4000	9.6	1.00E-11	126590	-20.5	-0.20	48.0
16	4000	4.8	1.00E-11	129490	-21.7	-0.77	48.5

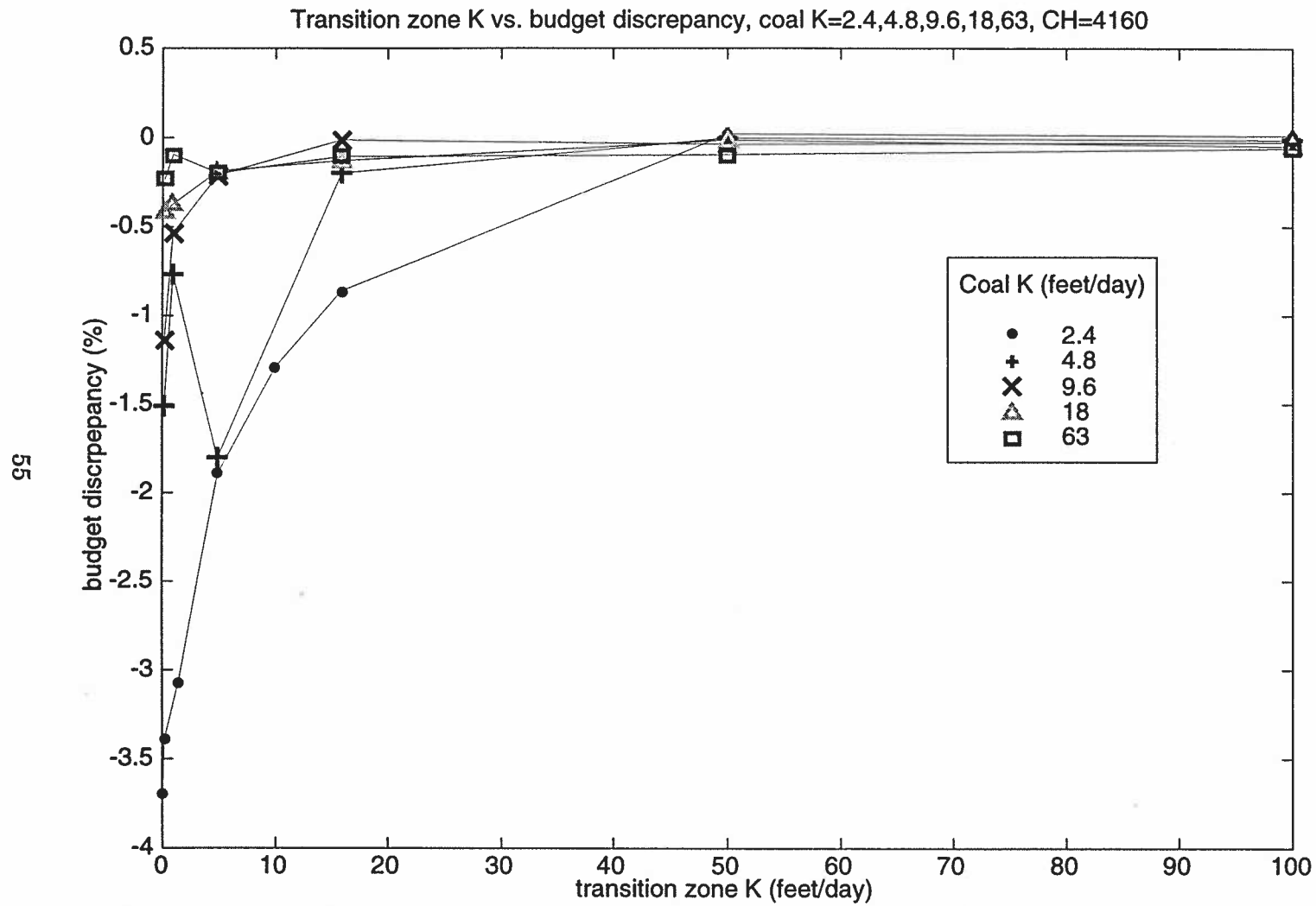


Figure 3-5. Case 2, homogeneous coal, homogeneous transition zone. Budget discrepancy as a function of transition zone K at given values of coal K. CH=4160.

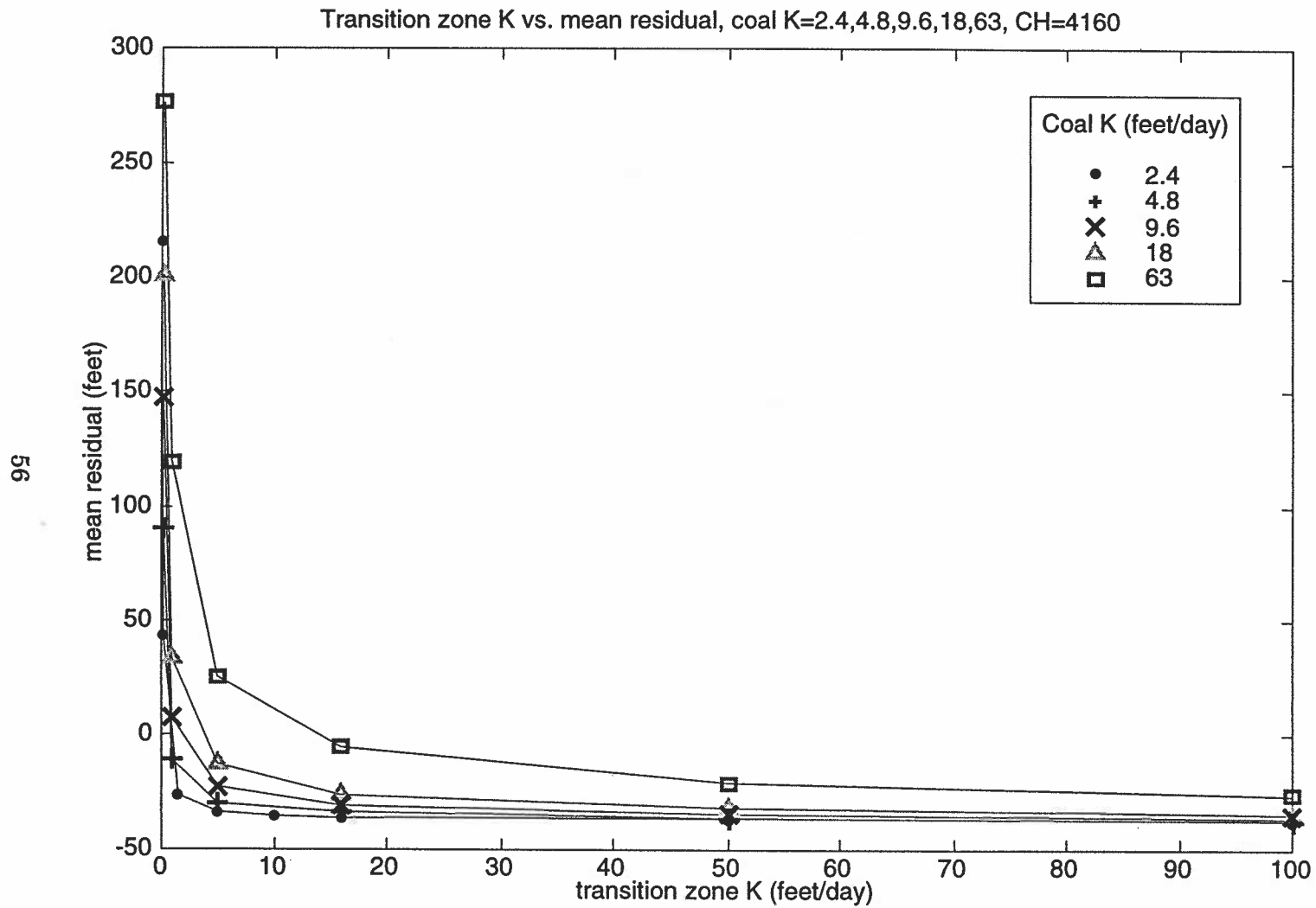


Figure 3-6. Case 2, homogeneous coal, homogeneous transition zone. Mean residual as a function of transition zone K at given values of coal K. CH=4160.

Table 3-2. Results from chapter 3 case 2

CH = 4160 feet, KV = 0.10E-10 feet/day

simulation no.	coal K (feet/day)	transition zone K (feet/day)	sum of the squared residuals	mean residual (feet)	budget discrepancy (%)	rmse (feet)
1	2.4	1.4	125060	-26.2	-3.06	47.7
2	2.4	0.1	220580	43.1	-3.39	63.3
3	2.4	0.01	3335700	216.0	-3.72	246.3
4	2.4	10	178400	-35.3	-1.29	57.0
5	18	1	164480	33.5	-0.37	54.7
6	18	0.1	2.89E+07	201.0	-0.42	724.9
7	41	1	614320	85.6	-0.31	105.7
8	2.4	5	166170	-33.5	-1.89	55.0
9	0.63	0.16	95588	-20.1	-8.41	41.7
10	6.3	1.6	87593	-13.9	-0.51	39.9
11	63	16	81847	-5.4	-0.10	38.6
12	630	160	108750	11.8	-0.01	44.5
13	2.4	16	183780	-36.3	-0.86	57.8
14	2.4	50	188570	-36.8	0.02	58.6
15	2.4	100	190500	-37.4	0.01	58.9
16	9.6	0.1	164164	148.0	-1.14	54.6
17	9.6	1	80320	7.4	-0.53	38.2
18	9.6	5	113870	-22.7	-0.21	45.5
19	9.6	16	152900	-30.9	-0.01	52.7
20	9.6	50	173980	-34.6	-0.03	56.2
21	9.6	100	181140	-36.0	-0.02	57.4
22	18	5	87204	-13.0	-0.19	39.8
23	18	16	128970	-26.1	-0.13	48.4
24	18	50	159390	-32.1	-0.01	53.8
25	18	10	171050	-34.3	-0.05	55.8
26	63	0.1	530170	276.0	-0.23	98.2
27	63	1	1111200	120.0	-0.09	142.1
28	63	5	132260	25.7	-0.20	49.0
29	63	50	112600	-20.6	-0.09	45.2
30	63	100	133810	-26.3	-0.06	49.3
31	4.8	1	81707	-10.8	-0.77	38.5
32	4.8	5	143340	-29.6	-1.80	51.1
33	4.8	16	171120	-34.0	-0.20	55.8
34	4.8	50	183510	-36.1	0.00	57.8
35	4.8	0.1	680220	90.9	-1.51	111.2
36	4.8	100	187530	-37.0	-0.01	58.4

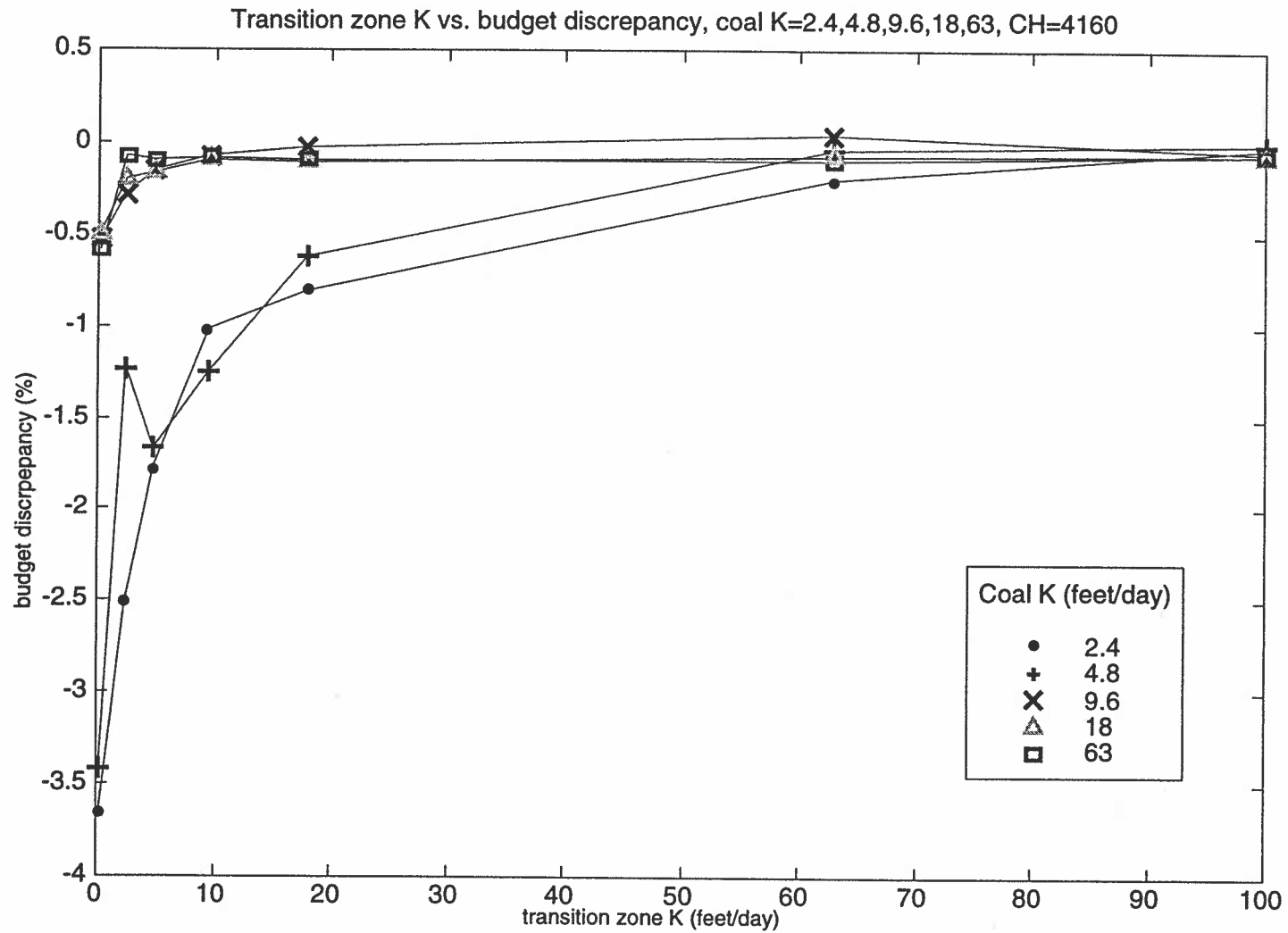


Figure 3-7. Case 3a, homogeneous coal, heterogeneous transition zone. Budget discrepancy as a function of transition zone K at given values of coal K, CH=4160.

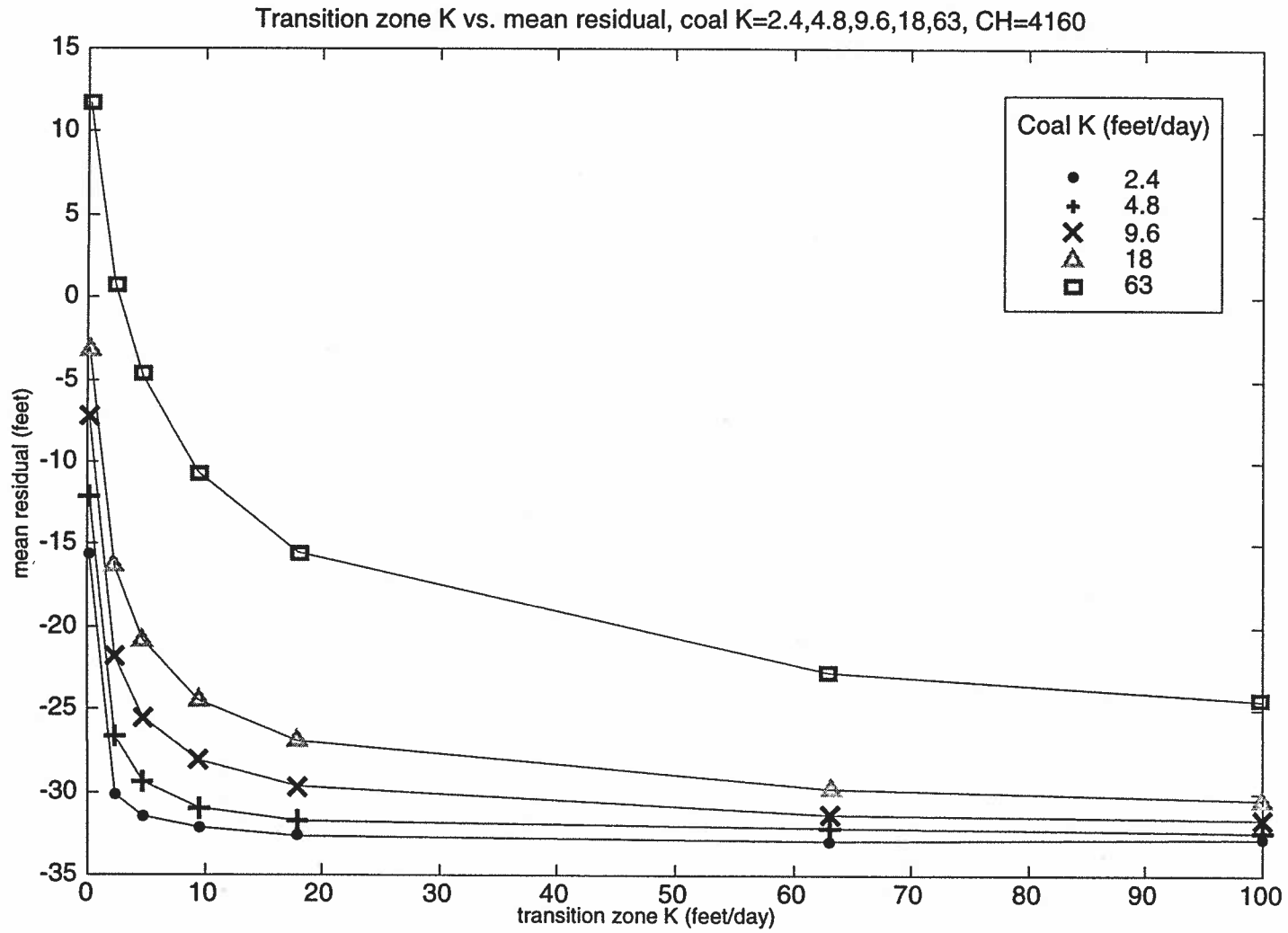


Figure 3-8. Case 3a, homogeneous coal, heterogeneous transition zone. Mean residual as a function of transition zone K at given values of coal K, CH=4160.

Table 3-3. Results from chapter 3 case 3a

CH = 4160 feet, KV = 0.10E-10 feet/day

simulation no.	coal K	transition zone K	transition zone K	sum of the squared residuals	mean residual (feet)	budget discrepancy (%)	rmse (feet)
	(feet/day)	(feet/day)	(feet/day)				
	zone 1	zone 2,3,4,6	zone 5				
1	2.4	0.1	2.4	87678	-15.6	-3.66	39.9
2	2.4	2.4	2.4	145550	-30.2	-2.51	51.4
3	2.4	4.8	2.4	155560	-31.5	-1.77	53.2
4	2.4	9.6	2.4	161920	-32.2	-1.02	54.3
5	2.4	18	2.4	165880	-32.7	-0.80	54.9
6	2.4	63	2.4	169290	-32.9	-0.20	55.5
7	2.4	100	2.4	169860	-32.8	-0.30	55.6
8	4.8	0.1	4.8	82546	-12.1	-3.42	38.7
9	4.8	2.4	4.8	127230	-26.7	-1.22	48.1
10	4.8	4.8	4.8	142210	-29.4	-1.67	50.8
11	4.8	9.6	4.8	152840	-31.0	-1.25	52.7
12	4.8	18	4.8	159360	-31.7	-0.62	53.8
13	4.8	63	4.8	166170	-32.2	-0.04	55.0
14	4.8	100	4.8	167410	-32.4	0.00	55.2
15	9.6	0.1	9.6	81951	-7.3	-0.53	38.6
16	9.6	2.4	9.6	107660	-21.9	-0.28	44.2
17	9.6	4.8	9.6	123210	-25.5	-0.15	47.3
18	9.6	9.6	9.6	137860	-28.1	-0.07	50.1
19	9.6	18	9.6	148200	-29.7	-0.02	51.9
20	9.6	63	9.6	160200	-31.3	0.04	54.0
21	9.6	100	9.6	162890	-31.6	-0.05	54.4
22	18	0.1	18	83246	-3.0	-0.49	38.9
23	18	2.4	18	91699	-16.4	-0.20	40.8
24	18	4.8	18	104340	-20.8	-0.16	43.6
25	18	9.6	18	119980	-24.4	-0.10	46.7
26	18	18	18	132860	-26.9	-0.11	49.1
27	18	63	18	151210	-29.8	-0.07	52.4
28	18	100	18	155450	-30.4	-0.06	53.2
29	63	0.1	63	113090	11.8	-0.59	45.3
30	63	2.4	63	85229	0.8	-0.07	39.4
31	63	4.8	63	80820	-4.8	-0.10	38.3
32	63	9.6	63	84035	-10.6	-0.08	39.1
33	63	18	63	93433	-15.5	-0.09	41.2
34	63	63	63	119910	-22.7	-0.10	46.7
35	63	100	63	128770	-24.5	-0.06	48.4

Case3b

The best fit for this scenario occurred with a coal $K=2.4$ feet/day and a transition zone $K=63$ feet/day, resulting in a budget discrepancy of -0.12% and a mean residual of 0.0126 feet. Complete results are shown in figures 3-9 and 3-10 and table 3-4. Head calculated for layer 2 in case 3b is shown in figure 3-11.

IV. Conclusions

Case 1

Increasing the coal K returns a smaller residual and a smaller budget discrepancy. However, the high values of coal K are unreasonable and indicate that this conceptual model is inadequate. Too much water is entering the model from the east, and, since CH has been fixed, coal K must be elevated to dissipate the water.

According to Darcy's law,

$$q = -K \frac{dh}{dl} \quad (\text{Anderson, 1992}),$$

where q = discharge rate (cubic feet/day)
 K = hydraulic conductivity (feet/day)
 h = hydraulic head (feet)
 l = flow-path length (feet)

if all variables are held constant, with the exception of dh and K , it is clear that these two variables are related inversely. In the case of the model, CH could be elevated to decrease the coal K . However, doing so increases both the mean residual and budget discrepancy (Figure 3-12). Therefore a plausible CH which allows for good calibration must be found and kept fixed. As shown in figure 3-12, this value is $CH=4160$ feet. Therefore, subsequent results are reported at $CH=4160$ feet.

Case 2

A high value of 63 feet/day for coal K runs counter to what is expected and indicates that this conceptual model is not adequate to describe the system. The coal K has, however, been reduced slightly.

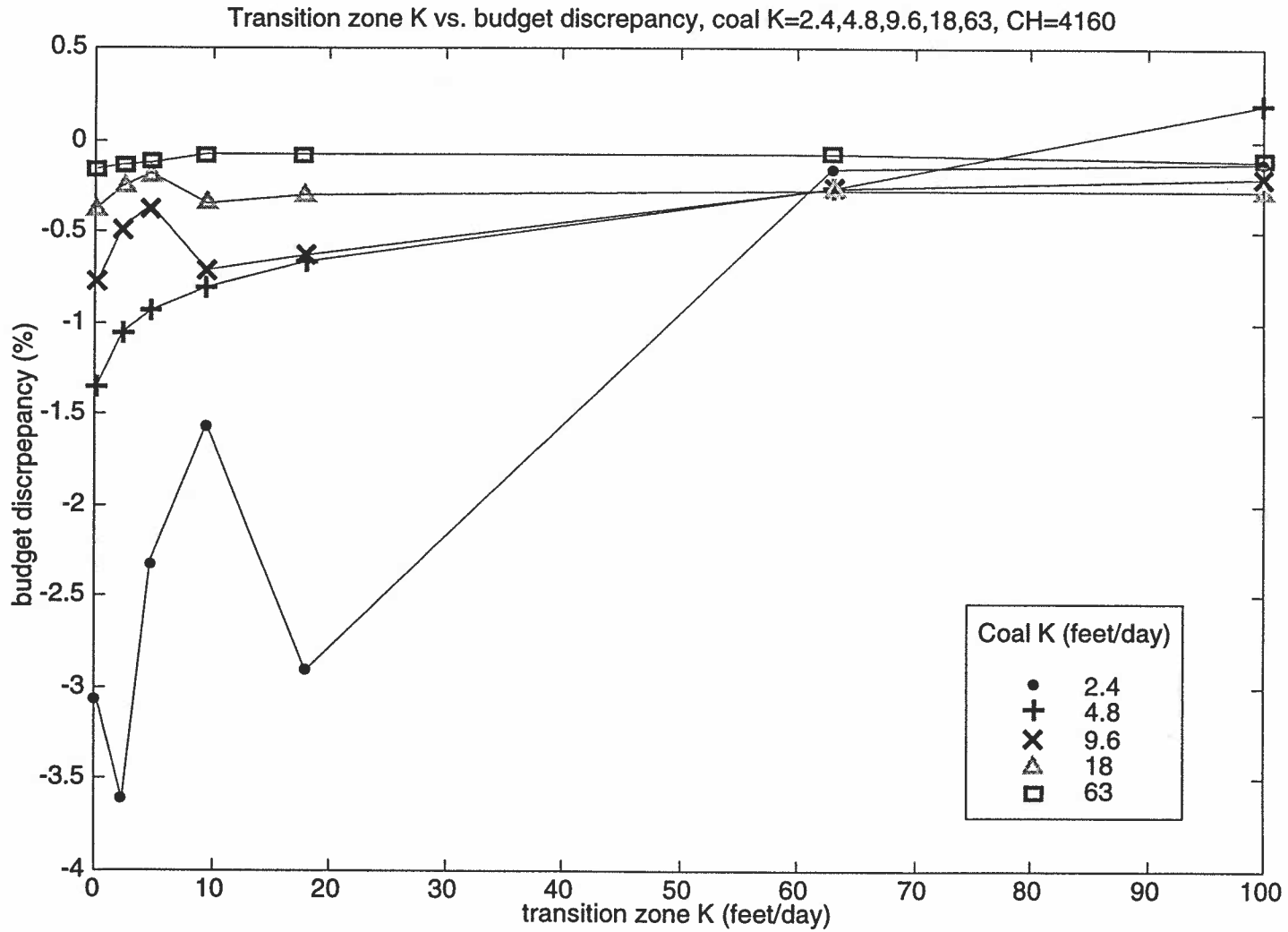


Figure 3-9. Case3b, homogeneous coal, heterogeneous transition zone. Non-clinker cropline cells inactive. Budget discrepancy as a function of transition zone K at given values of coal K, CH=4160.

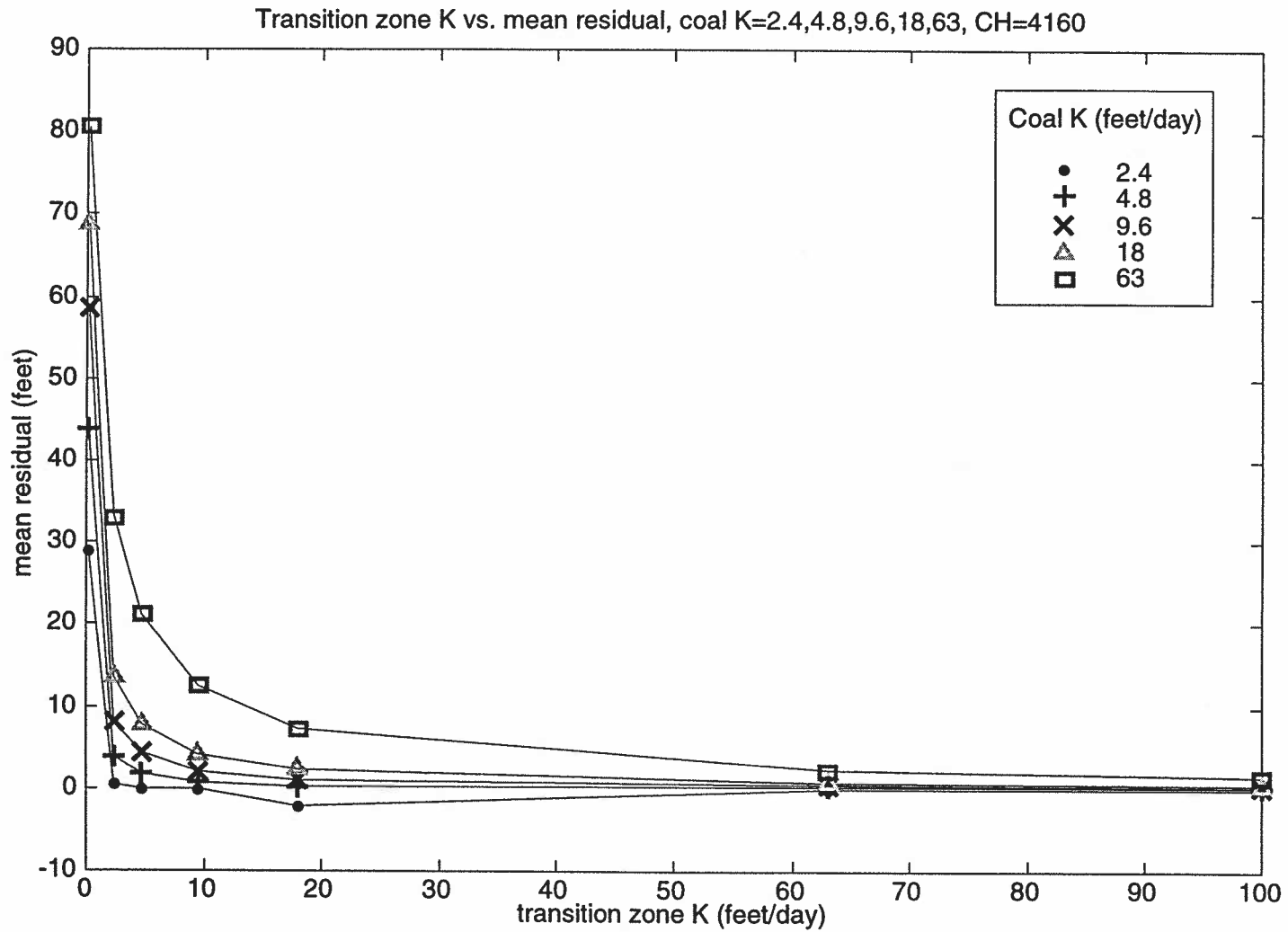


Figure 3-10. Case3b, homogeneous coal, heterogeneous transition zone. Non-clinker cropline cells inactive. Mean residual as a function of transition zone K at given values of coal K, CH=4160.

Table 3-4. Results from chapter 3 case 3b

CH = 4160 feet, KV = 0.10E-10 feet/day, non-clinker cropline cells inactive

simulation no.	coal K (feet/day)	transition zone K (feet/day)	transition zone K (feet/day)	sum of the squared residuals	mean residual (feet)	budget discrepancy (%)	rmse (feet)
	zone 1	zone 2,3,4	zone 5,6				
1	2.4	0.1	2.4	281700	28.90	-3.06	71.6
2	2.4	2.4	2.4	108190	0.49	-3.61	44.4
3	2.4	4.8	2.4	107270	-0.01	-2.31	44.2
4	2.4	9.6	2.4	107060	-0.17	-1.56	44.1
5	2.4	18	2.4	104160	-2.02	-2.91	43.5
6	2.4	63	2.4	107660	0.01	-0.16	44.2
7	2.4	100	2.4	107700	0.04	-0.12	44.3
8	4.8	0.1	4.8	449250	43.70	-1.35	90.4
9	4.8	2.4	4.8	117780	3.91	-1.05	46.3
10	4.8	4.8	4.8	111990	1.87	-0.93	45.1
11	4.8	9.6	4.8	109410	0.82	-0.80	44.6
12	4.8	18	4.8	108330	0.32	-0.66	44.4
13	4.8	63	4.8	107960	0.20	-0.26	44.3
14	4.8	100	4.8	107840	0.14	-0.19	44.3
15	9.6	0.1	9.6	677380	58.70	-0.78	111.0
16	9.6	2.4	9.6	132150	8.00	-0.47	49.0
17	9.6	4.8	9.6	118630	4.29	-0.36	46.4
18	9.6	9.6	9.6	112190	2.00	-0.71	45.2
19	9.6	18	9.6	109760	1.01	-0.63	44.7
20	9.6	63	9.6	108280	0.38	-0.26	44.4
21	9.6	100	9.6	108090	0.29	-0.21	44.3
22	18	0.1	18	861610	68.80	-0.04	125.2
23	18	2.4	18	160420	13.60	-0.25	54.0
24	18	4.8	18	131310	7.69	-0.18	48.9
25	18	9.6	18	117970	4.08	-0.35	46.3
26	18	18	18	112790	2.27	-0.30	45.3
27	18	63	18	108930	0.69	-0.27	44.5
28	18	100	18	108410	0.45	-0.28	44.4
29	63	0.1	63	1110300	80.50	-0.16	142.1
30	63	2.4	63	320170	33.30	-0.14	76.3
31	63	4.8	63	209560	21.20	-0.12	61.7
32	63	9.6	63	153520	12.50	-0.07	52.8
33	63	18	63	129730	7.37	-0.08	48.6
34	63	63	63	113230	2.41	-0.08	45.4
35	63	100	63	111200	1.58	-0.11	45.0

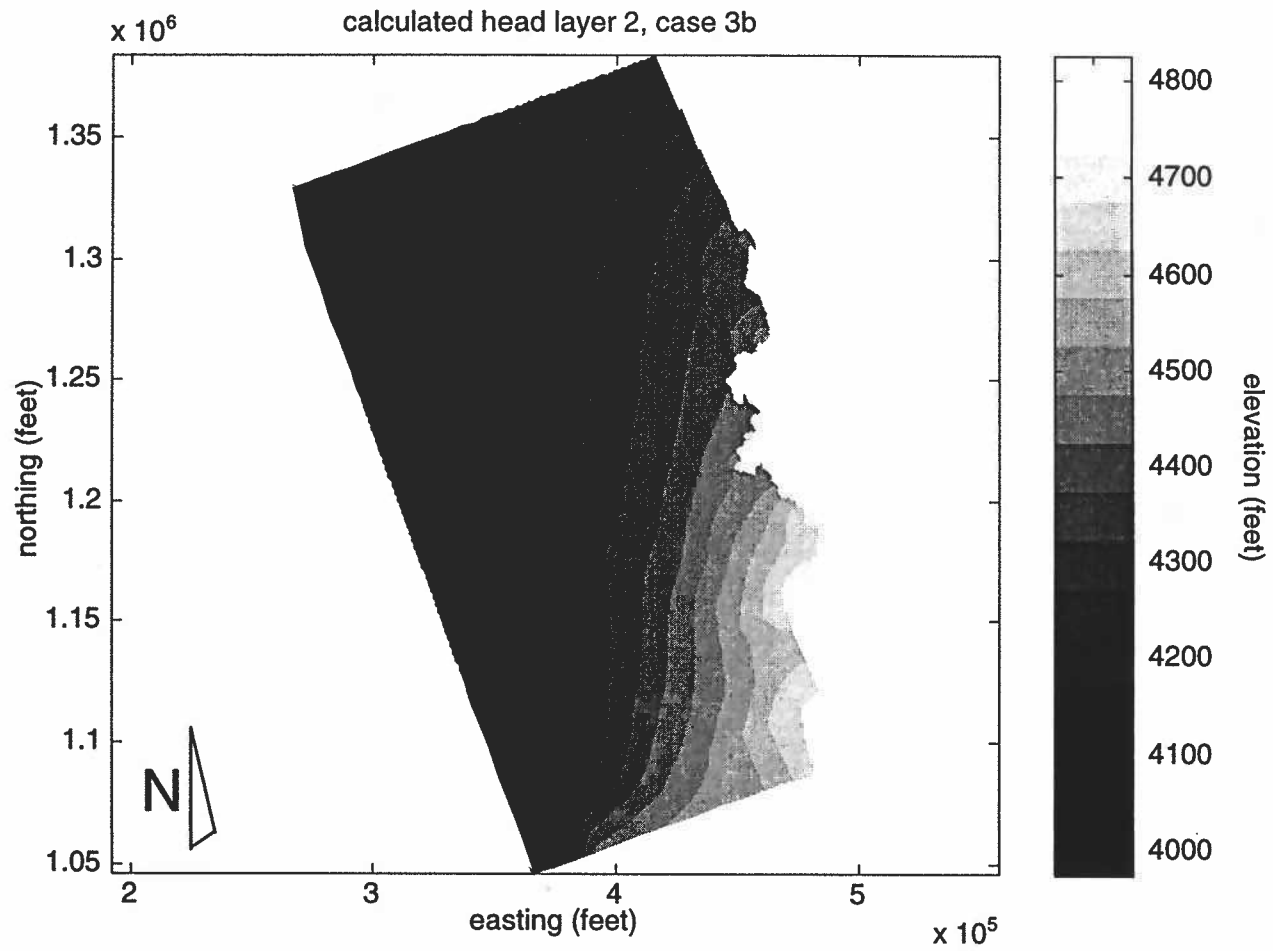


Figure 3-11. Head calculated in case 3b, layer 2; homogeneous coal, heterogeneous transition zone, non-clinker cropline cells inactive.

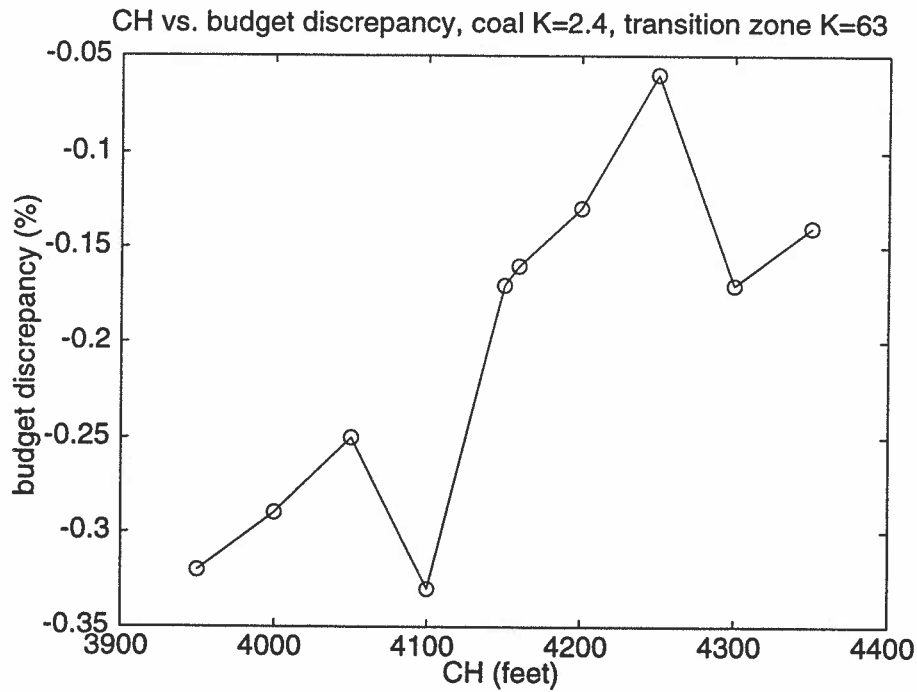
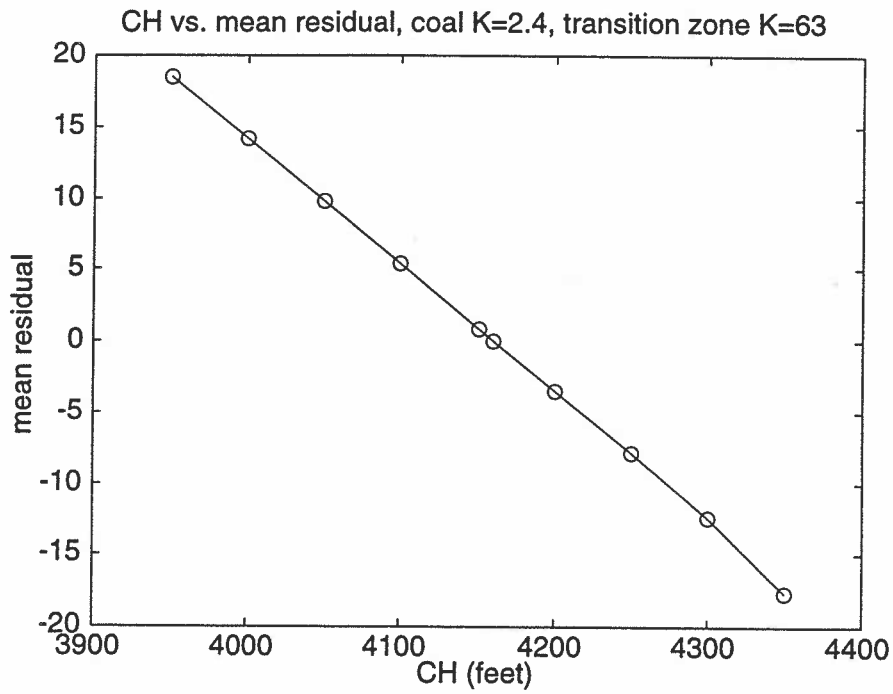


Figure 3-12. CH vs. mean residual and budget discrepancy. Coal K=2.4, transition zone K=63, heterogeneous transition zone, non-clinker cropline cells inactive.

Case3a

The results of case 3a are an exceptional fit. However, the coal and transition zone K's are reversed from what is expected from the data. Sixty-three is far too high for coal K. This may be due to too much water entering the model from the east, encouraging Modflowp to increase the coal K.

An interesting byproduct of this model is the indication by Modflowp that transition zones in the southern half of the model have a nearly 100% correlation with the coal of the rest of the model. This may indicate that either these transition zones have very low K, on the order of coal, that there is no transition zone in this area, or that the clinker in this area is not in connection with the coal due to a structural feature. For this and the following cases, the transition zones which correlated with coal were lumped back in with the coal.

Case3b

This is a model that is both plausible and fits our calibration criteria well. This model will be the starting point for investigations into the vertical hydraulic conductivity of the confining layer between the Wasatch sand lens and the Wyodak coal, and the heterogeneity of the coal.

CHAPTER 4. Investigations of vertical hydraulic conductivity in the confining bed separating the Wyodak coal from the overlying Wasatch sand lens aquifer.

I. Introduction

This investigation proceeds in similar fashion to that of chapter 3. The simplest case is considered first, and degrees of complexity are added in a step-wise fashion. The results of case 3b of chapter 3 are fixed in the cases of chapter 4; coal $K=2.4$, transition zone $K=63$, non-clinker cropline cells are inactive. Layer 1 remains as it was in chapter 3. The nature of the data available for layer 1 and the details of its construction do not allow for a systematic investigation of its aquifer properties. Layer 1 has been developed from all the available data in accordance with the conceptual model and its properties are not estimated in this study. Two additional monitoring wells are added inside the sand lens of layer 1, bringing the total number of calibration wells to 57. All 57 wells are used in the calculation of the mean residual or bias of the model. However, the two sand lens wells are also looked at apart from the rest of the wells to examine the fit of each model to the sand lens layer.

A range of plausible KV values and geometries given homogeneous coal are examined. The same investigation is conducted in chapter six given heterogeneous coal.

II. Method

Case KV1, homogeneous KV.

Case KV1 included only one KV zone over the entire model domain. The value of KV was varied in steps of half an order of magnitude from $1e-3$ to $1e-7$ feet/day. Once a value was arrived at, the estimate was refined by bisection.

Case KV2, heterogeneous KV, two zones.

Case KV2 broke the KV zone array into two zones, one underlying the sand lens (zone 1), and one underlying the Wasatch outside of the sand lens (zone 2) (Figure 4-1). KV in zones 1 and 2 was varied from $5e-5$ to $1e-7$ in steps of one-half an order of magnitude.

Case KV3, heterogeneous KV, three zones.

If one considers that KV may be different at either of the monitoring wells in the sand lens, a three-zone approach may prove beneficial (Figure 4-2). Consisting of three zones, the

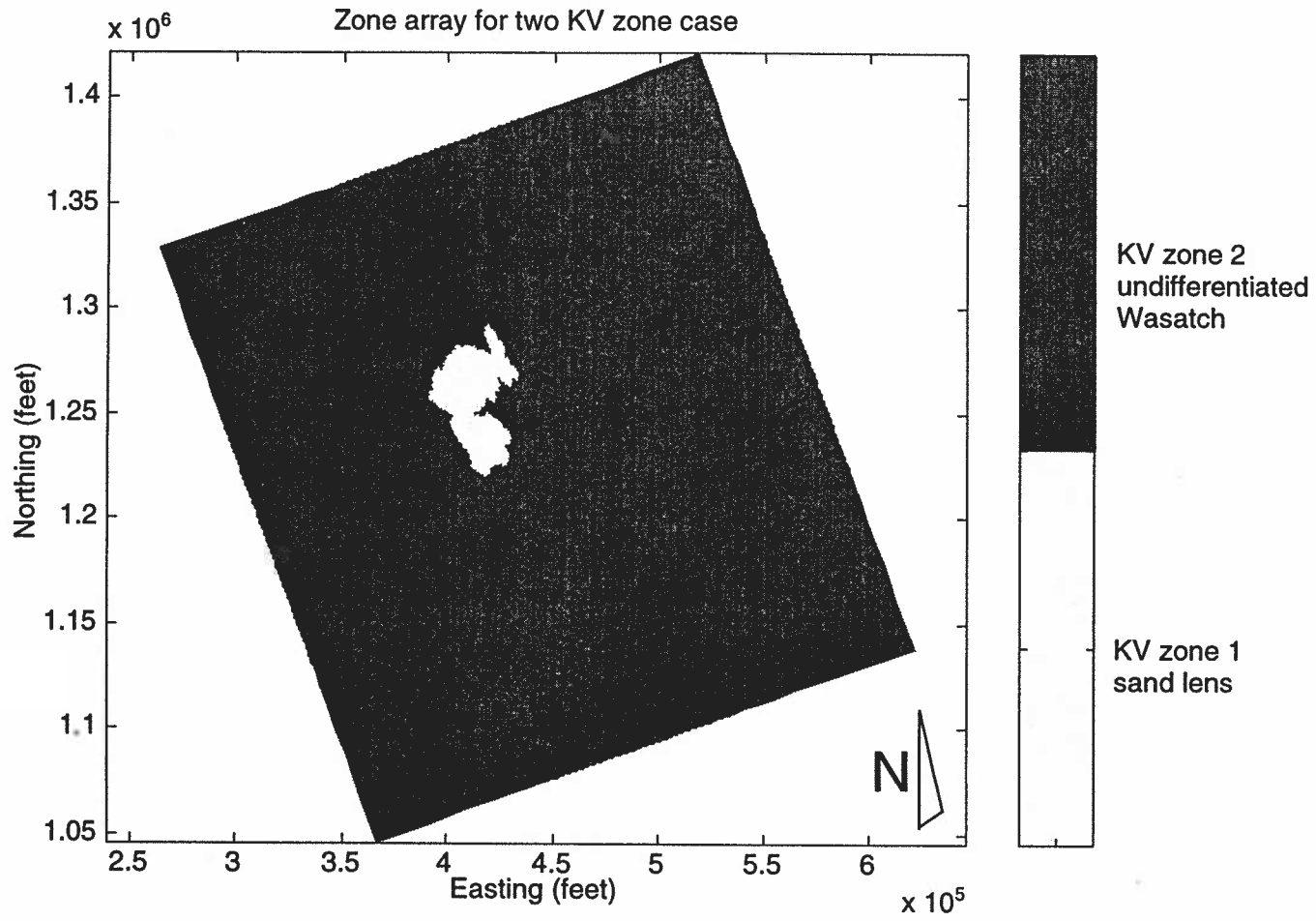


Figure 4-1. Zone array for KV, two zone case.

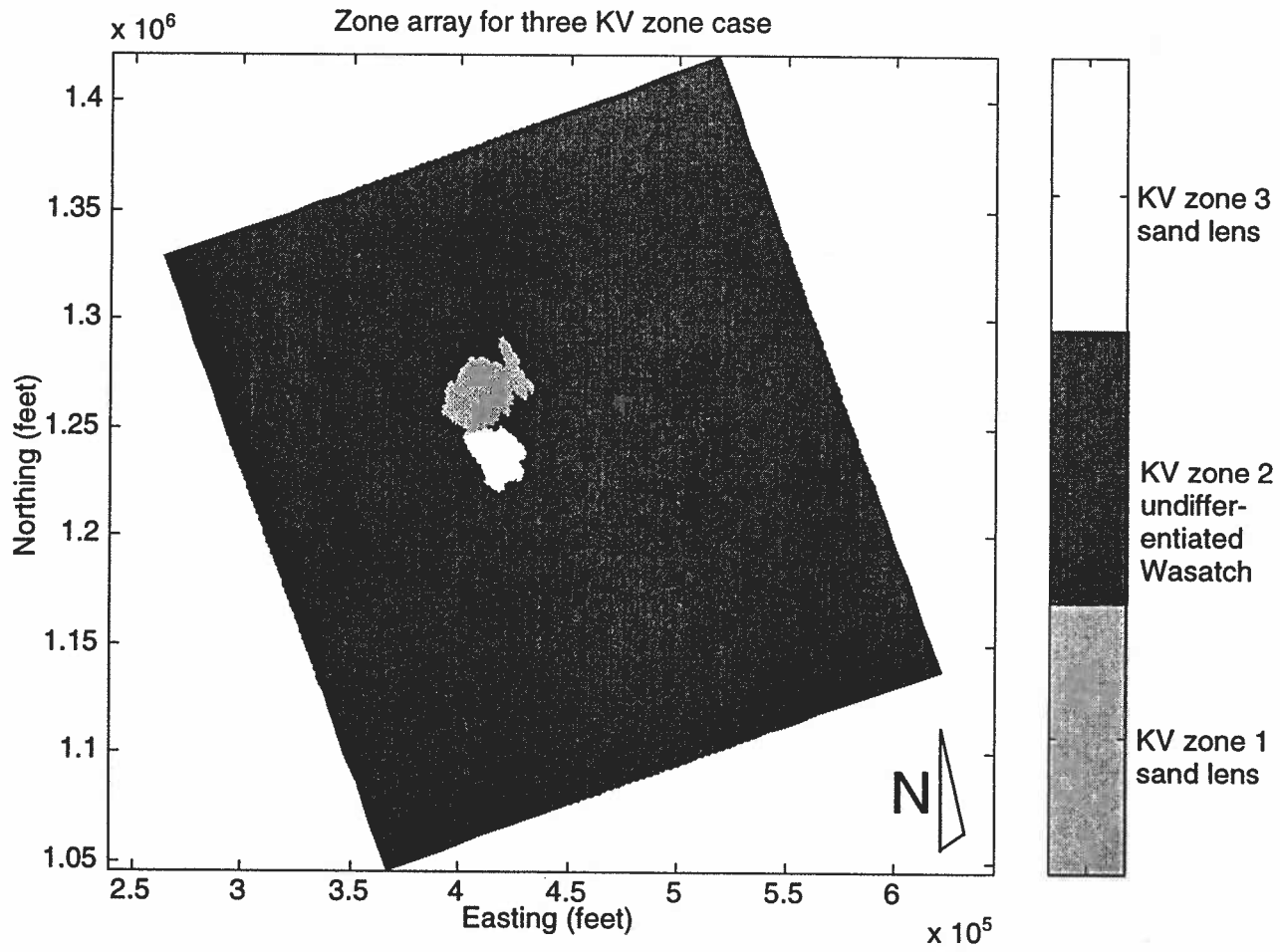


Figure 4-2. Zone array for KV, three zone case.

zone array for case KV3 was subdivided into two zones underlying the sand lens, one for each lobe (zones 1 and 3), and one zone underlying the Wasatch outside of the sand lens (zone 2). The KV in zones 1,2 and 3 was varied up and down from the best-fit scenario in case KV2 by an order of magnitude in steps of one-half an order of magnitude.

III. Results

Case KV1

The results indicate a best fit in the vicinity of $5e-6$ feet/day resulting in a mean residual of -4.64 a budget discrepancy of -0.47% and a mean sand lens residual of 8.535 feet (Figures 4-3, 4-4). Complete results are shown in figures 4-3 and 4-4 and table 4-1. The estimate was further refined by bisection to $4.5e-6$ feet/day. The head for layers 1 and 2, as calculated in case KV1 are shown in figures 4-5 and 4-6.

Case KV2

The best fit occurred with a KV in zone 1 equal to $1e-6$ feet/day and a KV in zone 2 equal to $5e-6$ feet/day. The resulting calibration values were a mean residual of -4.12 feet, a budget discrepancy of -0.19%, and a mean sand lens residual of -7.0. According to the charts (Figures 4-7 to 4-9) the mean sand lens residual may be improved to approximately 0 by moving KV of zone 1 to $2e-6$. Complete results are shown in figures 4-7 through 4-9 and table 4-2.

Case KV3

The best fit occurred with a KV in zone 1 of $5e-6$ feet/day, a KV in zone 2 of $5e-6$ feet/day and a KV in zone 3 of $5e-7$ feet/day. These values of KV result in a mean residual of -4.00 feet, a budget discrepancy of -0.20% and a mean sand lens residual of -3.62 feet. Complete results are shown in figures 4-10 through 4-12 and table 4-3.

IV. Conclusions

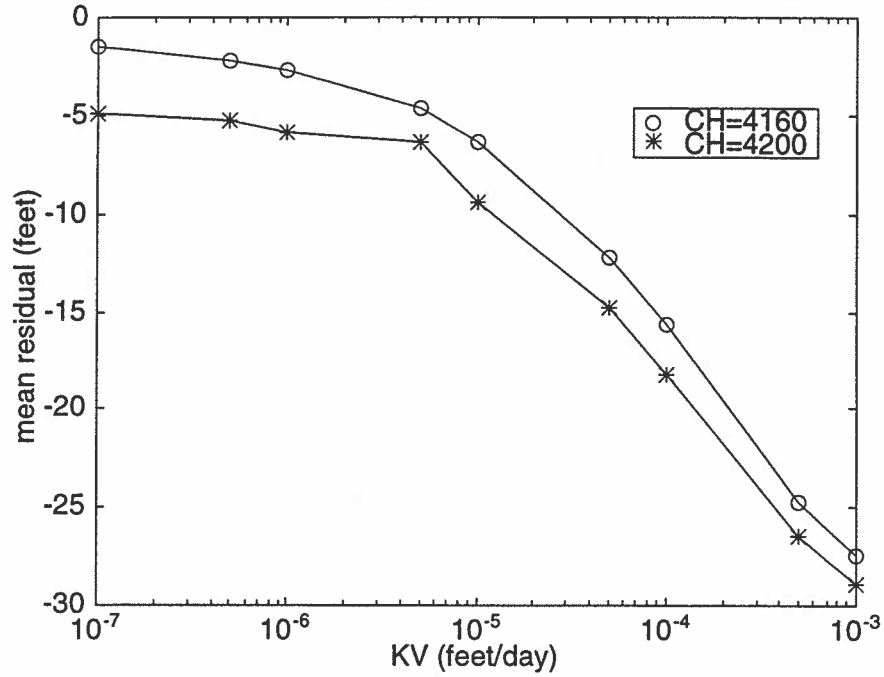
Case KV1

$4.5e-6$ feet/day is a good first order approximation of the KV for the entire model domain. The model is clearly sensitive to this parameter.

Case KV2

Case KV2 demonstrates that the model is not sensitive to the zonation of the confining

KV vs. mean residual, coal K=2.4, Transition zone K=63, CH=4160, 4200



KV vs. budget discrepancy, coal K=2.4, Transition zone K=63, CH=4160,4200

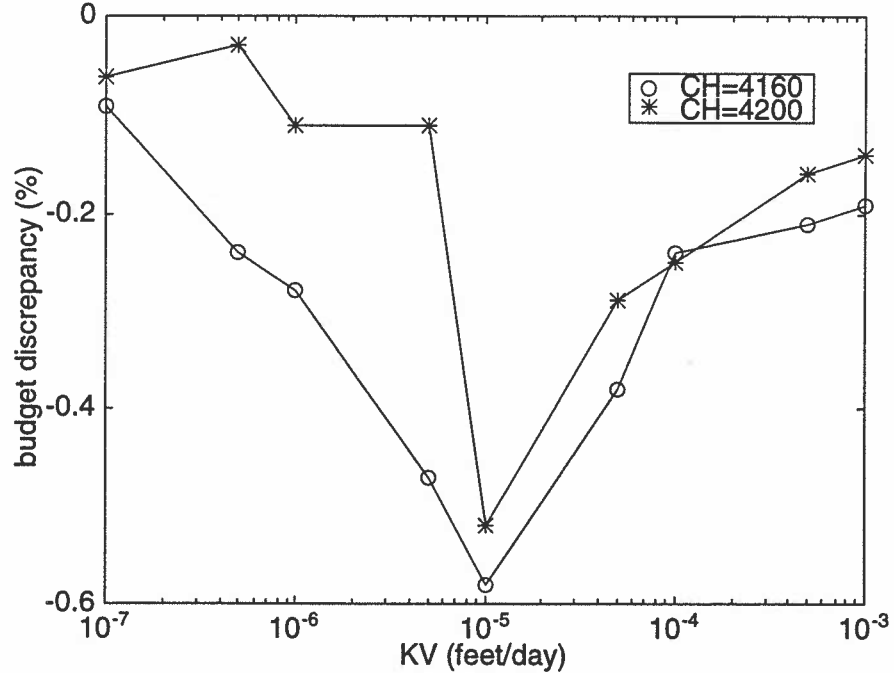


Figure 4-3. KV vs. mean residual and budget discrepancy for KV case 1; homogeneous KV, in one zone. Coal K=2.4, transition zone K=63, CH=4160 and 4200.

KV vs. mean sand lens residual, coal K=2.4, Transition zone K=63, CH=4160,4200

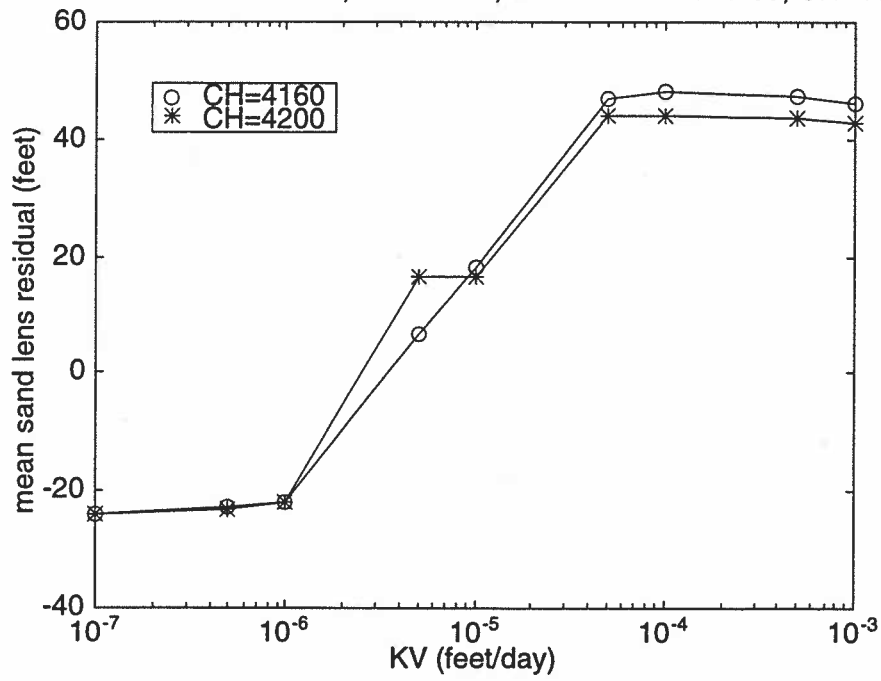


Figure 4-4. KV vs. mean sand lens residual for KV case 1; homogeneous KV, in one zone. Coal K=2.4, transition zone K=63, CH=4160 and CH=4200.

Table 4-1. Results of chapter 4 case KV1

CH=4160

simulation no.	KV (feet/day)	sum of the squared residuals	mean residual (feet)	budget discrepancy (%)	sand lens resid. #1	sand lens resid. #2	rmse (feet)
1	1.00E-04	119770	-15.7	-0.24	96.3	91.7	45.8
2	5.00E-05	114850	-12.3	-0.38	94.3	88.8	44.9
3	1.00E-05	99620	-6.4	-0.58	37.3	27.1	41.8
4	5.00E-06	100180	-4.6	-0.47	13.9	3.17	41.9
5	1.00E-06	111550	-2.8	-0.28	-43.7	-61.7	44.2
6	5.00E-07	113080	-2.2	-0.24	-45.5	-63.7	44.5
7	1.00E-07	114770	-1.5	-0.09	-47.7	-64.4	44.9
8	5.00E-04	142600	-24.7	-0.21	94.7	86.7	50.0
9	1.00E-03	153960	-27.4	-0.19	92.3	86.1	52.0

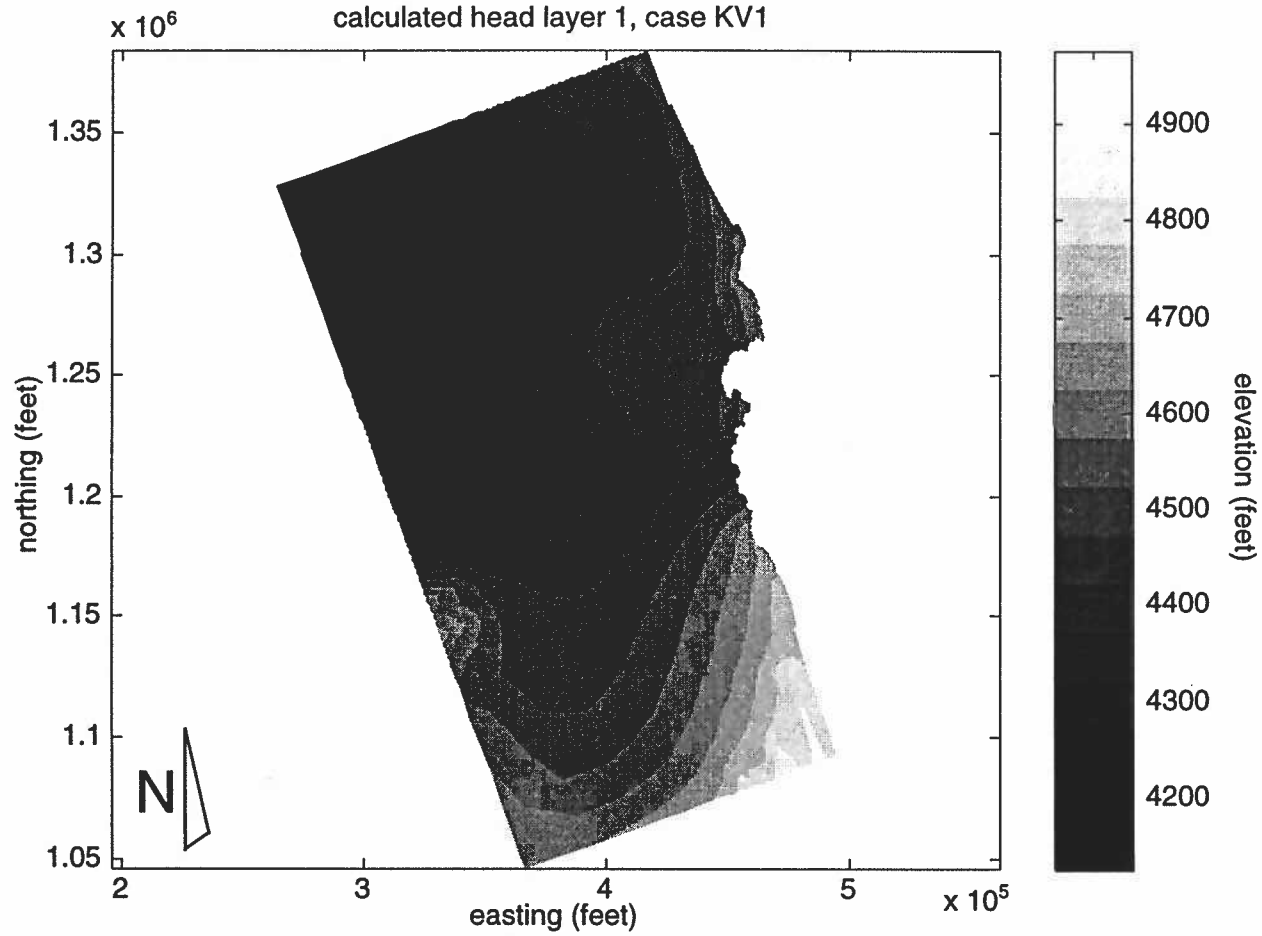


Figure 4-5. Head calculated in case KV1 layer 1; homogeneous coal, heterogeneous transition zone, non-clinker cropline cells inactive, $KV = 4.5E-06$ feet/day.

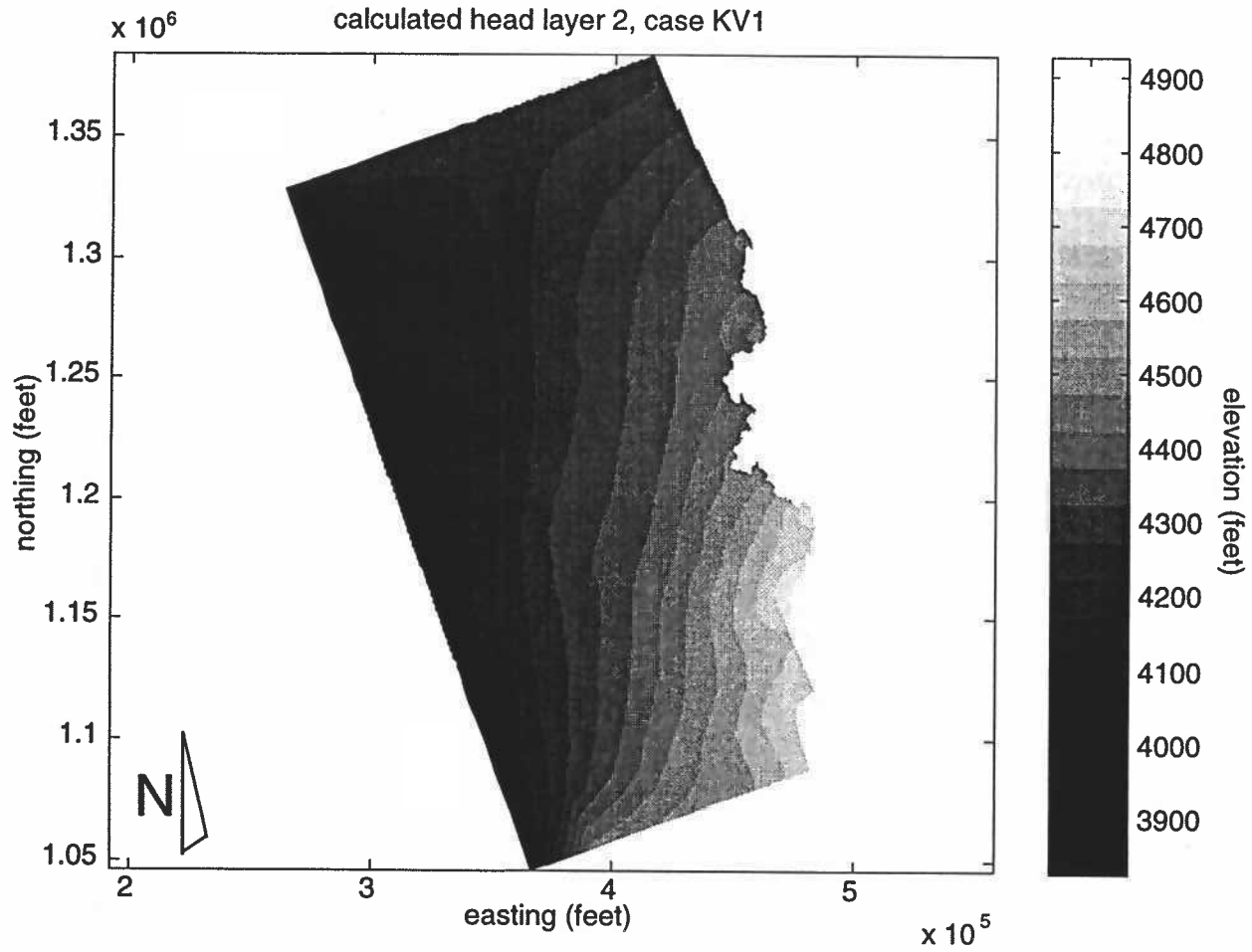


Figure 4-6. Head calculated in case KV1, layer 2; homogeneous coal, heterogeneous transition zone, non-clinker cropline cells inactive, $KV = 4.5E-06$ feet/day.

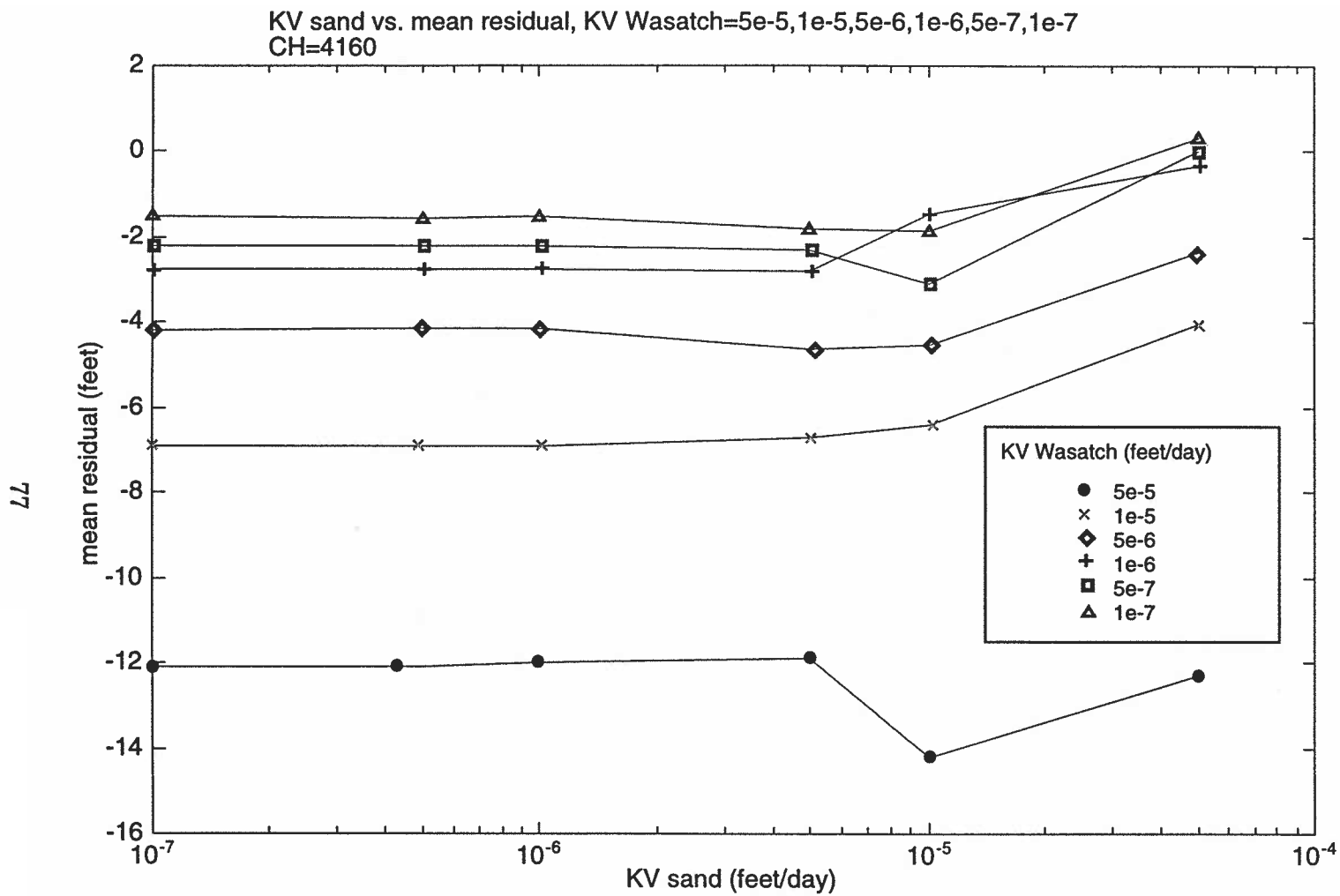


Figure 4-7. Case KV2. KV of the confining layer underlying the sand lens vs. mean residual. KV of the confining layer underlying the Wasatch, outside of the sand lens fixed at values shown in figure, CH fixed at 4160 feet.

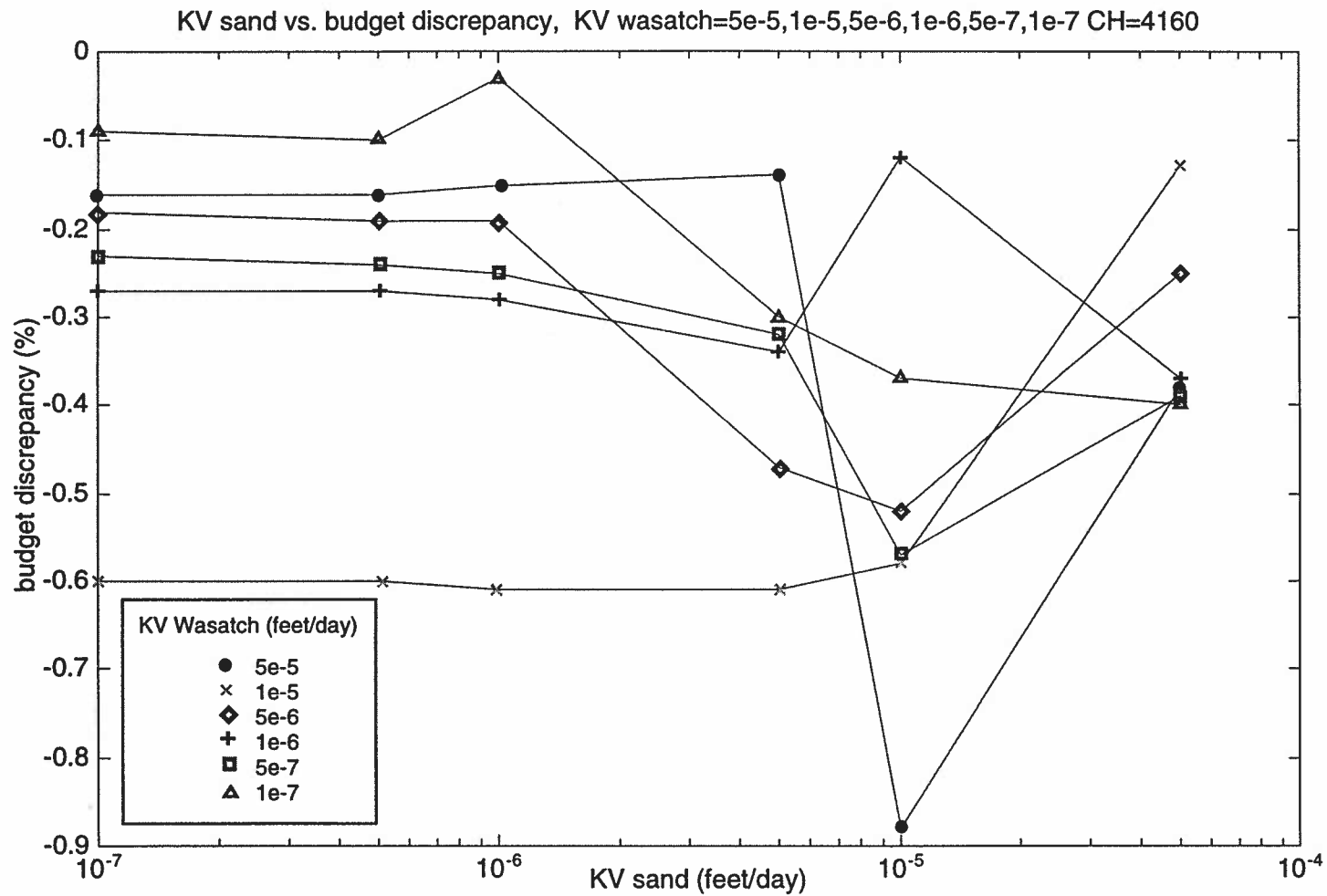


Figure 4-8. Case KV2. KV of the confining layer underlying the sand lens vs. budget discrepancy. KV of the confining layer underlying the Wasatch, outside of the sand lens fixed at values shown in figure, CH fixed at 4160 feet.

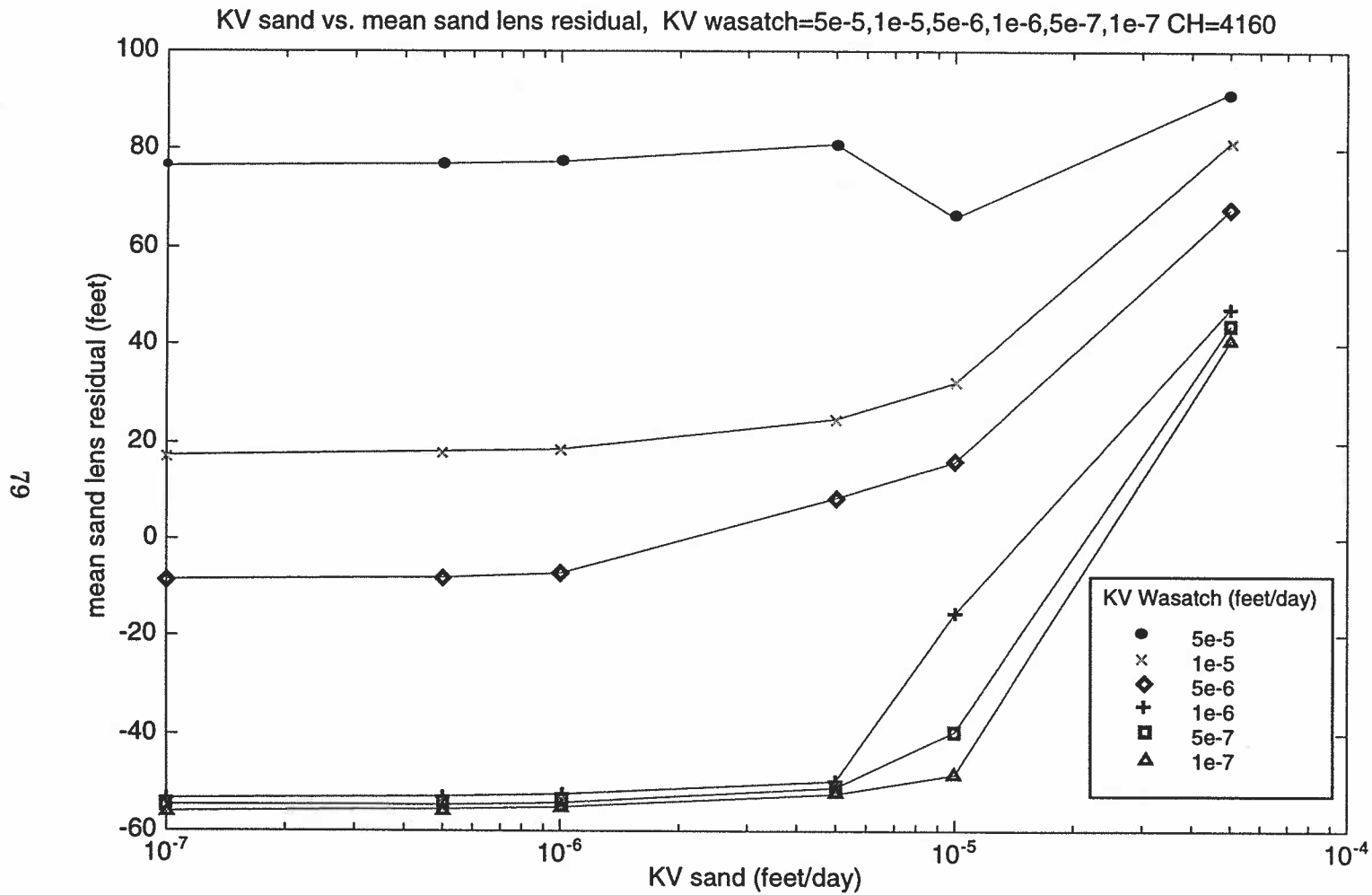


Figure 4-9. Case KV2. KV of the confining layer underlying the sand lens vs. mean sand lens residual. KV of the confining layer underlying the Wasatch, outside of the sand lens fixed at values shown in figure, CH fixed at 4160 feet.

Table 4-2. Results of chapter 4 case KV2

CH=4160 feet, KV zone 1 underlies the sand lens, KV zone 2 underlies the sand lens layer outside of the sand lens.

simulation no.	KV zone 1 (feet/day)	KV zone 2 (feet/day)	sum of the mean		budget discrepancy (%)	sand lens		rmse (feet)
			squared residuals	residual (feet)		resid. #1	resid. #2	
1	1.00E-05	1.00E-05	99620	-6.40	-0.58	37.3	27.1	41.8
2	1.00E-05	5.00E-06	100180	-4.53	-0.52	21.2	10.6	41.9
3	1.00E-05	1.00E-06	105480	-1.46	-0.12	-10.8	-20.2	43.0
4	1.00E-05	5.00E-07	108200	-3.11	-0.57	-33.5	-46.1	43.6
5	1.00E-05	1.00E-07	111290	-1.85	-0.37	-40.3	-57.1	44.2
6	1.00E-05	5.00E-05	107110	-14.20	-0.88	69.9	62.5	43.3
7	5.00E-05	5.00E-05	114850	-12.30	-0.38	94.3	88.8	44.9
8	5.00E-05	1.00E-05	111160	-4.01	-0.13	85.4	77.5	44.2
9	5.00E-05	5.00E-06	108520	-2.36	-0.25	71.8	63.9	43.6
10	5.00E-05	1.00E-06	107190	-0.31	-0.37	51.7	43.6	43.4
11	5.00E-05	5.00E-07	107190	0.03	-0.39	48.2	40.0	43.4
12	5.00E-05	1.00E-07	107250	0.34	-0.40	45.2	36.9	43.4
13	5.00E-06	5.00E-05	110490	-11.90	-0.14	85.9	76.2	44.0
14	5.00E-06	1.00E-05	98894	-6.70	-0.61	29.9	19.3	41.7
15	5.00E-06	5.00E-06	100180	-4.64	-0.47	13.9	3.2	41.9
16	5.00E-06	1.00E-06	110340	-2.78	-0.34	-41.0	-58.3	44.0
17	5.00E-06	5.00E-07	111610	-2.28	-0.32	-42.4	-60.0	44.3
18	5.00E-06	1.00E-07	112770	-1.82	-0.30	-43.6	-61.3	44.5
19	1.00E-06	5.00E-05	109370	-12.00	-0.15	82.5	72.8	43.8
20	1.00E-06	1.00E-05	98535	-6.89	-0.61	24.1	13.2	41.6
21	1.00E-06	5.00E-06	101350	-4.12	-0.19	-1.8	-12.2	42.2
22	1.00E-06	1.00E-06	111550	-2.75	-0.28	-43.7	-61.7	44.2
23	1.00E-06	5.00E-07	112910	-2.21	-0.25	-45.1	-63.3	44.5
24	1.00E-06	1.00E-07	114490	-1.49	-0.03	-47.0	-63.6	44.8
25	5.00E-07	5.00E-05	109230	-12.10	-0.16	82.0	72.3	43.8
26	5.00E-07	1.00E-05	98504	-6.91	-0.60	23.4	12.4	41.6
27	5.00E-07	5.00E-06	101400	-4.14	-0.19	-2.7	-13.1	42.2
28	5.00E-07	1.00E-06	111710	-2.74	-0.27	-44.1	-62.1	44.3
29	5.00E-07	5.00E-07	113080	-2.19	-0.24	-45.5	-63.7	44.5
30	5.00E-07	1.00E-07	114600	-1.54	-0.10	-47.4	-64.0	44.8
31	1.00E-07	5.00E-05	109110	-12.10	-0.16	81.7	71.9	43.8
32	1.00E-07	1.00E-05	98481	-6.92	-0.60	22.8	11.8	41.6
33	1.00E-07	5.00E-06	101440	-4.16	-0.18	-3.5	-13.8	42.2
34	1.00E-07	1.00E-06	111840	-2.73	-0.27	-44.3	-62.5	44.3
35	1.00E-07	5.00E-07	113230	-2.18	-0.23	-45.8	-64.0	44.6
36	1.00E-07	1.00E-07	114770	-1.53	-0.09	-47.7	-64.4	44.9

KV zone 3 vs. mean residual for given KV in zone 1, KV zone 2=1e-5, 5e-6, 1e-6

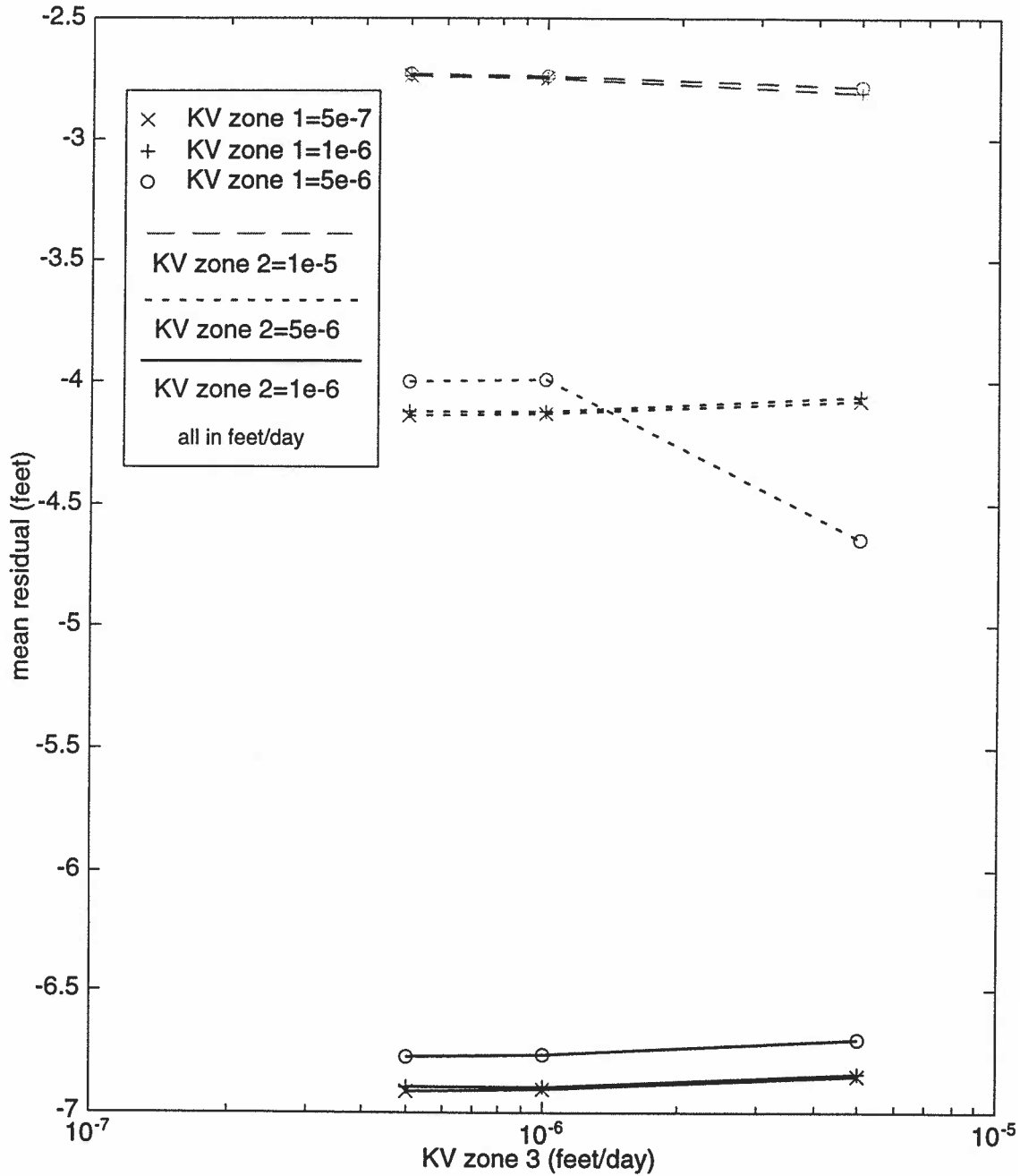


Figure 4-10. Case KV3. KV in zone 3 vs. mean residual . KV in zone 2 fixed as shown in figure, KV in zone 1 varies between 5e-7 and 5e-6. Zones 1 and 3 underlie the sand lens, zone 2 underlies the Wasatch outside of the sand lens.

KV zone 3 vs. budget discrepancy for given KV in zone 1, KV zone 2=1e-5, 5e-6, 1e-6

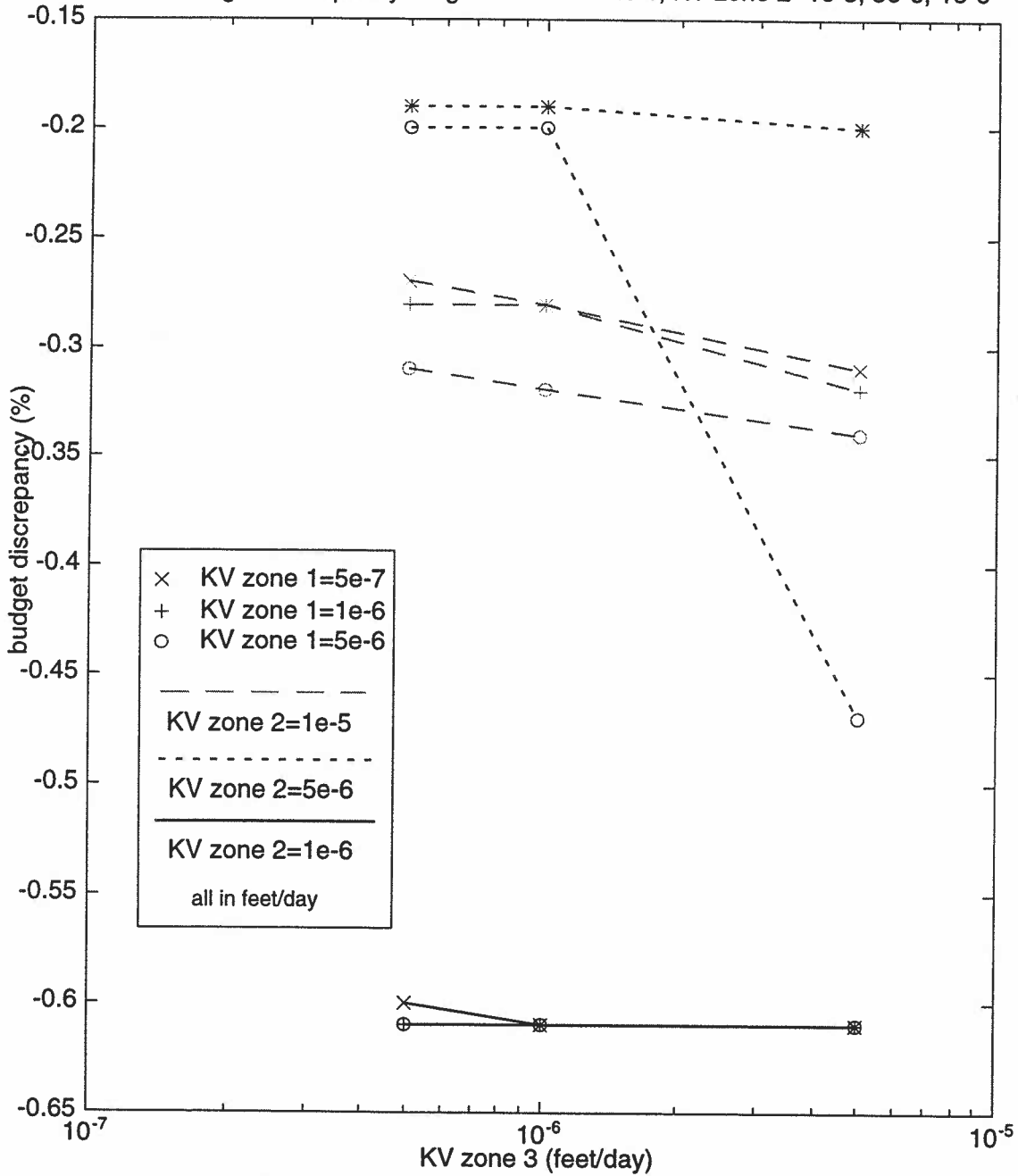


Figure 4-11. Case KV3. KV in zone 3 vs. budget discrepancy. KV in zone 2 fixed as shown in figure, KV in zone 1 varies between 5e-7 and 5e-6. Zones 1 and 3 underlie the sand lens, zone 2 underlies the Wasatch outside of the sand lens.

KV zone 3 vs. mean sand lens residual for given KV in zone 1, KV zone 2=1e-5, 5e-6, 1e-6

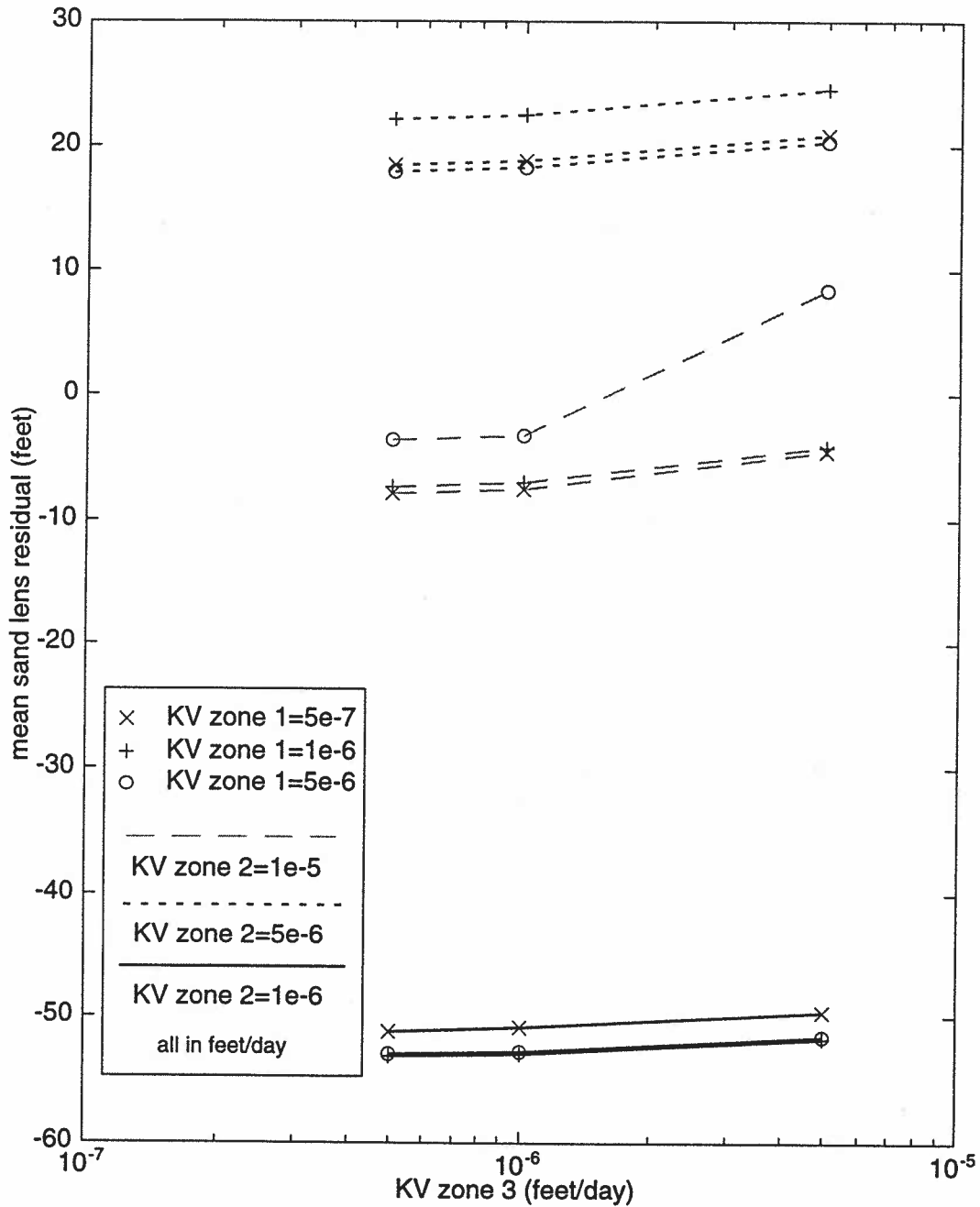


Figure 4-12. Case KV3. KV in zone 3 vs. mean sand lens residual. KV in zone 2 fixed as shown in figure, KV in zone 1 varies between 5e-7 and 5e-6. Zones 1 and 3 underlie the sand lens, zone 2 underlies the Wasatch outside of the sand lens.

Table 4-3 Results from chapter 4 case KV3

CH=4160

simulation no.	KV zone 1 (feet/day)	KV zone 2 (feet/day)	KV zone 3 (feet/day)	sum of the squared residuals	mean residual (feet)	budget discrepancy (%)	sand lens resid. #1	sand lens resid. #2	rmse (feet)
1	1.00E-05	5.00E-07	5.00E-07	98504	-6.91	-0.6	23.4	12.4	41.57091
2	1.00E-05	5.00E-07	1.00E-06	98518	-6.9	-0.61	23.7	12.6	41.57386
3	1.00E-05	5.00E-07	5.00E-06	98640	-6.85	-0.61	26.4	14.3	41.5996
4	1.00E-05	5.00E-06	5.00E-07	98701	-6.77	-0.61	26.9	17.3	41.61246
5	1.00E-05	5.00E-06	1.00E-06	98721	-6.76	-0.61	27.2	17.5	41.61667
6	1.00E-05	5.00E-06	5.00E-06	98894	-6.7	-0.61	29.9	19.3	41.65312
7	1.00E-05	1.00E-06	5.00E-07	98521	-6.89	-0.61	23.8	13	41.57449
8	1.00E-05	1.00E-06	1.00E-06	98535	-6.89	-0.61	24.1	13.2	41.57745
9	1.00E-05	1.00E-06	5.00E-06	98663	-6.84	-0.61	26.8	14.9	41.60444
10	5.00E-06	5.00E-06	5.00E-07	101180	-4	-0.2	0.954	-8.2	42.13179
11	5.00E-06	5.00E-06	1.00E-06	101170	-3.99	-0.2	1.39	-7.96	42.12971
12	5.00E-06	5.00E-06	5.00E-06	100180	-4.64	-0.47	13.9	3.17	41.92307
13	5.00E-06	1.00E-06	5.00E-07	101370	-4.12	-0.19	-2.28	-12.5	42.17133
14	5.00E-06	1.00E-06	1.00E-06	101350	-4.12	-0.19	-1.79	-12.2	42.16717
15	5.00E-06	1.00E-06	5.00E-06	101240	-4.06	-0.2	1.82	-10.2	42.14428
16	5.00E-06	5.00E-07	5.00E-07	98504	-4.14	-0.19	-2.71	-13.1	41.57091
17	5.00E-06	5.00E-07	1.00E-06	98518	-4.13	-0.19	-2.22	-12.8	41.57386
18	5.00E-06	5.00E-07	5.00E-06	98640	-4.08	-0.2	1.45	-10.7	41.5996
19	1.00E-06	5.00E-06	5.00E-07	110850	-2.73	-0.31	-43.3	-58.9	44.09917
20	1.00E-06	5.00E-06	1.00E-06	110790	-2.74	-0.32	-43	-58.8	44.08723
21	1.00E-06	5.00E-06	5.00E-06	110340	-2.78	-0.34	-41	-58.3	43.99761
22	1.00E-06	1.00E-06	5.00E-07	111610	-2.74	-0.28	-44	-61.8	44.25009
23	1.00E-06	1.00E-06	1.00E-06	111550	-2.75	-0.28	-43.7	-61.7	44.23819
24	1.00E-06	1.00E-06	5.00E-06	111070	-2.81	-0.32	-41.8	-61.2	44.14291
25	1.00E-06	5.00E-07	5.00E-07	111710	-2.74	-0.27	-44.1	-62.1	44.26991
26	1.00E-06	5.00E-07	1.00E-06	111650	-2.75	-0.28	-43.8	-62.1	44.25802
27	1.00E-06	5.00E-07	5.00E-06	111160	-2.81	-0.31	-41.8	-61.6	44.16079

layer. Although the mean sand lens residual jumps from one side of the decimal point to the other there is little change in its magnitude. There is very little change in the mean residual, indicating about the same quality of fit. The only real improvement seems to be in the budget. The results indicate that mean residual and mean sand lens residual are not affected by KV of the confining layer below the sand lens with a KV in this zone below $1.0E-5$ feet/day. This indicates that the model is not sensitive to KV of the confining layer under the sand and that subdivision of the confining layer is not reasonable. Above KV of zone 2= $1E-5$ feet/day, the budget discrepancy is sensitive to even minor alterations of the KV in zones 1 or 2, indicating that values of KV higher than this are unreasonable.

Case KV3

In comparison with the KV values for the sand lens in case KV2, the southern lobe of the sand lens has been lowered by a half order of magnitude while the northern lobe has been raised by a half order of magnitude. Figures 4-10 to 4-12 show that the model is sensitive only to the KV of zone 2. It is possible that the heterogeneity of the confining layer should be considered. However, the changes in the estimated KV resulting from zonation of the confining layer are limited to an order of magnitude between case KV1 and case KV3 and only in the southern lobe of the sand lens. Over the scale of the study domain, the estimate of $4.5e-6$ feet/day arrived at in case KV1 is the most reasonable.

Chapter 5. Investigation of heterogeneity in the coal.

I. Introduction

Throughout the investigations to this point, a coal layer with homogeneous hydraulic conductivity (K) has been used. However, the pump-test data indicate that the coal is heterogeneous. In addition, the poor fit of the models from chapters 3 and 4 indicate that the use of homogeneous coal results in inadequate calibration. The amount of K data which has been collected is limiting, but it can be shown that the introduction of heterogeneity into the coal will improve the calibration of the model. First to be demonstrated is that the introduction of heterogeneity in the coal improves calibration and second is that manipulation of the heterogeneity further improves calibration.

II. Method

Log transformed hydraulic conductivity, estimated from 38 aquifer tests, was used to investigate the directional range of correlation for hydraulic conductivity in the coal aquifer. Figure 5-1 shows the directional correlation functions in the directions N52E and S38E respectively. Although 38 data points is only marginally sufficient to deduce anisotropy, it can be seen that the range of influence is substantially longer in the S38E direction than in the N52E direction. An approximate ratio of anisotropy ranging from 2:1 to 3:1 can be seen, with a dominant wavelength in the northwest-southeast direction of approximately 20000 feet, and 10000 feet in the northeast-southwest direction. When a physical process exhibits nearly periodic behavior in space, the dominant wavelength is approximately 4 times the range of influence in the covariance function (Kern, 1995).

Modflowp was run with a kriged K array (Figure 5-2), which was constructed utilizing all of the available data of adequate quality (Kern, 1997b). Six conditioning points were then chosen from the kriged array, and an heterogeneous K array was conditionally simulated (Borgman, 1994) and run through Modflowp (Figure 5-3). Finally, using the result of the previous run, ten additional conditioning points were chosen by observing where there were large magnitude residuals resulting from calibration (Figure 5-4). A K array was conditionally simulated using these sixteen points and run through Modflowp in an attempt to further improve

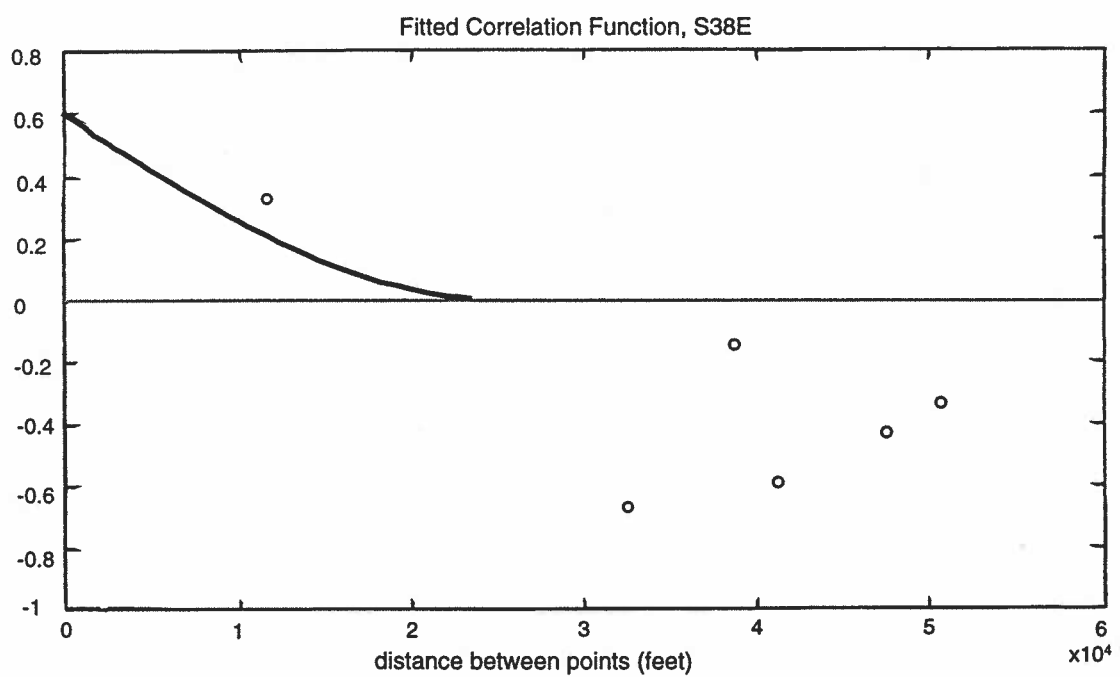
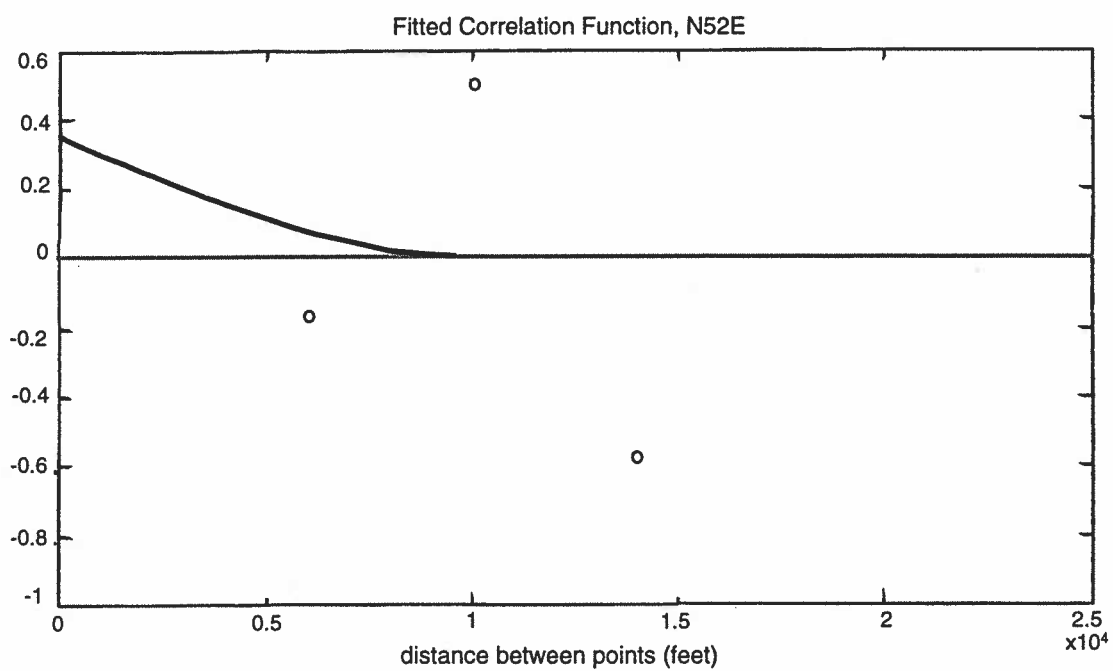


Figure 5-1. Fitted correlation functions for kriging of coal K data.

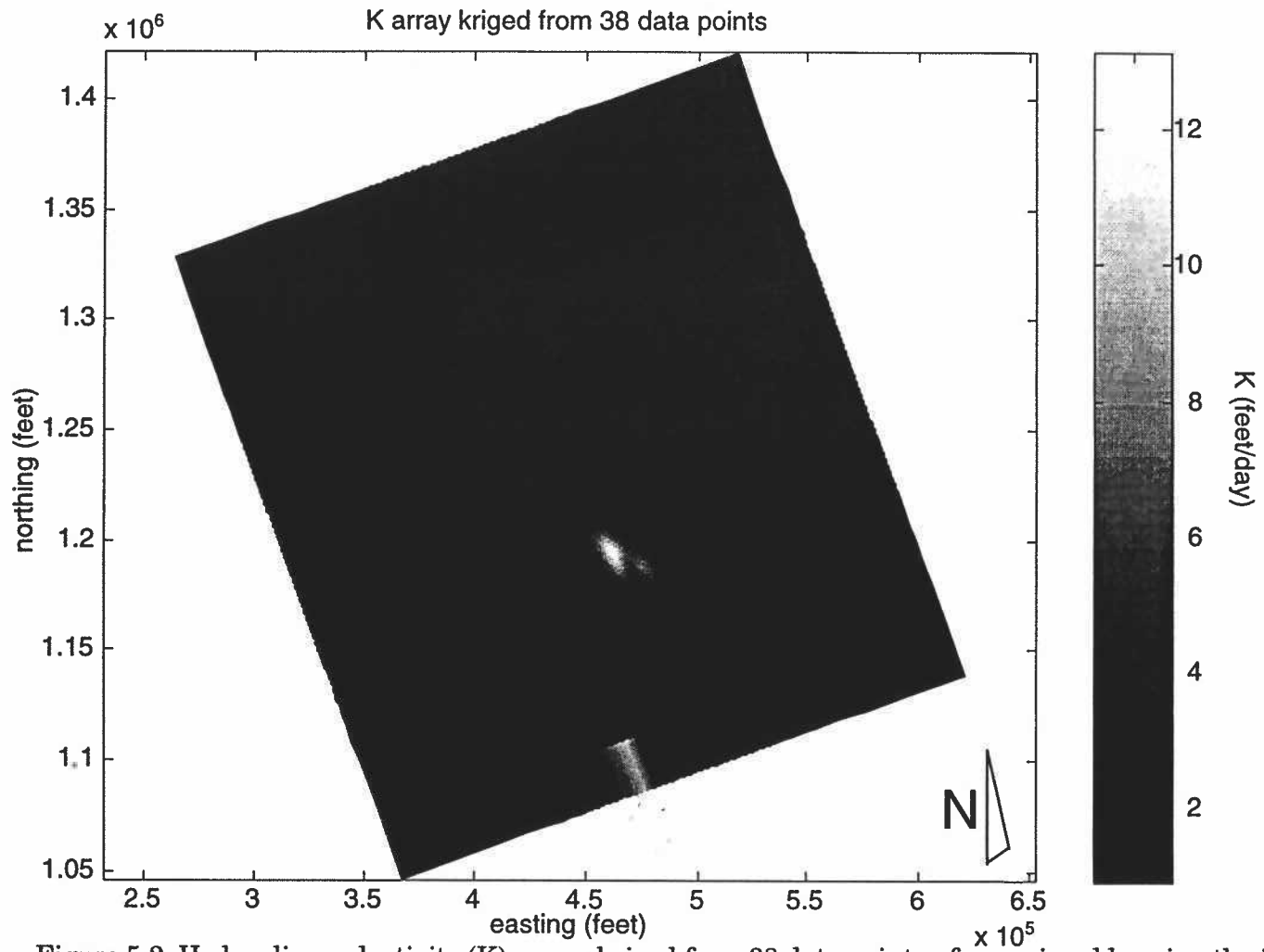


Figure 5-2 Hydraulic conductivity (K) array, kriged from 38 data points, for use in addressing the issue of heterogeneity in the coal.

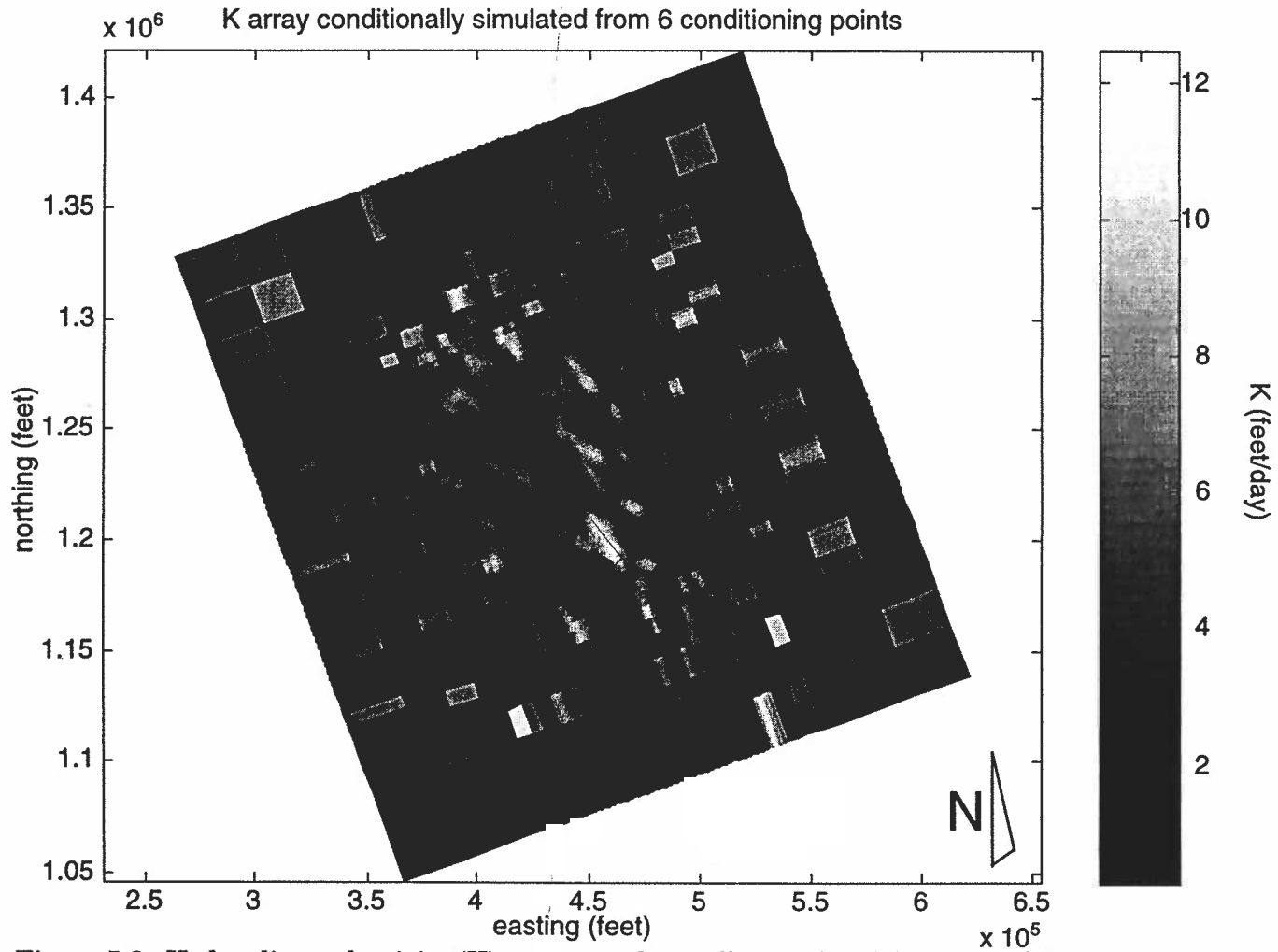


Figure 5-3. Hydraulic conductivity (K) array, conditionally simulated from 6 conditioning points, for use in addressing the issue of heterogeneity in the coal.

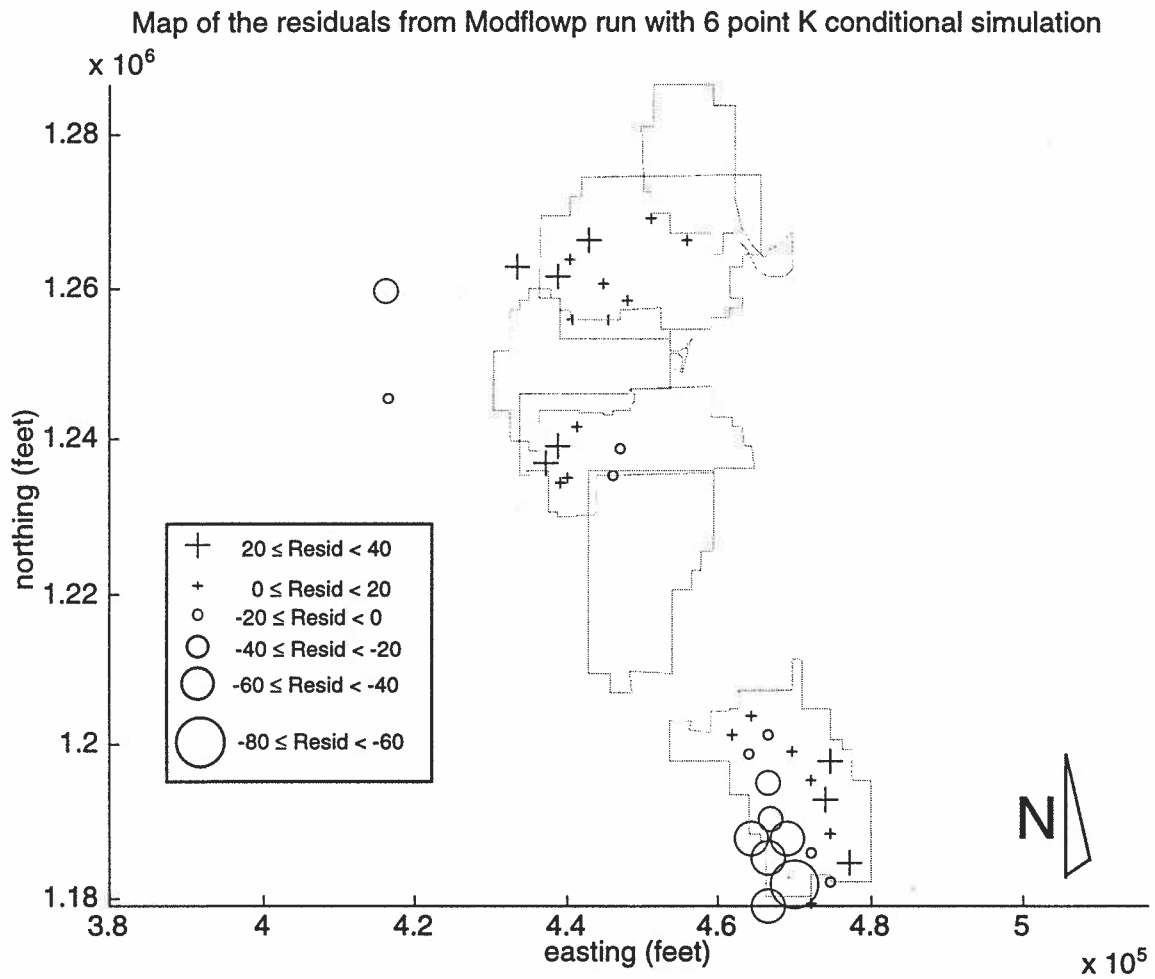


Figure 5-4. Residuals resulting from Modflow run with coal K array conditionally simulated from 6 conditioning points.

calibration (Figure 5-5). The residuals from this run are shown in figure 5-6. The magnitudes of the conditioning points used in the conditional simulations were somewhat arbitrary. Where a high positive residual was observed, it was replaced with a conditioning point of 10 feet/day, where a low negative residual was observed, it was replaced with a conditioning point of 1 foot/day.

The conditional simulation technique allowed simulation of arrays of heterogeneous hydraulic conductivity with the same mean, variance, statistical distribution and spatial correlation structure as that observed in the aquifer test data. In addition, the simulated conductivity surfaces also interpolated the known aquifer test values.

In these simulations CH was fixed at 4160 feet. Models were run using the best-fit results of chapter 4. A one zone KV equal to $4.5E-6$ feet/day was used first, a two zone KV equal to $1E-6$ and $5E-6$ feet/day was used second, and a three zone KV equal to $5E-6$, $5E-6$ and $5E-7$ feet/day was used third.

In order to draw a more reasonable picture of the system, the calibration wells for this portion of the study were limited to the forty wells found within the fully refined area of the model grid. Seventeen wells were discounted because they were located in unrefined grid cells. As a test of how this would affect the root mean squared (rms) error for subsequent models, the best fit scenario from chapter 4 with three zone KV was run with the forty calibration wells. The root mean squared error for this run improved by 17.67 feet, from 42.13 feet to 24.46 feet.

III. Results

Complete results of these simulations are presented in table 5-1. The results were similar no matter which configuration of the confining layer was used. The kriged K array yielded rms errors of approximately 29 feet. The K array conditionally simulated with six points yielded rms errors of approximately 28 feet. The K array conditionally simulated with 16 points yielded rms errors in the neighborhood of 22 feet. Mean residuals ranged from 7.79 to -2.00 feet. The budget discrepancies ranged from -1.26 to -0.85% . The sand lens residuals were in the vicinity of -35 to -50 feet. The heads calculated with the 16 point conditionally simulated K array for layers 1 and 2 are shown in figures 5-7 and 5-8.

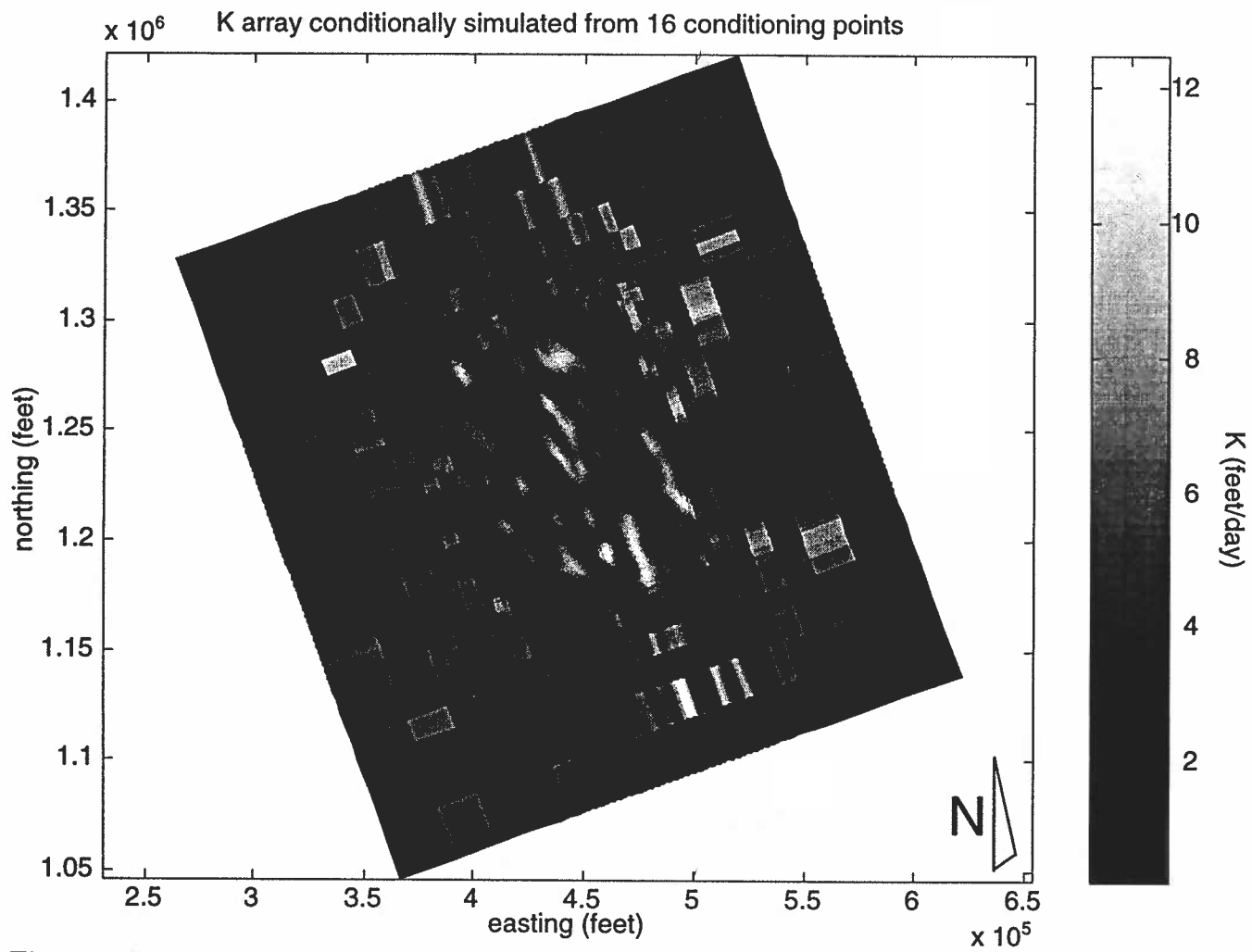


Figure 5-5. Hydraulic conductivity (K) array, conditionally simulated from 16 conditioning points, for use in addressing the issue of heterogeneity in the coal.

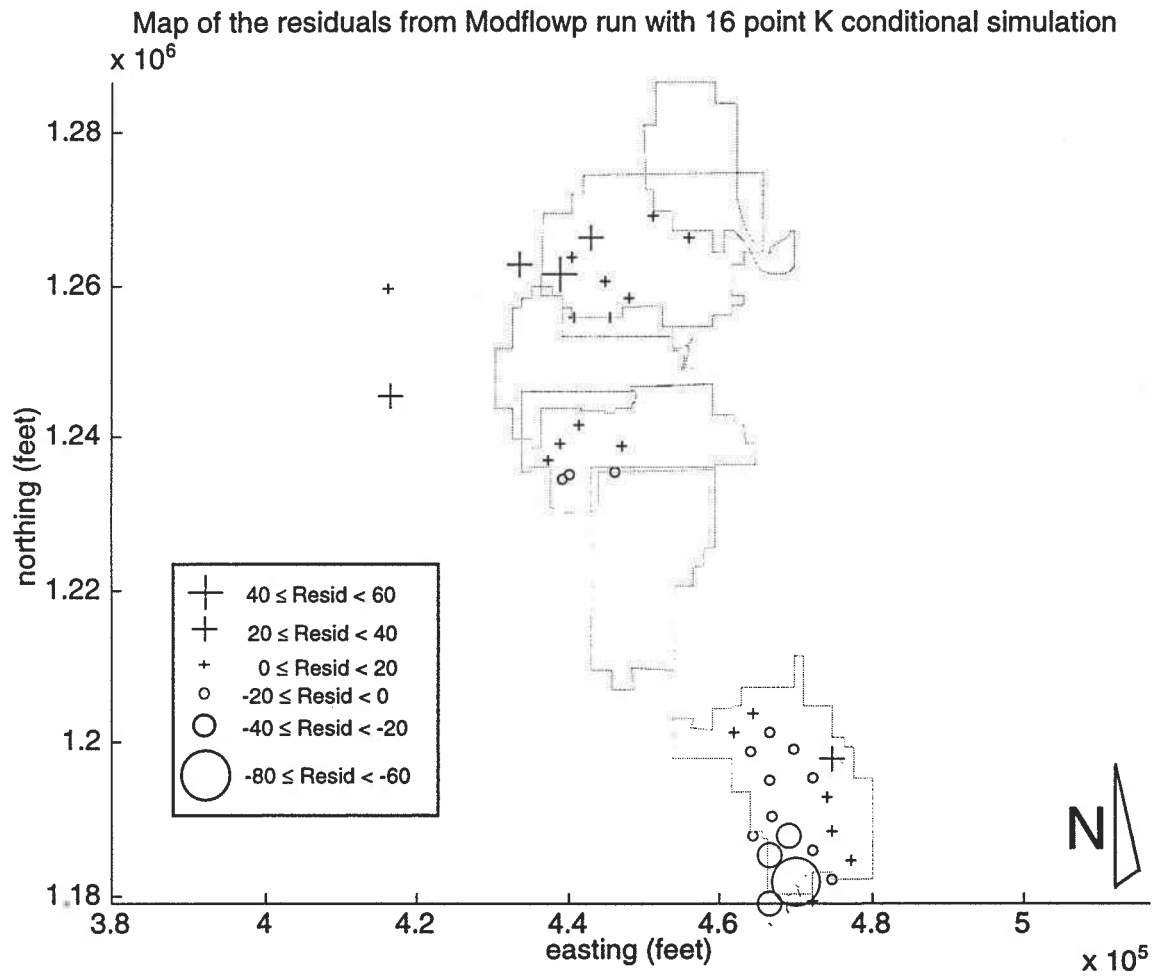


Figure 5-6. Residuals resulting from Modflow run with coal K array conditionally simulated from 16 conditioning points.

Table 5-1. Results from investigations of heterogeneous coal

CH=4160

simulation no.	coal K array	KV zone 1 (feet/day)	KV zone 2 (feet/day)	KV zone 3 (feet/day)	sum of the mean squared residuals	residual (feet)	budget discrepan cy (%)	sand lens resid. #1	sand lens resid. #2	rmse (feet)
1	kriged	4.50E-06	NA	NA	33494	7.79	-0.86	-33.0	-49.1	28.9
2	kriged	1.00E-06	5.00E-06	NA	33658	7.52	-0.88	-34.6	-51.3	29.0
3	kriged	5.00E-06	5.00E-06	5.00E-07	33119	7.61	-0.85	-34.0	-48.2	28.8
4	6pt. cond. sim.	4.50E-06	NA	NA	30598	-1.82	-1.26	-33.9	-50.8	27.7
5	6pt. cond. sim.	1.00E-06	5.00E-06	NA	31100	-2.08	-1.24	-35.3	-52.9	27.9
6	6pt. cond. sim.	5.00E-06	5.00E-06	5.00E-07	30430	-2.00	-1.25	-34.8	-50.0	27.6
7	16pt. cond. sim.	4.50E-06	NA	NA	20014	0.05	-1.04	-34.3	-50.6	22.4
8	16pt. cond. sim.	1.00E-06	5.00E-06	NA	20403	-0.23	-1.04	-35.8	-52.7	22.6
9	16pt. cond. sim.	5.00E-06	5.00E-06	5.00E-07	19798	-0.14	-1.03	-35.2	-49.8	22.2

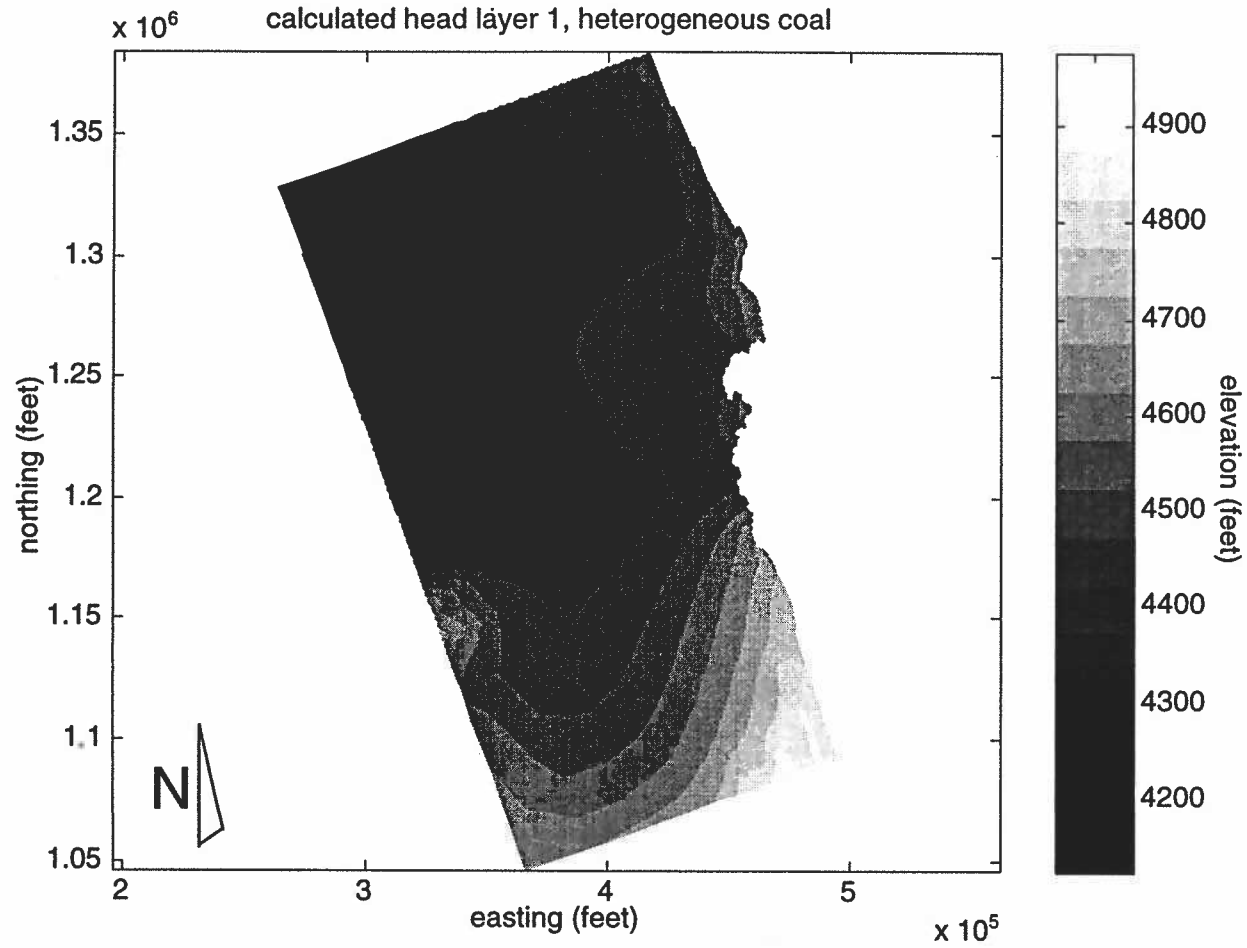


Figure 5-7. Head calculated with heterogeneous coal, layer 1; heterogeneous coal, heterogeneous transition zone, non-clinker cropline cells inactive, $KV = 4.5E-06$ feet/day. Coal K array conditionally simulated with 16 conditioning points.

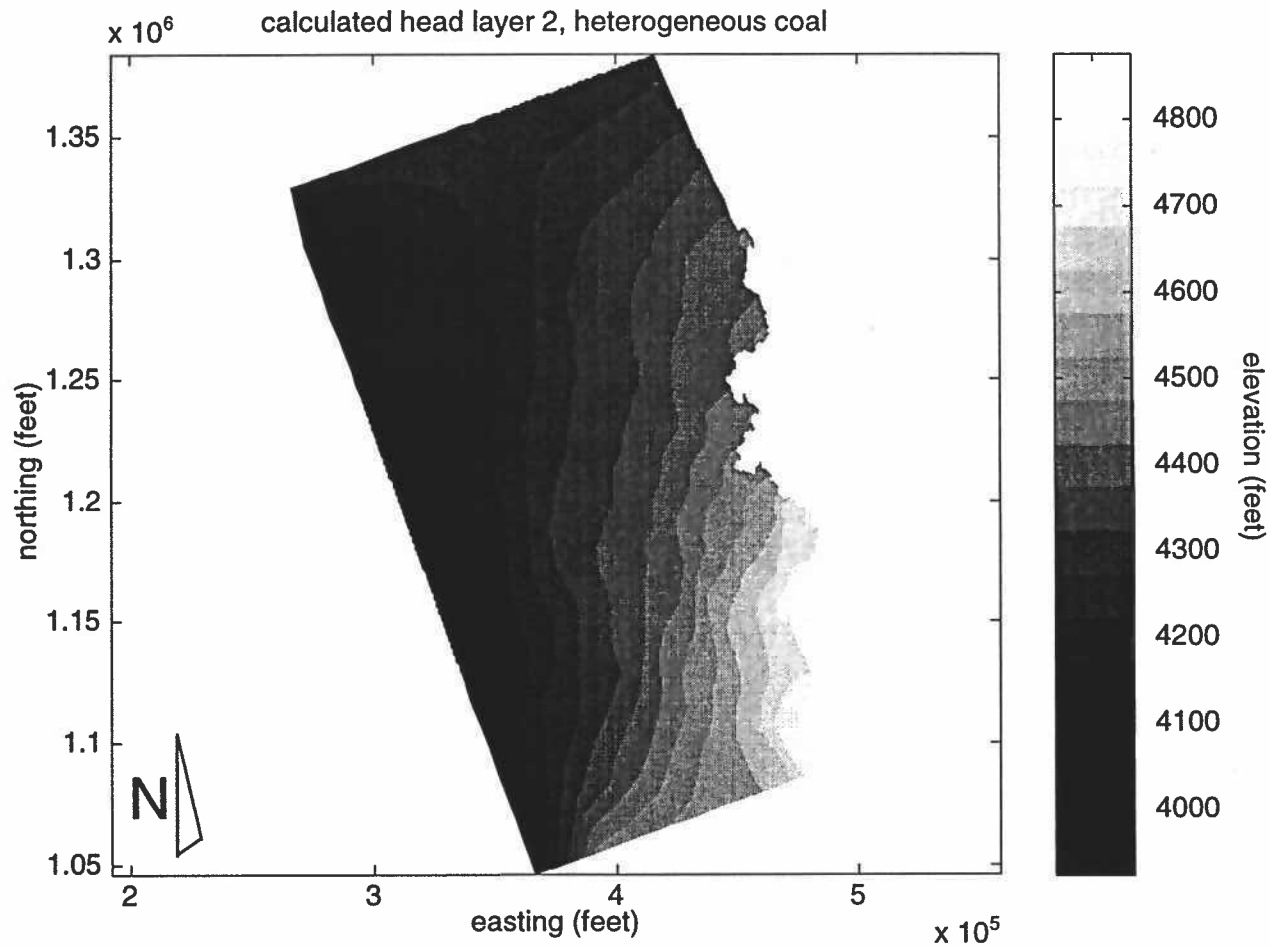


Figure 5-8. Head in layer 2 calculated with heterogeneous coal; heterogeneous coal, heterogeneous transition zone, non-clinker cropline cells inactive, $KV = 4.5E-06$ feet/day. Coal K array conditionally simulated with 16 conditioning points.

IV. Conclusions

It is fair to say that a heterogeneous coal layer improves calibration. The method used to show this was somewhat arbitrary, being based loosely on a kriged K array. The conditioning points were located at points where high magnitude residuals were found. The magnitude of the conditioning points was also arbitrary. It is intuitive that a coal heterogeneity based on more complete observation of the aquifer parameters and including some knowledge of the structure of the layer would result in an even better fit.

Chapter 6. Estimation of vertical hydraulic conductivity given best estimate heterogeneous coal.

I. Introduction

As was demonstrated in chapter 5, the inclusion of some degree of heterogeneity in the coal improves the calibration of the model. However, using estimates of KV from models constructed with homogeneous coal yielded budget discrepancies and sand lens residuals which were relatively high. Estimation of KV, given heterogeneous coal, should result in lower budget discrepancies and sand lens residuals.

II. Method

The procedure for finding the best-fit KV for the heterogeneous coal layer paralleled the procedure for finding the best fit KV for the homogeneous coal layer. The procedure included testing a grid of plausible KV values in one, two, and three zones. The coal K array used in these simulations was the array conditionally simulated from 16 points.

III. Results

One KV zone

Results of these simulations are shown in figures 6-1 and 6-2, and in table 6-1. The best fit for this scenario occurs with a KV of $9E-6$ feet/day, and results in a root mean squared error of 19.6 feet, a budget discrepancy of -0.80% , and a mean sand lens residual of 16.1 feet. The heads calculated in this case for layers 1 and 2 are shown in figures 6-3 and 6-4.

Two KV zones

Results of these simulations are shown in figures 6-5 to 6-7, and in table 6-2. The best fit for this scenario occurs with a KV of zone 1 equal to $1E-6$ feet/day and a KV of zone 2 equal to $1.25E-5$ feet/day. These values result in a root mean squared error of 19.4 feet, a budget discrepancy of -0.73% , and a mean sand lens residual of 13.4 feet.

Three KV zones

Results of these simulations are shown in figures 6-8 to 6-10, and in table 6-3. The best fit for this scenario occurs with a zone 1 KV of $1E-6$ feet/day, a zone 2 KV of $1.25E-5$ feet/day,

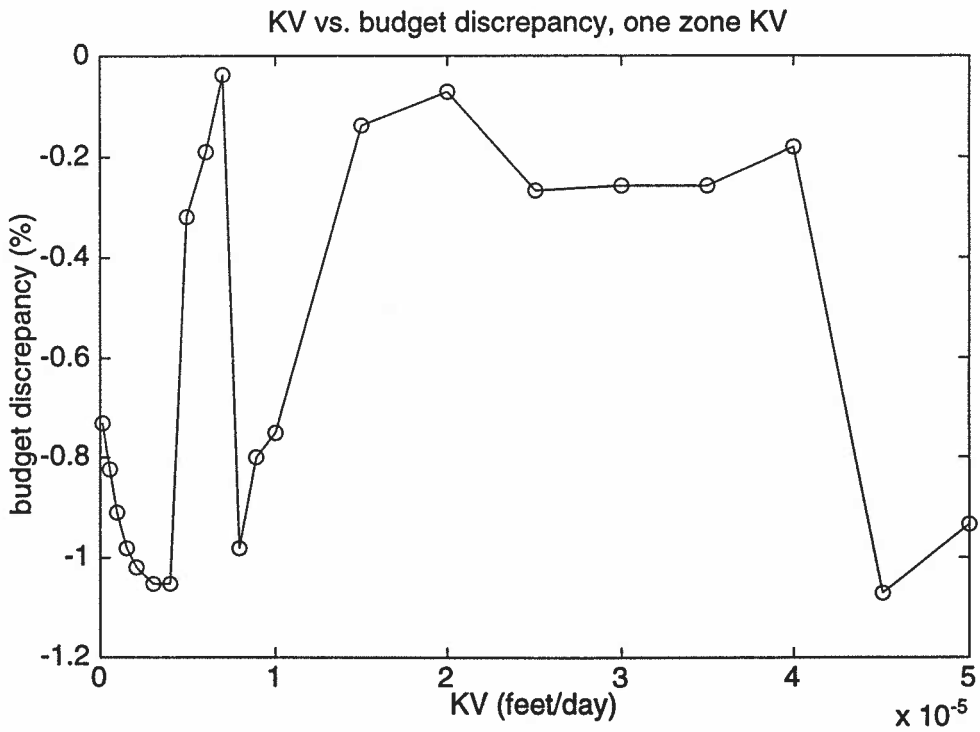
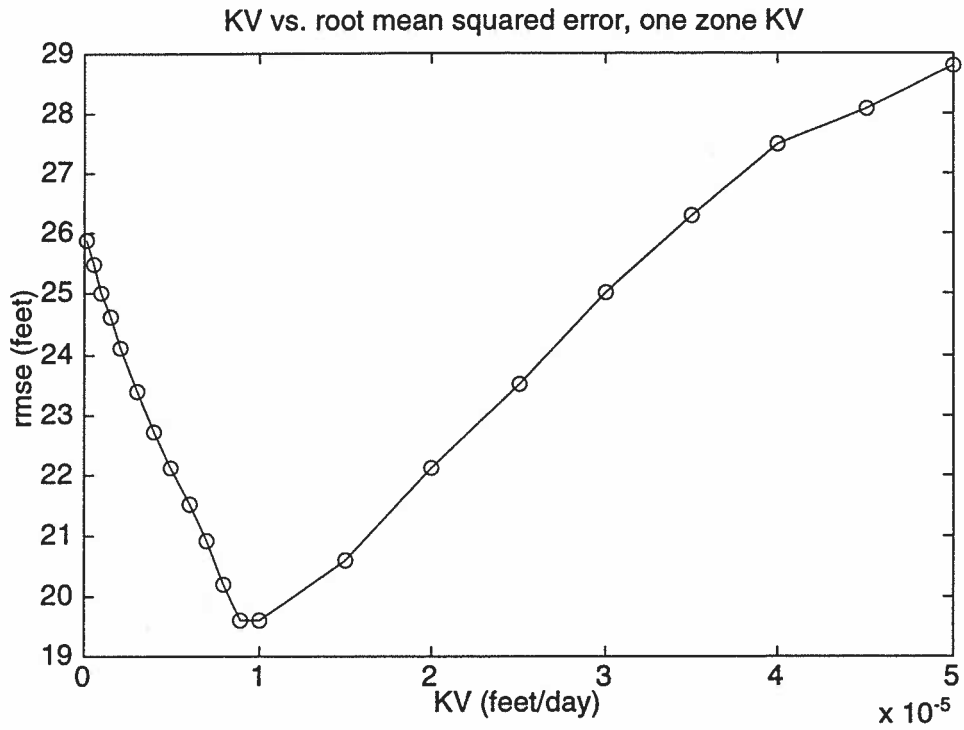


Figure 6-1. KV vs. rmse (root mean squared error) and budget discrepancy. KV is in one zone only, and the coal is heterogeneous.

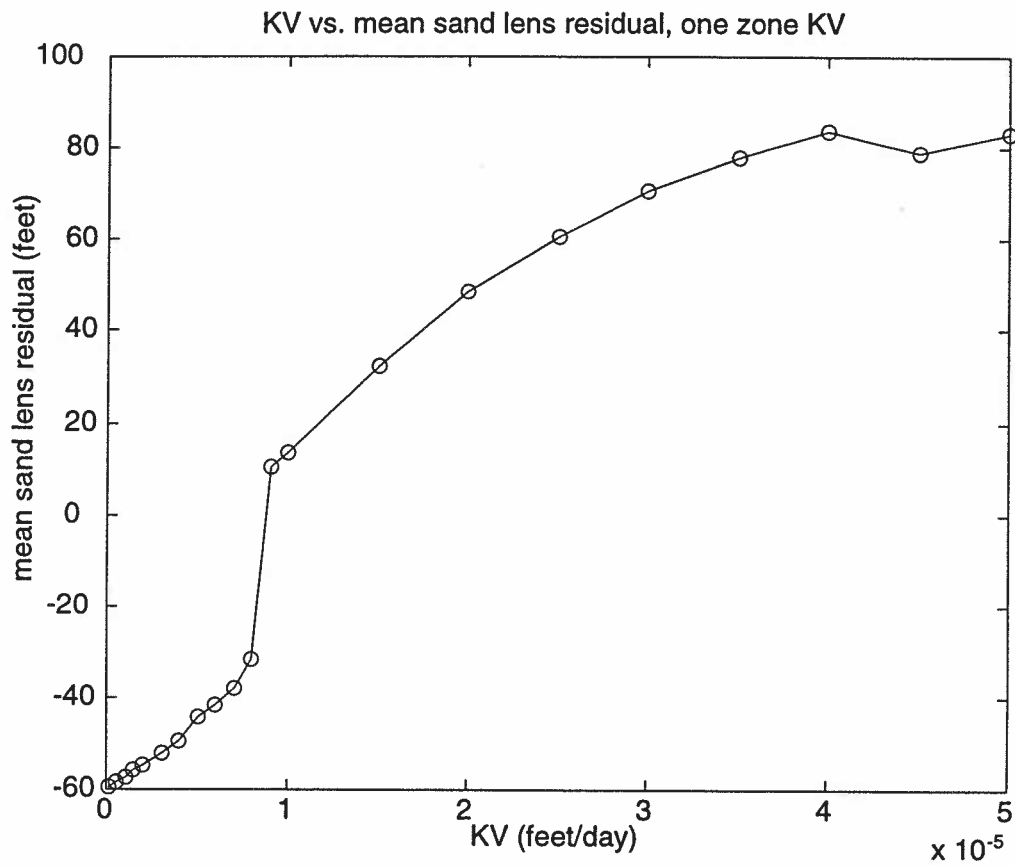


Figure 6-2. KV vs. mean sand lens residual. KV is in one zone and the coal is heterogeneous.

Table 6-1. Results from KV estimation, one zone

CH=4160, heterogeneous coal

simulation no.	KV zone 1 (feet/day)	sum of the squared residuals	mean residual (feet)	budget discrepancy (%)	sand lens resid. #1	sand lens resid. #2	rmse (feet)
1	5.00E-05	33074	-5.58	-0.93	81.5	74.2	28.8
2	4.50E-05	31565	-5.27	-1.07	78.6	71.1	28.1
3	4.00E-05	30278	-3.12	-0.18	85.9	76.2	27.5
4	3.50E-05	27768	-2.51	-0.26	81.3	71.7	26.3
5	3.00E-05	25042	-1.94	-0.26	75.0	65.5	25.0
6	2.50E-05	22066	-1.38	-0.27	66.6	57.3	23.5
7	2.00E-05	19530	-0.91	-0.07	55.9	46.5	22.1
8	1.50E-05	16899	-0.37	-0.14	41.7	31.8	20.6
9	1.00E-05	15363	0.14	-0.75	24.9	13.9	19.6
10	9.00E-06	15407	0.28	-0.80	21.7	10.5	19.6
11	8.00E-06	16294	-0.77	-0.98	-21.3	-32.1	20.2
12	7.00E-06	17502	-0.17	-0.04	-27.4	-39.0	20.9
13	6.00E-06	18447	0.00	-0.19	-30.0	-42.9	21.5
14	5.00E-06	19504	0.22	-0.32	-32.6	-46.6	22.1
15	4.00E-06	20594	0.22	-1.05	-35.5	-52.2	22.7
16	3.00E-06	21857	0.63	-1.05	-38.0	-55.5	23.4
17	2.00E-06	23298	1.17	-1.02	-40.6	-58.9	24.1
18	1.50E-06	24111	1.50	-0.98	-42.1	-60.6	24.6
19	1.00E-06	25005	1.87	-0.91	-43.6	-62.3	25.0
20	5.00E-07	26004	2.29	-0.82	-45.3	-64.1	25.5
21	1.00E-07	26898	2.67	-0.73	-46.7	-65.5	25.9

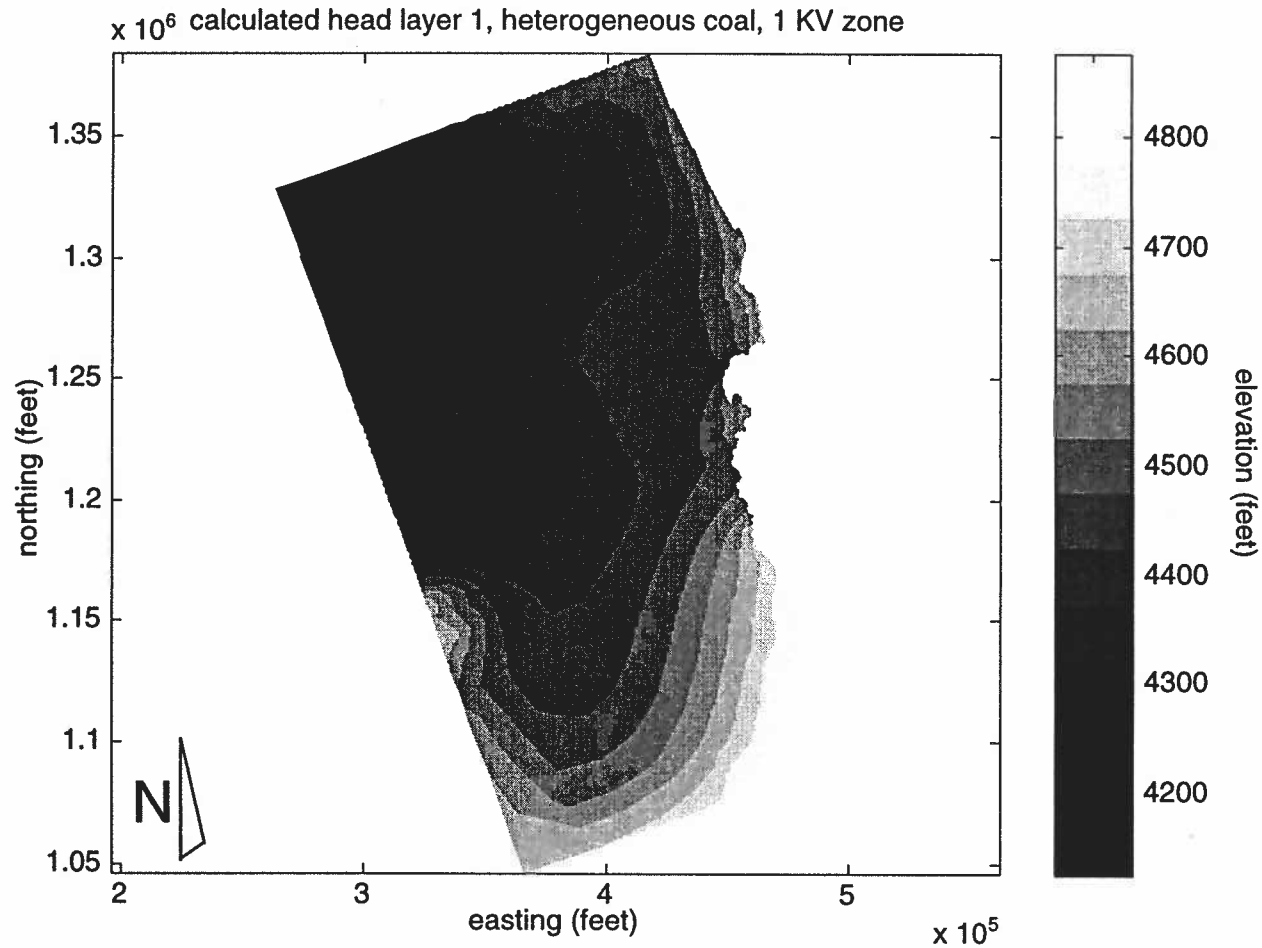


Figure 6-3. Head in layer 1 calculated with heterogeneous coal; heterogeneous coal, heterogeneous transition zone, non-clinker cropline cells inactive, KV = 9.0E-06 feet/day. Coal K array conditionally simulated with 16 conditioning points.

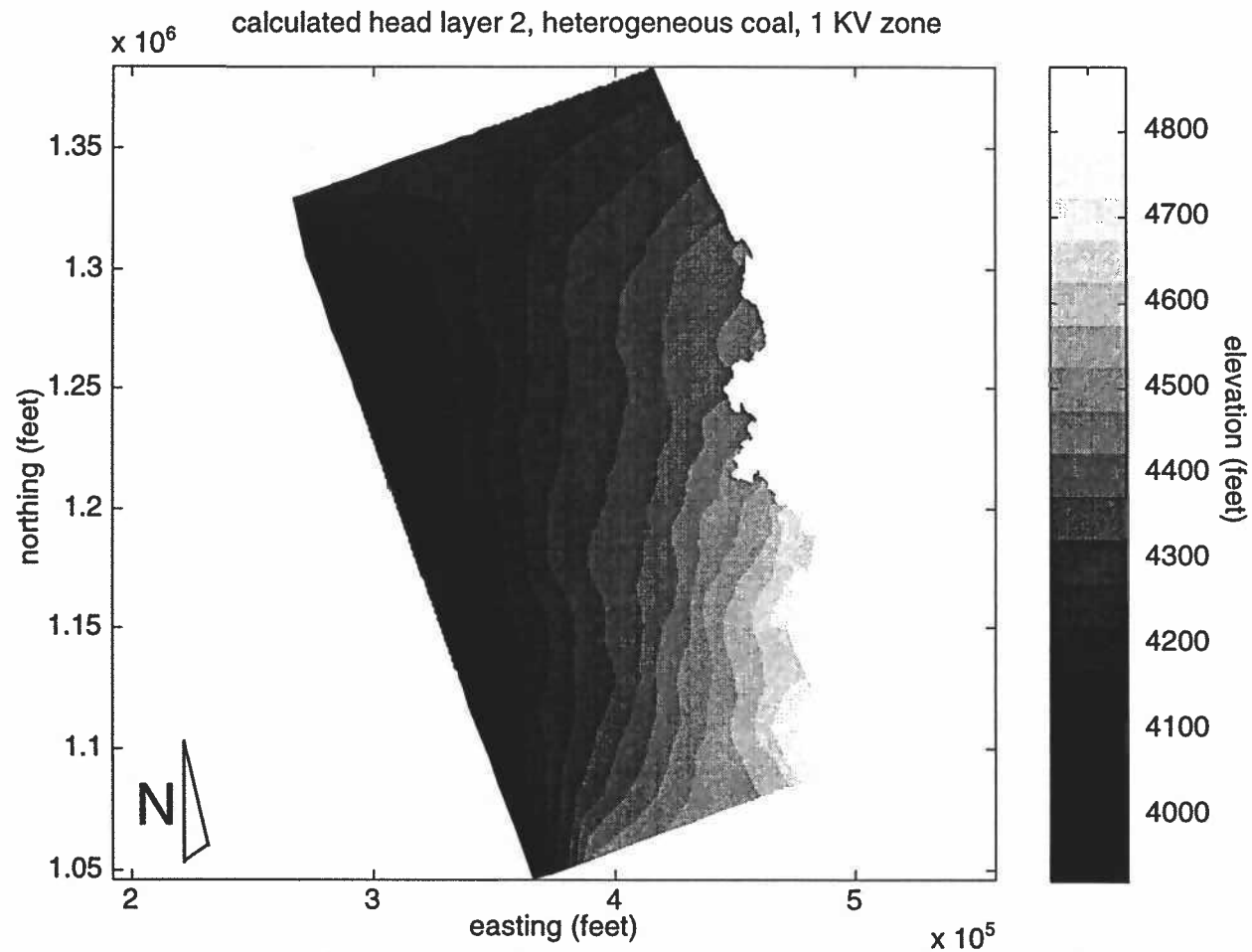


Figure 6-4. Head in layer 2 calculated with heterogeneous coal; heterogeneous coal, heterogeneous transition zone, non-clinker cropline cells inactive, $KV = 9.0E-06$ feet/day. Coal K array conditionally simulated with 16 conditioning points.

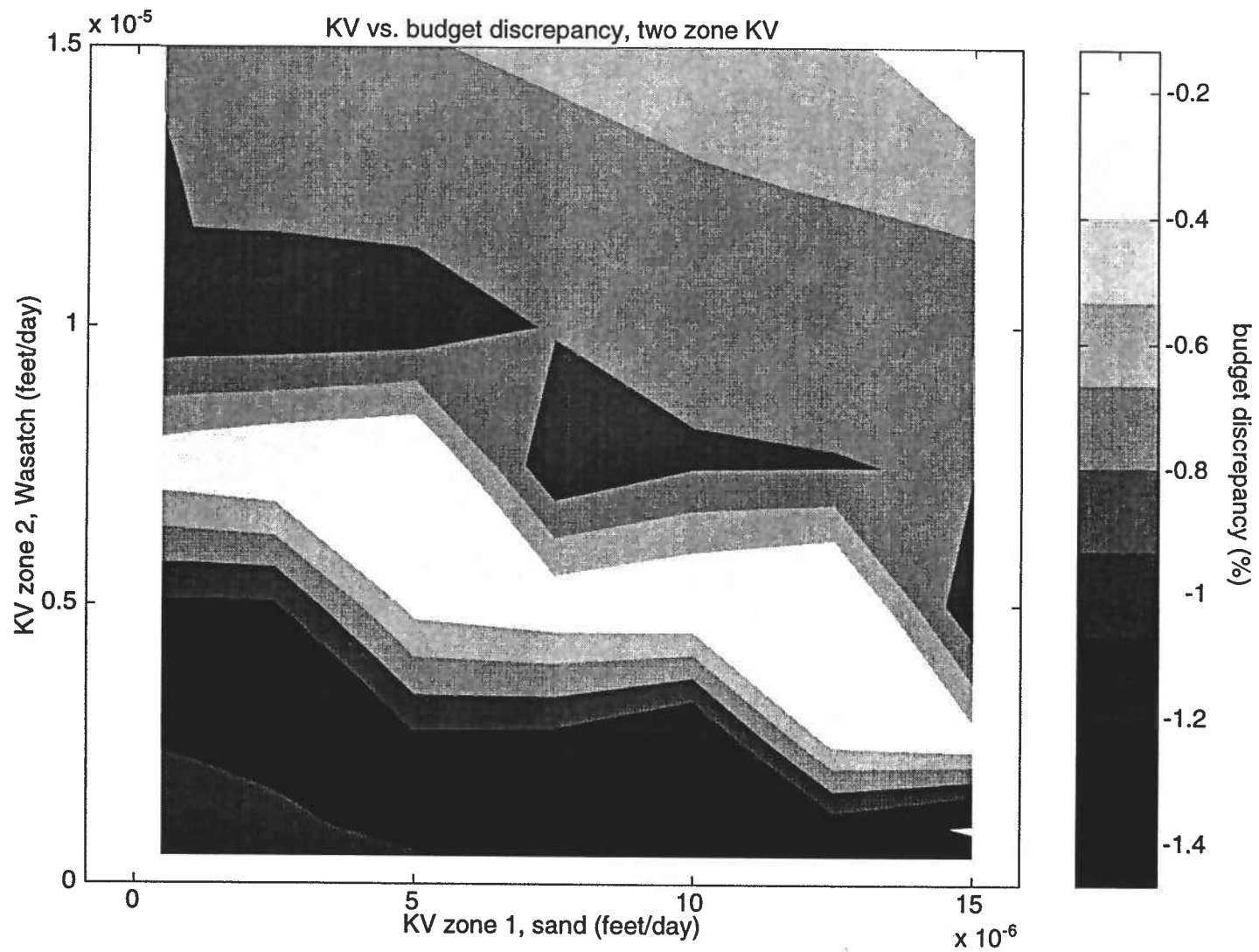


Figure 6-5. Topography of the solution, in terms of budget discrepancy, for the estimation of KV in two zones with heterogeneous coal.

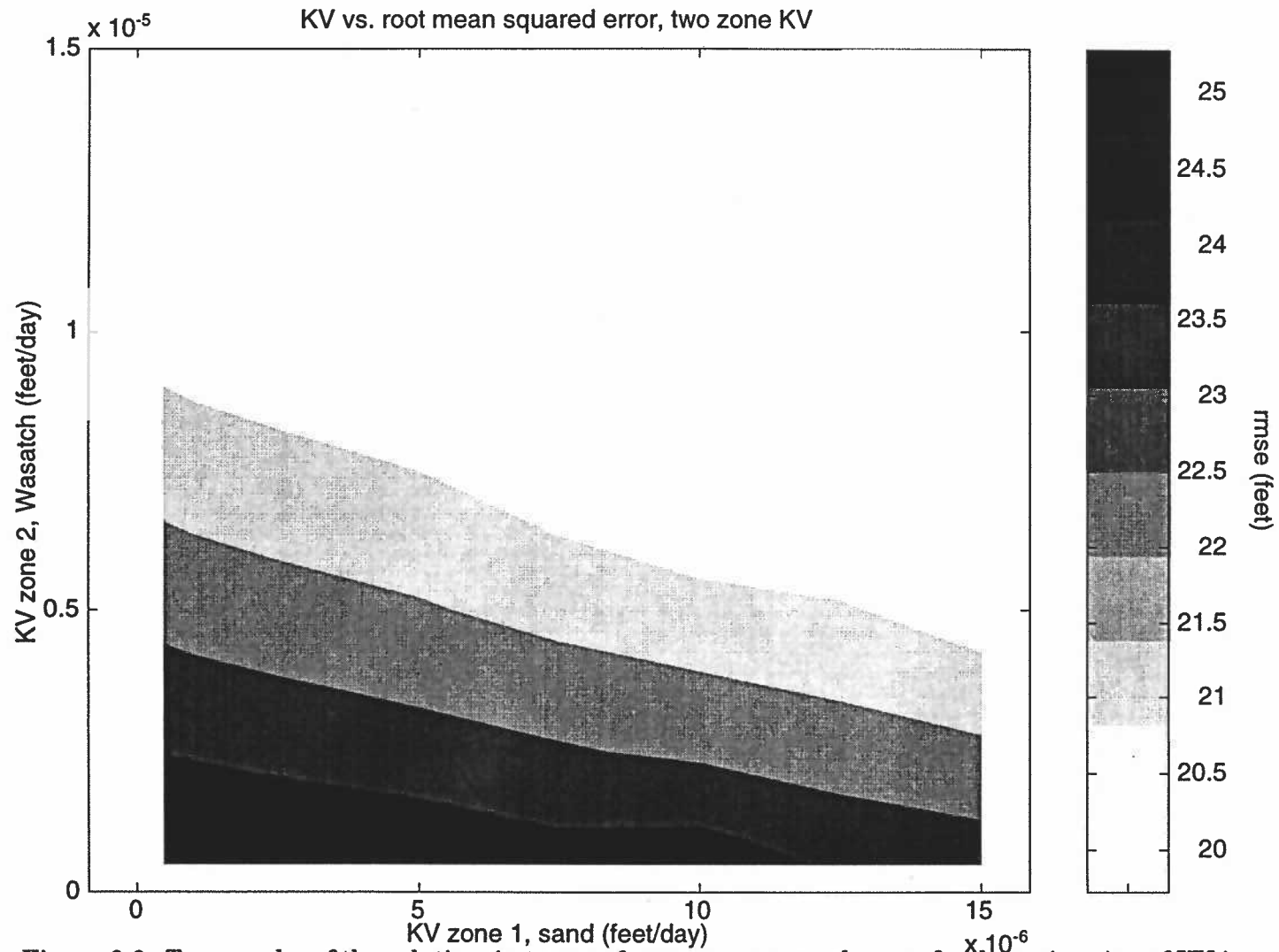


Figure 6-6. Topography of the solution, in terms of root mean squared error, for the estimation of KV in two zones with heterogeneous coal.

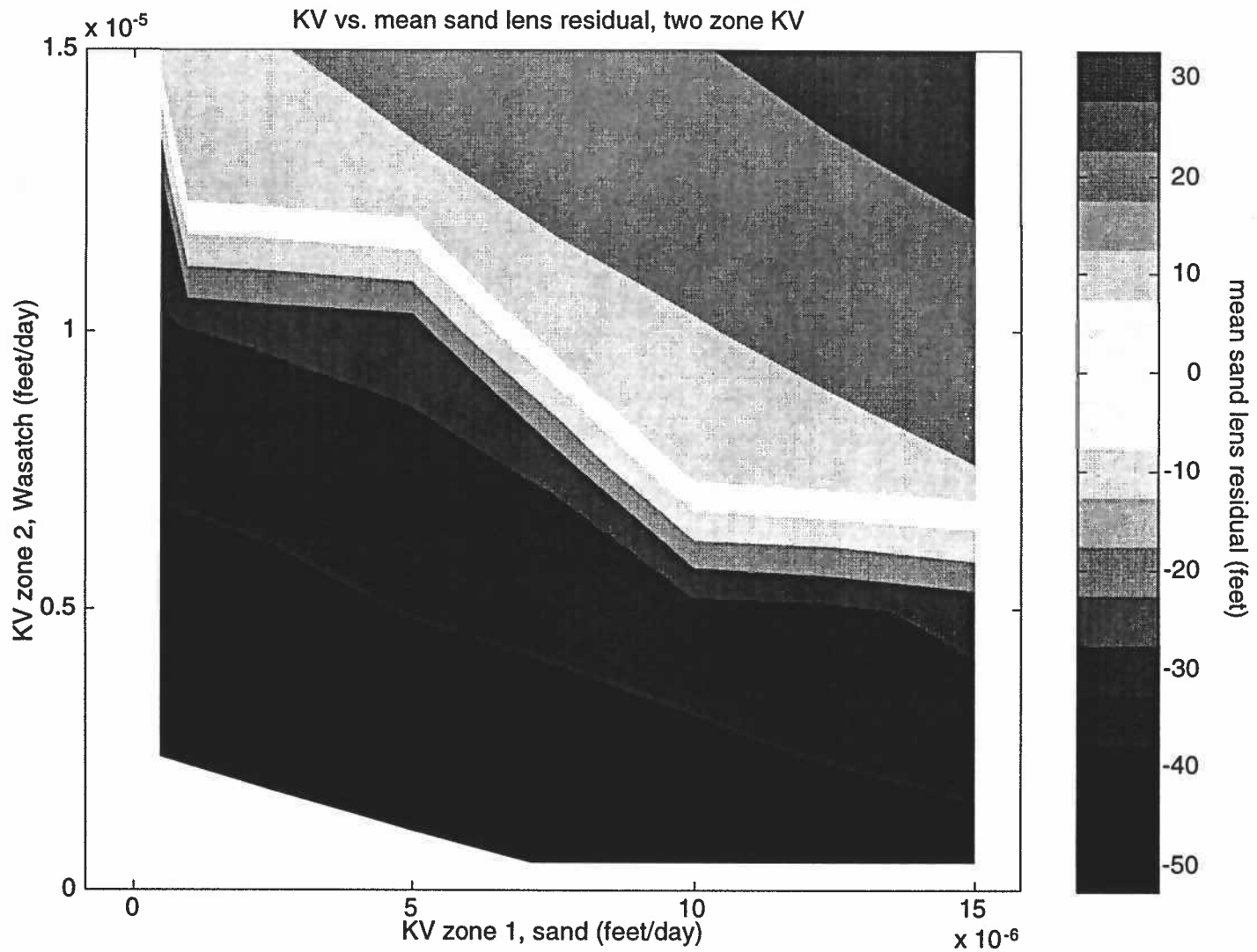


Figure 6-7. Topography of the solution, in terms of mean sand lens residual, for the estimation of KV in two zones with heterogeneous coal.

Table 6-2. Results from KV estimation, two zones

CH=4160, heterogeneous coal

simulation no.	KV zone 1 (feet/day)	KV zone 2 (feet/day)	sum of the mean		budget discrepancy (%)	sand lens		rmse (feet)
			squared residuals	residual (feet)		resid. #1	resid. #2	
1	1.50E-05	1.50E-05	16899	-0.37	-0.14	41.7	31.8	20.6
2	1.50E-05	1.25E-05	15918	0.06	-0.55	36.3	26.1	19.9
3	1.50E-05	1.00E-05	15654	0.45	-0.69	30.8	20.3	19.8
4	1.50E-05	7.50E-06	15683	0.99	-0.78	25.2	14.2	19.8
5	1.50E-05	5.00E-06	16794	0.47	-0.98	-21.1	-31.8	20.5
6	1.50E-05	2.50E-06	19735	1.57	-0.29	-30.4	-43.3	22.2
7	1.50E-05	1.00E-06	21596	2.17	-1.45	-34.5	-49.7	23.2
8	1.50E-05	5.00E-07	22211	2.30	-1.16	-36.0	-52.7	23.6
9	1.25E-05	1.50E-05	16042	-0.47	-0.49	38.8	27.7	20.0
10	1.25E-05	1.25E-05	15634	-0.10	-0.59	33.1	22.6	19.8
11	1.25E-05	1.00E-05	15481	0.29	-0.72	27.9	17.0	19.7
12	1.25E-05	7.50E-06	15615	0.85	-0.81	22.4	11.3	19.8
13	1.25E-05	5.00E-06	17808	0.67	-0.04	-26.7	-37.9	21.1
14	1.25E-05	2.50E-06	20301	1.44	-0.37	-32.3	-46.0	22.5
15	1.25E-05	1.00E-06	22056	1.92	-1.14	-36.3	-53.1	23.5
16	1.25E-05	5.00E-07	22810	2.25	-1.15	-37.6	-54.8	23.9
17	1.00E-05	1.50E-05	15720	-0.64	-0.53	34.7	24.2	19.8
18	1.00E-05	1.25E-05	15410	-0.27	-0.62	30.0	19.3	19.6
19	1.00E-05	1.00E-05	15363	0.14	-0.75	24.9	13.9	19.6
20	1.00E-05	7.50E-06	15592	0.71	-0.82	19.7	8.4	19.7
21	1.00E-05	5.00E-06	18354	0.50	-0.15	-28.8	-40.9	21.4
22	1.00E-05	2.50E-06	20818	1.22	-1.39	-34.3	-49.5	22.8
23	1.00E-05	1.00E-06	23430	2.22	-1.11	-39.2	-56.8	24.2
24	7.50E-06	1.50E-05	15461	-0.81	-0.57	31.5	20.8	19.7
25	7.50E-06	1.25E-05	15246	-0.44	-0.66	26.9	15.9	19.5
26	7.50E-06	1.00E-05	15298	-0.01	-0.78	22.8	10.8	19.6
27	7.50E-06	7.50E-06	16687	-0.68	-0.99	-22.8	-34.2	20.4
28	7.50E-06	5.00E-06	18920	0.35	-0.24	-30.8	-43.8	21.7
29	7.50E-06	2.50E-06	21329	0.97	-1.09	-36.1	-53.0	23.1
30	7.50E-06	1.00E-06	23284	1.85	-1.09	-39.5	-57.3	24.1
31	7.50E-06	5.00E-07	24070	2.21	-1.06	-40.7	-58.8	24.5
32	5.00E-06	1.50E-05	15265	-0.98	-0.61	28.3	17.4	19.5
33	5.00E-06	1.25E-05	15141	-0.60	-0.69	23.9	12.7	19.5
34	5.00E-06	1.00E-05	15927	-1.40	-0.95	-20.4	-30.4	20.0
35	5.00E-06	7.50E-06	17623	-0.42	-0.07	-28.2	-40.1	21.0
36	5.00E-06	5.00E-06	19504	0.22	-0.32	-32.6	-46.6	22.1
37	5.00E-06	2.50E-06	21932	0.92	-1.07	-37.7	-55.1	23.4
38	5.00E-06	1.00E-06	23927	1.84	-1.04	-41.0	-59.2	24.5
39	5.00E-06	5.00E-07	24735	2.22	-0.99	-42.3	-60.7	24.9
40	2.50E-06	1.50E-05	15130	-1.14	-0.64	25.2	14.0	19.4
41	2.50E-06	1.25E-05	15091	-0.76	-0.72	20.9	9.5	19.4
42	2.50E-06	1.00E-05	16462	-1.55	-0.97	-22.9	-34.3	20.3
43	2.50E-06	7.50E-06	18196	-0.58	-0.17	-30.2	-43.2	21.3
44	2.50E-06	5.00E-06	20048	-0.18	-1.03	-34.8	-51.3	22.4
45	2.50E-06	2.50E-06	22551	0.89	-1.04	-39.3	-57.2	23.7
46	2.50E-06	1.00E-06	24593	1.85	-0.97	-42.6	-61.2	24.8
47	2.50E-06	5.00E-07	25427	2.25	-0.91	-44.0	-62.6	25.2
48	1.00E-06	1.50E-05	15077	-1.24	-0.66	23.4	12.0	19.4
49	1.00E-06	1.25E-05	15085	-0.85	-0.73	19.1	7.7	19.4
50	1.00E-06	1.00E-05	16798	-1.64	-0.97	-24.4	-36.3	20.5
51	1.00E-06	7.50E-06	18548	-0.67	-0.23	-31.4	-44.9	21.5
52	1.00E-06	5.00E-06	20403	-0.23	-1.04	-35.8	-52.7	22.6
53	1.00E-06	2.50E-06	22930	0.87	-1.02	-40.2	-58.4	23.9
54	1.00E-06	1.00E-06	25005	1.87	-0.91	-43.6	-62.3	25.0
55	1.00E-06	5.00E-07	25858	2.28	-0.84	-44.9	-63.7	25.4
56	5.00E-07	1.50E-05	15064	-1.28	-0.66	22.8	11.4	19.4
57	5.00E-07	1.25E-05	15876	-2.16	-0.92	-20.6	-31.0	19.9
58	5.00E-07	1.00E-05	16913	-1.67	-0.97	-24.9	-36.9	20.6
59	5.00E-07	7.50E-06	18667	-0.70	-0.25	-31.8	-45.5	21.6
60	5.00E-07	5.00E-06	20552	-0.24	-1.03	-36.1	-53.1	22.7
61	5.00E-07	2.50E-06	23057	0.87	-1.01	-40.5	-58.8	24.0
62	5.00E-07	1.00E-06	25145	1.87	-0.89	-43.9	-62.7	25.1
63	5.00E-07	5.00E-07	26004	2.29	-0.82	-45.3	-64.1	25.5

KV zone 3 vs. budget discrepancy for given KV in zone 1, KV zone 2=2.5E-5, 1.25E-5, 6.3E-6

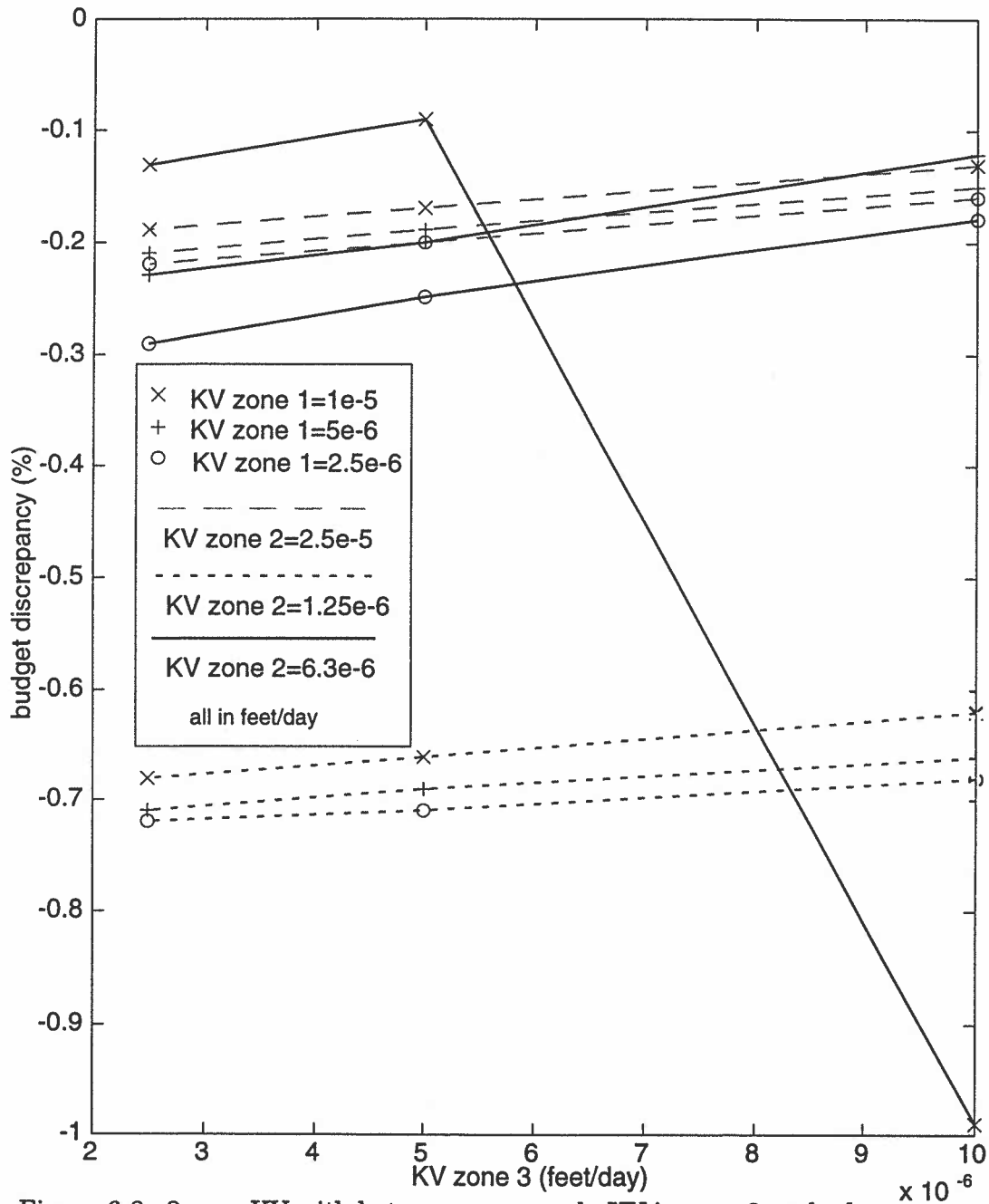


Figure 6-8. 3 zone KV with heterogeneous coal. KV in zone 3 vs. budget discrepancy. KV in zone 2 fixed as shown in figure, KV in zone 1 varies between 1e-5 and 2.5e-6. Zones 1 and 3 underlie the sand lens, zone 2 underlies the Wasatch outside of the sand lens.

KV zone 3 vs. rms error for given KV in zone 1, KV zone 2=2.5E-5, 1.25E-5, 6.3E-6

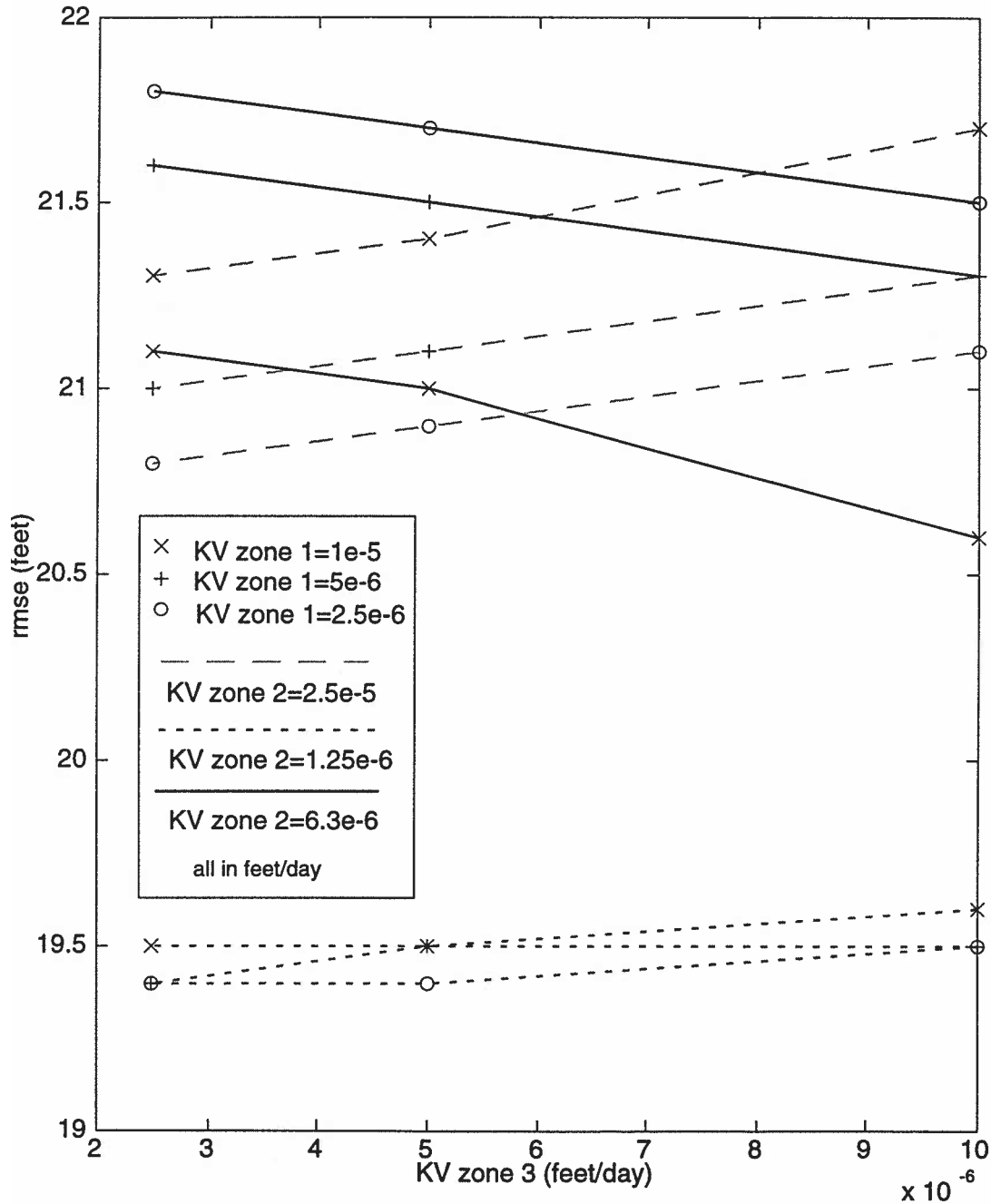


Figure 6-9. 3 zone KV with heterogeneous coal. KV in zone 3 vs. root mean squared error. KV in zone 2 fixed as shown in figure, KV in zone 1 varies between 1×10^{-5} and 2.5×10^{-6} . Zones 1 and 3 underlie the sand lens, zone 2 underlies the Wasatch outside of the sand lens.

KV zone 3 vs. mean sand lens residual for given KV in zone 1, KV zone 2=2.5E-5, 1.25E-5, 6.3E-6

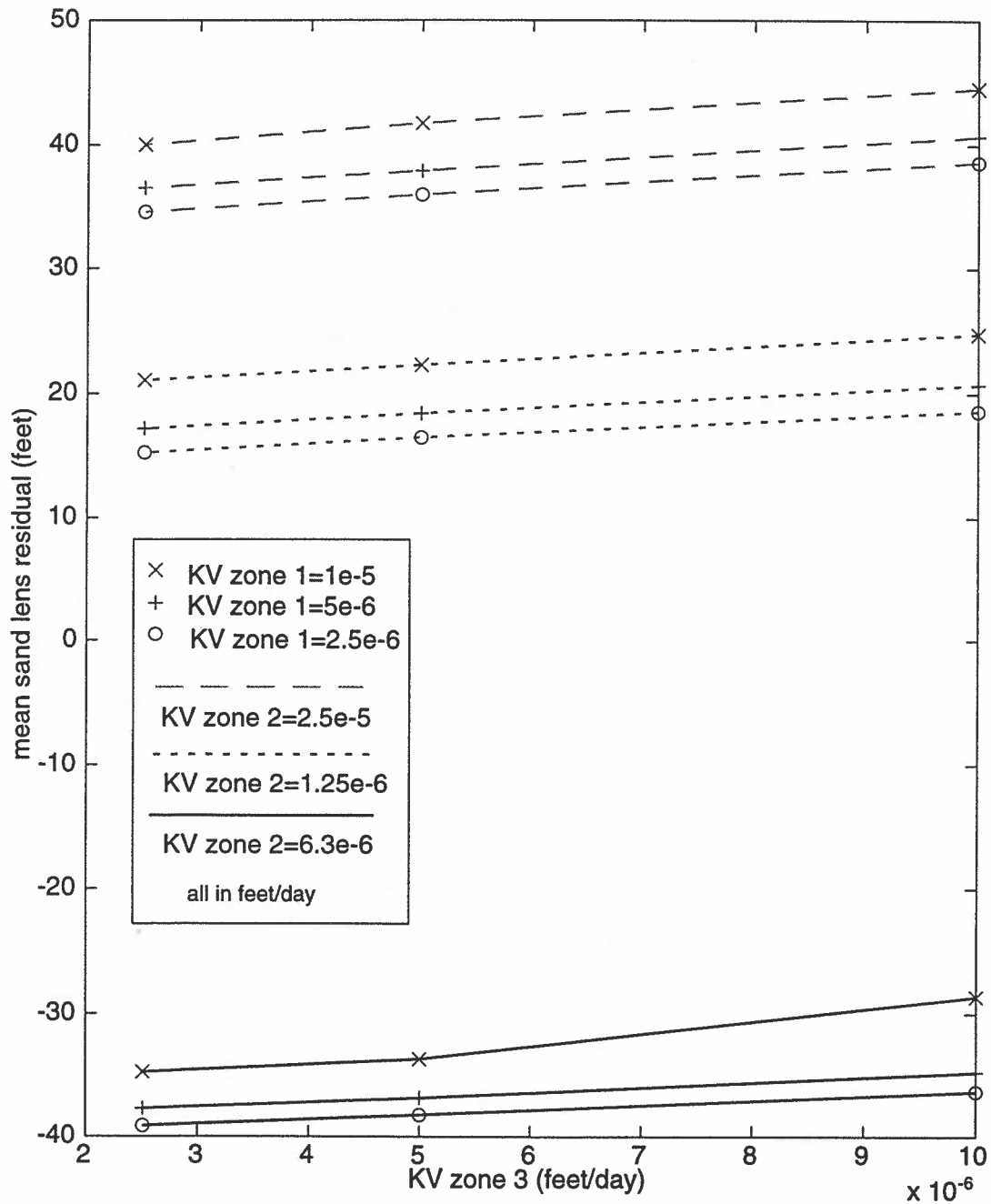


Figure 6-10. 3 zone KV with heterogeneous coal. KV in zone 3 vs. mean sand lens residual. KV in zone 2 fixed as shown in figure, KV in zone 1 varies between 1e-5 and 2.5e-6. Zones 1 and 3 underlie the sand lens, zone 2 underlies the Wasatch outside of the sand lens.

Table 6-3. Results from KV estimation, three zones

CH=4160, heterogeneous coal

simulation no.	KV zone 1 (feet/day)	KV zone 2 (feet/day)	KV zone 3 (feet/day)	sum of the mean squared residuals	mean residual (feet)	budget discrepancy (%)	sand lens resid. #1	sand lens resid. #2	rmse (feet)
1	100	250	100	18765	-2.17	-0.13	49.5	39.7	21.7
2	100	250	50	18324	-2.31	-0.17	46.4	37.2	21.4
3	100	250	25	18117	-2.38	-0.19	44.0	36.0	21.3
4	100	125	100	15410	-0.27	-0.62	30.0	19.3	19.6
5	100	125	50	15261	-0.40	-0.66	27.0	17.3	19.5
6	100	125	25	15199	-0.47	-0.68	25.5	16.4	19.5
7	100	63	100	16907	-0.21	-0.99	-22.9	-34.3	20.6
8	100	63	50	17700	0.07	-0.09	-28.9	-38.6	21.0
9	100	63	25	17890	0.01	-0.13	-30.3	-39.3	21.1
10	50	250	100	18148	-2.33	-0.15	46.2	35.2	21.3
11	50	250	50	17762	-2.47	-0.19	43.1	32.8	21.1
12	50	250	25	17583	-2.54	-0.21	41.5	31.6	21.0
13	50	125	100	15236	-0.47	-0.66	26.7	14.5	19.5
14	50	125	50	15141	-0.60	-0.69	23.9	12.7	19.5
15	50	125	25	15104	-0.66	-0.71	22.4	11.8	19.4
16	50	63	100	18079	-0.02	-0.12	-27.7	-41.9	21.3
17	50	63	50	18450	-0.13	-0.20	-30.3	-43.2	21.5
18	50	63	25	18641	-0.19	-0.23	-31.6	-43.9	21.6
19	25	250	100	17859	-2.42	-0.16	44.4	32.9	21.1
20	25	250	50	17502	-2.55	-0.20	41.3	30.5	20.9
21	25	250	25	17338	-2.62	-0.22	39.8	29.3	20.8
22	25	125	100	15186	-0.57	-0.68	25.1	12.1	19.5
23	25	125	50	15117	-0.70	-0.71	22.3	10.4	19.4
24	25	125	25	15091	-0.76	-0.72	20.9	9.5	19.4
25	25	63	100	18473	-0.13	-0.18	-28.4	-44.3	21.5
26	25	63	50	18845	-0.23	-0.25	-30.9	-45.5	21.7
27	25	63	25	19035	-0.28	-0.29	-32.2	-46.1	21.8

and a zone 3 KV of $1\text{E-}6$ feet/day. These values are identical to those determined in the two KV zone case and therefore result in the same mean residual, budget discrepancy, and mean sand lens residual.

IV. Conclusions

The improvement in rms error, budget discrepancy, and mean sand lens residual, is minimal between the three cases outlined above. Subdivision of the confining layer into two or three zones is unwarranted. This result is in agreement with Modflowp in that it shows that the calibration wells are generally insensitive to KV in zones 1 and 3. This indicates that $9.0\text{E-}6$ feet/day is the best estimate available for the vertical hydraulic conductivity in the confining layer separating the overlying Wasatch sand lens from the underlying Wyodak coal seam.

Chapter 7. Conclusions

I. Aquifer parameters

Boundaries

An understanding of boundary conditions is of paramount importance in the construction of any ground water flow model. In this study relatively little is known about the boundary conditions of the model. The conceptual model of the study domain has governed the application of boundary conditions. For example, recharge was expected from the clinker nodes on the cropline, the head gradient was expected to be to the northwest in both layers, and the head gradient was expected to be flatter than the dip of the coal layer. These conditions were set at the beginning of the modeling effort and adhered to throughout. In the absence of data in these areas this is a reasonable approach, and one that has been used previously (Peacock, 1997b). This study has shown, however, that the model can be quite sensitive to head values on the boundary, which is to be expected from the PDE being solved. Although questions were answered regarding other model parameters, they were all based on the assumption that the boundary conditions were correct. This study established boundary conditions which were plausible, but would have benefited from a better understanding of the boundary conditions.

Coal heterogeneity

The conclusion that a heterogeneous coal layer better represents the system is important. Even conditionally simulated heterogeneous coal hydraulic conductivities represent the coal better than a homogeneous mean coal K value. Although homogeneous coal might be useful in generating a first order approximation of the flow system, a better assessment of the heterogeneity of the coal and its distribution will allow for the creation of a much better model.

Vertical hydraulic conductivity of the confining layer

It is clear from the results of this study that the value given to the vertical K of the confining layer dictates whether a calibration with the Wasatch sand lens can be achieved. This study has determined that $9.0E-06$ is the best available estimate for the vertical hydraulic conductivity of the confining layer. It is interesting to note that the estimates of vertical hydraulic conductivity in the homogeneous coal case and the heterogeneous coal case differ only by a factor of two.

II. Recommendations for future study

Boundary conditions

Collection of data which will aid in the understanding of boundary conditions should be the first priority in any modeling effort. The two areas of most pressing need for this study are the western and eastern boundaries of the model. Wells should be drilled, and heads measured, in the vicinity of the western boundary of the domain.

Along the eastern boundary a better understanding of the nature of the aquifers is necessary. A tracer test would benefit the model by determining a recharge rate along the eastern boundary. A bomb tritium or chlorofluorocarbon tracer test would be ideal in this location because not only would the delineation of the tracer front allow for the calculation of a volumetric inflow rate, but a study of the geometry of the tracer front might shed some light on how areas of the cropline behave as recharge zones.

The nature of the clinker needs to be addressed along the cropline. An examination of the connection between clinker and coal would be beneficial. The transition zone should also be examined, and its hydrologic properties assessed.

Hydrogeologic properties of the Wasatch

The heterogeneity of the Wasatch makes it difficult to model. The scale of variation within the Wasatch Formation prohibits a good assessment of its aquifer characteristics. As this study has shown, a large sand body does exist within the Wasatch. Presumably there are others. This model would benefit from more aquifer tests in the Wasatch aimed at determining the degree of interconnection between this and other sand lenses. A few aquifer tests in the sand lens itself should be done to assess its hydrogeologic parameters. The boundaries of this model layer should be addressed as well.

Leaky aquifer test

The author recommends that a leaky aquifer test be done. The coal should be pumped while the sand lens is monitored. This would further address the premise of the study; the connection between the Wyodak coal and the Wasatch sand lens.

III. Modeling

The question remains, how much modeling can be supported by how much data? In this case the model domain was constructed in order to include sufficient area to model a transient state simulation at a later date. In so doing, much of the domain is without data, even though data from all available sources has been acquired. The result is a model which weighs heavily on a conceptualization of the domain, and methods, such as kriging, to fill the model with plausible parameter values. In addition, due to the size of the model, many simplifications of the stratigraphy were necessary. Such simplifications may have had an effect on the predicted heads and hence the estimated parameter values. Therefore, the estimates arrived at in this model are only internally consistent. About the behavior of the natural system which the model represents, there is far less certainty. Before applying these results outside of this model, the error resulting from simplification and estimation must be accounted for. If it is accepted that a model of near infinite complexity can describe the natural system, it must be accepted that the estimates of aquifer parameters and heads are only reliable to the degree that the model has been simplified.

The non-uniqueness of the model results is significant. If plausible values for model inputs are chosen, there can be some confidence that the results of the model will be plausible. However, it is necessary to accept that by balancing all of the factors involved, the result is not unique. And that the more numerous the parameters involved, the more numerous the possible solutions. Hence, the parameter estimates provided in this work should not be accepted directly into further models of the Powder River Basin. They may, however, provide a starting point to be used as a first approximation in such models.

REFERENCES

- Anderson, M. P., W. W., Woessner, 1992, Applied groundwater modeling. Academic Press, San Diego, 381p.
- Ayers, W. B., 1986, Lacustrine and fluvial-deltaic depositional systems, Fort Union Formation (Paleocene), Powder River Basin, Wyoming and Montana. AAPG Bulletin, v. 70, p. 1651-1673.
- Ayers, W. B., 1984, Depositional systems and coal occurrence in the Fort Union Formation (Paleocene), Powder River Basin, Wyoming and Montana: Ph.D dissertation, University of Texas at Austin, Austin Texas, 208 p.
- Borgman, L. E., C. D., Miller, S. R., Signorini, R. C., Faucette, 1994, Stochastic interpolation as a means to estimate oceanic fields. Atmosphere-Ocean, v. 32, no. 2, p395-419.
- Brogan, M., J., Meyer, 1996, Marquiss project – water monitoring wells, unpublished data.
- Brown, J. L., 1993, Sedimentary and postdepositional history of the lower Paleocene Tullock Member of the Fort Union Formation, Powder River Basin, Wyoming and Montana. USGS Bulletin 1917-L, 42 p.
- Cherven, V. B., A. R., Jacob, 1985, Evolution of Paleogene depositional systems, Williston Basin in response to global sea level changes. In: Cenozoic Paleogeography of west-central United States, Flores and Kaplan eds., Rocky Mountain Paleogeography Symposium 3, SEPM, Rocky Mountain Section, p. 127-170.
- Curry, W. H. III., Laramide structural history of the Powder River Basin, Wyoming. In: Wyoming Geological Association Guidebook, 23rd. Annual Field Conference, p. 49-60.
- Dickinson, W. R., M. A., Klute, M. J., Hayes, S. U., Janecke, E. R., Lundin, M. A., Mckittrick, M. D., Olivares, 1988, Paleogeographic and paleotectonic setting of Laramide sedimentary basins in the central Rocky Mountain region. GSA Bulletin, v. 100, p. 1023-1039.
- Dobson, C. W., 1996, Anisotropy of horizontal transmissivity in the Anderson-Wyodak coal aquifer of the Powder River Basin, Wyoming. MS thesis, University of Wyoming, 185p.
- Dynamic Graphics, Inc., 1996, Earth Vision, computer software.

- Fogg, J. L., M. W., Martin, P. B., Daddow, Geohydrology and potential effects of coal mining in 12 coal-lease areas, Powder River structural basin, northeastern Wyoming. USGS Water Resources Investigations, WRI-87-4102, 49 p.
- Freeze, R. A., J. A., Cherry, 1979, Groundwater, Prentice-Hall, New Jersey, 604p.
- Fullerton, D. S., 1977, Surficial geology of the Coyote Draw quad., Campbell County, Wyoming. USGS Miscellaneous Field Studies Map, MF-895.
- Garabedian, P. R., 1964, Partial differential equations, John Wiley & Sons, New York, 672p.
- Glass, G. B., R. W., Jones, 1991, Coal fields and coal beds of Wyoming. In: Wyoming Geological Association Guidebook, 42nd. Annual Field Conference, p. 133-167.
- Hefferin, E., 1997, Clinker maps, unpublished data.
- Hill, M. C., 1990, MODFLOWP: a computer program for estimating parameters of a transient, three-dimensional ground-water flow model using nonlinear regression. USGS Open-file Report, 317p.
- Kern, J. W., 1995, Spectra and cross spectra models for large scale frequency domain simulations
of d-variate n-dimensional random functions: applications in groundwater modeling and a statistical examination of Pierre Gy's sampling procedures. Phd Thesis, University of Wyoming, 201p.
- Kern, J. W., 1996, Geomat, unpublished computer software.
- Kern, J. W., 1997a, Personal communication, 9-3-1997
- Kern, J. W., 1997b, Personal communication, 10-25-97
- Lewis, B. D., W. R., Hotchkiss, 1981, Thickness, percent sand, and configuration of shallow hydrologic units in the Powder River Basin, Montana and Wyoming. USGS Miscellaneous Investigations Series, I-1317.
- Lisenbee, A. L., 1978, Laramide structure of the Black Hills uplift, South Dakota-Wyoming-Montana. GSA Memoir 151, p. 165-196.

- Lisenbee, A. L., 1988, Tectonic history of the Black Hills uplift, In: Wyoming Geological Association Guidebook, 39th. Annual Field Conference, p. 45-52.
- Lowry, M. E., J. G., Rankl, 1987, Hydrology of the White Tail Butte area, northern Campbell County, Wyoming. USGS Water Resources Investigations, WRI-82-4117, 47 p.
- Marston, R. A., ed., 1990, Wyoming Water Atlas, University of Wyoming, 124 p.
- Martin, L. J., D. L., Naftz, H. W., Lowham, J. G., Rankl, 1988, Cumulative potential hydrologic impacts of surface coal mining in the eastern Powder River structural basin, northeastern Wyoming. USGS Water Resources Investigations, WRI 88-4046, 201 p.
- Mathworks, Inc., 1996, Matlab, computer software.
- Matson, R. E., J. M., Pinchock, 1976, Geology of the Tongue River member, Fort Union Formation of eastern Montana. In: D. K. Murray ed., 1976 symposium on the geology of Rocky Mountain coal: Colorado Geological Survey Resources Series 1, p. 91-114.
- McDonald, M. G., A. W., Harbaugh, 1988, A modular three-dimensional finite-difference ground-water flow model. Techniques of Water Resources Investigations 06-A1, USGS, 576p.
- Mears, B., S. S., Agard, W. M., Sutherland, D. A., Coates, Powder River Basin, In: Quaternary Geology of the Northern Great Plains. Morrison and Assoc. 1991, p. 441-476.
- Peacock, K., 1997a, Personal communication, 1-20-1997.
- Peacock, K., 1997b, Personal communication, 8-12-1997.
- Rehm, B. W., G. H., Groenewold, K. A., Morin, 1980, Hydraulic properties of coal and related materials, Northern Great Plains. Ground Water, v. 18. no. 6, p. 551-561.
- Robinson, C. S., W. J., Mapel, M. H., Bergendahl, 1964, Stratigraphy and structure of the northern and western flanks of the Black Hills uplift, Wyoming, Montana, and South Dakota. USGS Prof. Paper 404 134 p.
- Seeland, D., 1988, Laramide paleogeographic evolution of the eastern Powder River Basin, Wyoming and Montana. In: Wyoming Geological Association Guidebook, 39th. Annual Field Conference, p. 29-34.

- Stone, R., D. F., Snoeberger, 1977, Cleat orientation and areal hydraulic anisotropy of a Wyoming coal aquifer. *Ground Water*, v. 15, no. 6, p. 434-438.
- Stoner, J. D., 1981, Horizontal anisotropy determined by pumping in two Powder River Basin coal aquifers, Montana. *Ground Water*, v. 19, no. 1, p. 34-40.
- StratiFact Software, Inc., 1995, Stratifact, computer software.
- Wang, H. F., M. P., Anderson, 1982, Introduction to groundwater modeling: finite difference and finite element methods. W. H. Freeman, San Francisco, 256p.
- Weaver, J. N., R. M., Flores, 1987, Sedimentologic and stratigraphic framework of the upper part of the Fort Union Formation, western Powder River Basin, Wyoming. USGS Miscellaneous Field Studies Map, MF-1929.
- Williams, V. S., 1978, Surficial geologic map of the Fortin Draw quad., Campbell County, Wyoming. USGS Miscellaneous Field Studies Map, MF-929.
- Williams, V. S., 1978, Surficial geologic map of the Gillette East quadrangle, Campbell County, Wyoming. USGS Miscellaneous Field Studies Map, MF-947.
- Williams, V. S., 1978, Surficial geologic map of the Moyer Springs quadrangle, Campbell County, Wyoming. USGS Miscellaneous Field Studies Map, MF-950.

This page intentionally left blank.